

CA-200
and
CA-608

RHO-BWI-C-5

MASTER

THREE-DIMENSIONAL GRAVITY INVESTIGATION OF THE HANFORD RESERVATION

BY

BENJAMIN H. RICHARD
CONSULTANT

AND

RAUL A. DEJU
ROCKWELL HANFORD OPERATIONS

NOTICE

The report was prepared as an account of work sponsored by the United States Government. Neither the United States nor the United States Department of Energy, nor any of their employees, nor any of their contractors, subcontractors, or their employees, makes any warranty, express or implied, or assumes any legal liability or responsibility for the accuracy, completeness, or usefulness of any information, apparatus, product or process disclosed, or represents that its use would not infringe privately owned rights.

JULY 1977

NOTICE MN ONLY

PORTIONS OF THIS REPORT ARE ILLEGIBLE. It
has been reproduced from the best available
copy to permit the broadest possible avail-
ability.

PREPARED FOR ROCKWELL HANFORD OPERATIONS,
A PRIME CONTRACTOR TO THE U. S. DEPARTMENT OF ENERGY,
UNDER CONTRACT NUMBER EY-77-C-06-1030

DISTRIBUTION OF THIS DOCUMENT IS UNLIMITED

THREE-DIMENSIONAL GRAVITY INVESTIGATION
OF THE HANFORD RESERVATION

Raul A. Deju
Benjamin H. Richard

July 1977

Prepared for

Research Department
Research and Engineering
Rockwell International
Atomics International Division
Rockwell Hanford Operations
Richland, Washington 99352

This report was prepared as an account of work sponsored by the United States Government. Neither the United States, nor the United States Department of Energy, nor any of their employees, nor any of their contractors, subcontractors, or their employees, makes any warranty, express or implied, or assumes any legal liability or responsibility for the accuracy, completeness, or usefulness of any information, apparatus, product or process disclosed, or represents that its use would not infringe privately owned rights.

TABLE OF CONTENTS

	<u>Page</u>
ABSTRACT	8
INTRODUCTION	9
PURPOSE AND SCOPE	9
PREVIOUS WORK	9
GEOLOGY	9
GRAVITY	18
GRAVITY CORRECTIONS	19
LIMITATIONS	20
DATA BASE	21
DATA REDUCTION	21
PROCESSING OF DATA	24
COMPUTER PROGRAMS USED FOR PROCESSING	60
INTERPRETATION	60
RESOLUTION OF DATA	60
SENSITIVITY	61
CONCLUSIONS	62
USEFULNESS OF THE GRAVITY-BEDROCK MODEL	62
DETAIL OBTAINED FROM THE MODEL	63
SIGNIFICANCE OF THE STUDY	64
APPENDIX A - DATA USED TO CONSTRUCT THE THREE-DIMENSIONAL MODELS	65
APPENDIX B - PERSPECTIVE VIEWS OF THE HANFORD RESERVATION GRAVITY STUDIES	86
REFERENCES	111
DISTRIBUTION	111

LIST OF FIGURES

<u>FIGURE NUMBER</u>		<u>Page</u>
1	THE SETTING OF THE PASCO BASIN	10
2	BLOCK DIAGRAM SHOWING TOPOGRAPHY PRIOR TO RELEASE OF GLACIAL FLOOD WATERS	14
3	BLOCK DIAGRAM SHOWING HANFORD AREA INUNDATED BY ICEBERG-LADEN WATERS	15
4	BLOCK DIAGRAM SHOWING EMERGING TOPOGRAPHIC "HIGHS" WITH CONTINUED DOWN-CUTTING BY FLOOD WATERS	16
5	BLOCK DIAGRAM SHOWING LOWER FLOOD WATER STAGE WITH DOWN-CUTTING NEAR GABLE MOUNTAIN	17
6	LOCATION OF BOUGUER GRAVITY DATA USED IN THIS STUDY	22
7	1960 HANFORD RESERVATION WATER TABLE MAP	23
8	499-POINT BOUGUER GRAVITY MAP OF THE HANFORD RESERVATION	25
9	499-POINT TERRAIN-CORRECTED BOUGUER GRAVITY MAP OF THE HANFORD RESERVATION	26
10	166-POINT CORRECTION FOR UNSATURATED MATERIALS ABOVE THE WATER TABLE	28
11	499-POINT WATER TABLE AND TERRAIN-CORRECTED BOUGUER GRAVITY MAP	29
12	LOCATION OF THE DATA USED TO CONSTRUCT THE REGIONAL GRAVITY SURFACE FOR THE 499-POINT THREE-DIMENSIONAL MODEL	30
13	REGIONAL GRAVITY SURFACE USED IN THE 499-POINT STUDY	31
14	499-POINT GRAVITY-BEDROCK MAP CONSTRUCTED BY SUBTRACTING FIGURE 13 FROM FIGURE 11	32
15	GRAVITY POINT LOCATIONS IN THE 499-POINT STUDY WITHIN THE AREA SHOWN IN FIGURE 14	33
16	GRAVITY STATIONS USED TO CALCULATE THE REGIONAL GRAVITY SURFACE FOR THE 499-POINT STUDY THAT ARE WITHIN THE AREA SHOWN IN FIGURE 13	34

<u>FIGURE NUMBER</u>		<u>Page</u>
17	LOCATION OF BOUGUER GRAVITY STATIONS USED FOR THE 344-POINT THREE-DIMENSIONAL MODEL	35
18	344-POINT BOUGUER GRAVITY MAP OF THE HANFORD RESERVATION	36
19	344-POINT TERRAIN-CORRECTED BOUGUER GRAVITY MAP OF THE HANFORD RESERVATION	37
20	344-POINT WATER TABLE AND TERRAIN-CORRECTED BOUGUER GRAVITY MAP OF THE HANFORD RESERVATION	38
21	344-POINT GRAVITY-BEDROCK MAP CONSTRUCTED BY SUBTRACTING FIGURE 13 FROM FIGURE 20	39
22	GRAVITY POINT LOCATIONS IN THE 344-POINT STUDY WITHIN THE AREA SHOWN IN FIGURE 20	40
23	LOCATION OF BOUGUER GRAVITY STATIONS USED FOR THE 166-POINT THREE-DIMENSIONAL MODEL	41
24	166-POINT BOUGUER GRAVITY MAP OF THE HANFORD RESERVATION	42
25	166-POINT TERRAIN-CORRECTED BOUGUER GRAVITY MAP OF THE HANFORD RESERVATION	43
26	166-POINT WATER TABLE AND TERRAIN-CORRECTED BOUGUER GRAVITY MAP OF THE HANFORD RESERVATION	44
27	LOCATION OF THE DATA USED TO CONSTRUCT THE REGIONAL GRAVITY SURFACE FOR THE 166-POINT THREE-DIMENSIONAL MODEL	45
28	REGIONAL GRAVITY SURFACE USED IN THE 166-POINT STUDY	46
29	166-POINT GRAVITY-BEDROCK MAP CONSTRUCTED BY SUBTRACTING FIGURE 28 FROM FIGURE 26	47
30	GRAVITY STATION LOCATIONS USED IN THE 166-POINT STUDY THAT ARE WITHIN THE AREA SHOWN IN FIGURE 29	48
31	GRAVITY STATIONS USED TO CALCULATE THE REGIONAL GRAVITY SURFACE FOR THE 166-POINT STUDY WITHIN THE AREA OF FIGURE 28	49
32	LOCATION OF BOUGUER GRAVITY STATIONS USED FOR THE 88-POINT THREE-DIMENSIONAL MODEL	50

<u>FIGURE NUMBER</u>		<u>Page</u>
33	88-POINT BOUGUER GRAVITY MAP OF THE HANFORD RESERVATION	51
34	88-POINT TERRAIN-CORRECTED BOUGUER GRAVITY MAP OF THE HANFORD RESERVATION	52
35	88-POINT CORRECTION FOR UNSATURATED MATERIALS ABOVE THE WATER TABLE	53
36	88-POINT WATER TABLE AND TERRAIN-CORRECTED BOUGUER GRAVITY MAP OF THE HANFORD RESERVATION	54
37	LOCATION OF THE DATA USED TO CONSTRUCT THE REGIONAL GRAVITY SURFACE FOR THE 88-POINT STUDY	55
38	REGIONAL GRAVITY SURFACE USED IN THE 88-POINT STUDY	56
39	88-POINT GRAVITY-BEDROCK MAP CONSTRUCTED BY SUBTRACTING FIGURE 38 FROM FIGURE 36	57
40	GRAVITY STATION LOCATIONS USED IN THE 88-POINT STUDY THAT ARE WITHIN THE AREA SHOWN IN FIGURE 39	58
41	GRAVITY STATIONS USED TO CALCULATE THE REGIONAL GRAVITY SURFACE FOR THE 88-POINT STUDY WITHIN THE AREA OF FIGURE 38	59
B-1	HANFORD RESERVATION PETERSON-BOUGUER GRAVITY MAP, SOUTH VIEW	87
B-2	HANFORD RESERVATION PETERSON-BOUGUER GRAVITY MAP, WEST VIEW	88
B-3	HANFORD RESERVATION PETERSON-BOUGUER GRAVITY MAP, NORTH VIEW	89
B-4	HANFORD RESERVATION PETERSON-BOUGUER GRAVITY MAP, EAST VIEW	90
B-5	HANFORD RESERVATION DEJU AND RICHARD RESIDUAL GRAVITY MAP, SOUTH VIEW	91
B-6	HANFORD RESERVATION DEJU AND RICHARD RESIDUAL GRAVITY MAP, WEST VIEW	92
B-7	HANFORD RESERVATION DEJU AND RICHARD RESIDUAL GRAVITY MAP, NORTH VIEW	93

<u>FIGURE NUMBER</u>	<u>Page</u>
B-8 HANFORD RESERVATION DEJU AND RICHARD RESIDUAL GRAVITY MAP, EAST VIEW	94
B-9 HANFORD RESERVATION 499-POINT GRAVITY BEDROCK MAP, SOUTH VIEW	95
B-10 HANFORD RESERVATION 499-POINT GRAVITY BEDROCK MAP, WEST VIEW	96
B-11 HANFORD RESERVATION 499-POINT GRAVITY BEDROCK MAP, NORTH VIEW	97
B-12 HANFORD RESERVATION 499-POINT GRAVITY BEDROCK MAP, EAST VIEW	98
B-13 HANFORD RESERVATION 344-POINT GRAVITY BEDROCK MAP, SOUTH VIEW	99
B-14 HANFORD RESERVATION 344-POINT GRAVITY BEDROCK MAP, WEST VIEW	100
B-15 HANFORD RESERVATION 344-POINT GRAVITY BEDROCK MAP, NORTH VIEW	101
B-16 HANFORD RESERVATION 344-POINT GRAVITY BEDROCK MAP, EAST VIEW	102
B-17 HANFORD RESERVATION 166-POINT GRAVITY BEDROCK MAP, SOUTH VIEW	103
B-18 HANFORD RESERVATION 166-POINT GRAVITY BEDROCK MAP, WEST VIEW	104
B-19 HANFORD RESERVATION 166-POINT GRAVITY BEDROCK MAP, NORTH VIEW	105
B-20 HANFORD RESERVATION 166-POINT GRAVITY BEDROCK MAP, EAST VIEW	106
B-21 HANFORD RESERVATION 88-POINT GRAVITY BEDROCK MAP, SOUTH VIEW	107
B-22 HANFORD RESERVATION 88-POINT GRAVITY BEDROCK MAP, WEST VIEW	108
B-23 HANFORD RESERVATION 88-POINT GRAVITY BEDROCK MAP, NORTH VIEW	109
B-24 HANFORD RESERVATION 88-POINT GRAVITY BEDROCK MAP, EAST VIEW	110

LIST OF TABLES

<u>TABLE NUMBER</u>		<u>Page</u>
A-I	LISTING OF DATA USED IN MODEL CALCULATIONS	66

A B S T R A C T

Models of the basalt surface buried under the Hanford reservation are constructed from gravity data. The method uses a modified third order polynomial surface to remove the regional effects and a gravity-geologic method to remove the water table effects. When these influences are subtracted from previous data, the anomaly remaining directly reflects the irregularity of the underlying basalt surface. The Umbanum Anticline and the Cold Creek Syncline are delineated beneath the overlying surficial deposits. Along the crest of the Umbanum Anticline, a number of gravity lows are evident. These may identify locations of breaching by an ancestral river.

In addition, the data are examined to determine optimum gravity data spacing for modeling. Optimum results were obtained using a station separation of one per four square miles. Less will delineate only the major underlying structures. It is also very important to have all data points distributed in a regularly spaced grid.

INTRODUCTION

PURPOSE AND SCOPE

This study uses the original gravity data gathered by Peterson^(1,2) which were studied further by Deju and Richard⁽³⁾ to construct a three-dimensional geologic model of the Hanford reservation. The model was reconstructed four times using a maximum of 499 data points and a minimum of 88 data points. These models were evaluated to establish:

1. The usefulness of gravity data in constructing three-dimensional geologic models;
2. The data distribution needed for model construction; and,
3. The geologic information that may be inferred from this technique.

PREVIOUS WORK

Gravity data were initially collected by Peterson.^(1,2) These data, along with:

1. A Bouguer gravity map of the Hanford reservation on a 1:62,000 scale with station locations and values for the stations; and,
2. Notes containing data to calculate the Bouguer values, were reduced by Deju and Richard⁽³⁾ to produce a residual gravity map of the Hanford reservation.

GEOLOGY

The Hanford reservation is located in south-central Washington within the Columbia Plateau physiographic province. The reservation presently encompasses 576 square miles in the structural and topographic low known as the Pasco Basin. The Pasco Basin (Figure 1) is delineated by the Saddle Mountains to the north, the Umtanum and Yakima ridges to the west, the Rattlesnake and Horse Heaven Hills to the south, and a broad regional monocline (known locally as the Jackass Mountain Monocline) to the east.

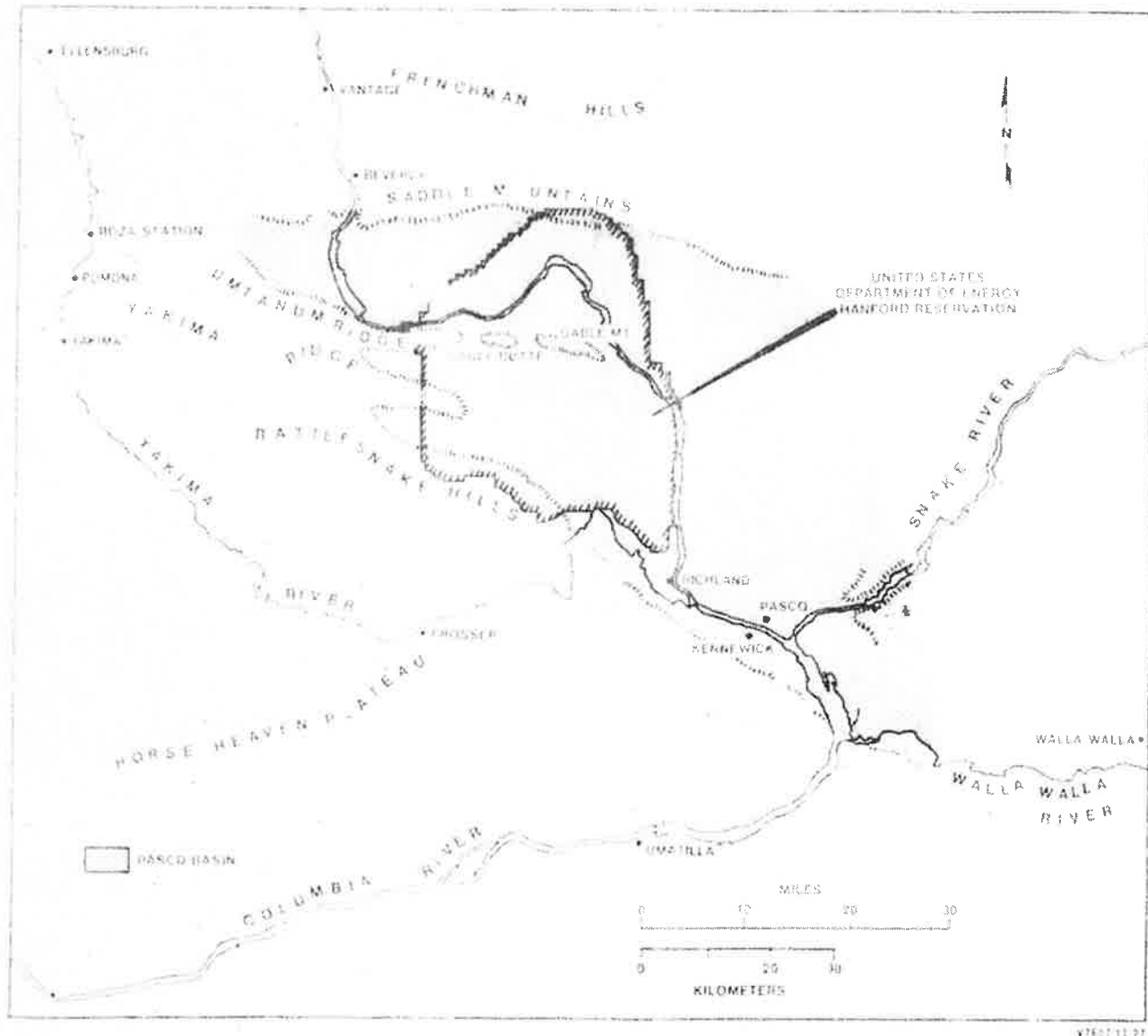


FIGURE 1
THE SITTING OF THE PASCO BASIN

During the Tertiary Period, the Columbia Plateau was the scene of numerous lava outpourings emanating from extensive fissure systems. The viscous fluids covered the surrounding terrain and flowed into the regional low areas, such as the Pasco Basin. As basining continued, thick sections of basalt accumulated in these low regions. At one location in the Pasco Basin, the basalt rock and intercalated sediments appear to be more than 10,000 feet (3,000 meters) thick.

The youngest flow dated within the Pasco Basin is about eight million years old and is confined to the eastern and southeastern sections. Between periods of lava outpourings, the basalt surface was subjected to various degrees of weathering and erosion. As a consequence, a thin layer of sediments accumulated on some of the basalt surfaces prior to being covered by later flows. One sedimentary horizon, the Vantage Sandstone (Formation), is identified over a broad region; however, most sedimentary horizons between basalt flows are of limited horizontal extent.

Although the Columbia River now flows through the center of the Pasco Basin, it is believed that the river's course has been extensively changed in the past by basalt flows entering the Pasco Basin. The Columbia River represents the base level of the regional unconfined ground water flow system. Confined ground water is present within some of the basalt flows beneath the Hanford reservation and may originate as far away as the Cascade Mountains to the west. Both the vesicular and rubbly zones near the tops of the basalt flows and the sedimentary interbeds provide the permeability for ground water movement. The dense inner sections of the flow units comprise the confining material.

During the Pliocene Epoch, the number and size of fissure eruptions markedly decreased. Though the volcanic activity eventually ceased, basining continued and was apparently accompanied by a regional north-south compression. As a result of this compression acting on the basalt rocks, a number of

east-west-trending anticlinal ridges; e.g., Saddle Mountains, developed in the western part of the Columbia Plateau. The formation of these ridges had a significant effect on the course of the Columbia River. Where the river was able to erode the basalt at a rate equal to or faster than the anticlinal ridges were rising, little change occurred in the course of the Columbia River. Where the ridges rose faster than the river was able to erode, its flow was temporarily halted and the water ponded behind the ridges. This appears to have occurred during the rise of the Horse Heaven Hills. A shallow lake covering over 10,000 square miles (25,000 square kilometers) was created. It was into this lake that sediments began accumulating about three million years ago. As basining continued, sediments continued to fill the Pasco Basin. These lacustrine and fluvial deposits overlying the basalt are known as the Ringold Formation. The upper portion of this formation presently comprises the steep cliffs exposed just east of the Columbia River, known as the White Bluffs. The total thickness of the Ringold Formation in the Pasco Basin is about 1,000 feet (300 meters) and is characterized by a lower clay, middle cemented gravel and an upper section of silt and sand units. The presence of gravel beds throughout the Ringold Formation tends to indicate that at no time during deposition did the Horse Heaven Hills completely impound the Columbia River for a significantly long time.

By late Pleistocene (300,000 years ago), Ringold deposition ceased. Basining decreased on a regional scale and, instead, the land within the Pasco Basin was uplifted (the present surface of the Ringold Formation in the White Bluffs area is 1,000 feet [305 meters] above mean sea level). A period of down-cutting followed, during which the ancestral Columbia River eroded more than 600 feet (180 meters) into the Ringold sediments in the central part of the Pasco Basin.

At the close of the Ice Age (perhaps 20,000 to 40,000 years ago), the continental ice sheet, which covered much of northern Washington, melted and gradually retreated northward. As a result, large volumes of meltwater were released from the melting

ice and from the ice marginal lakes. The block diagram shown in Figure 2 illustrates the topography as it would have appeared just prior to the release of the glacial floodwaters.

Eighteen to twenty thousand years ago, a deep lake, 2,000 feet (600 meters) at the deepest point, called Lake Missoula, formed behind an ice cork that plugged the surface drainage of portions of western Montana and northern Idaho. This blockage was the result of ice filling a narrow valley where the Clark Fork River empties into Pend Oreille Lake in Idaho. When the ice dam failed, water flowed through the gap at the rate of 9.5 cubic miles (40 cubic kilometers) per hour. This compares with the present average flow of the Columbia River of 8.7×10^{-6} cubic miles (3.6×10^{-5} cubic kilometers) per hour.

Figure 3 shows the basin filled with iceberg-laden waters. It is estimated that over 500 cubic miles (2,000 cubic kilometers) of water poured into the Pasco Basin. Within a few months, the floodwater receded to the stage shown in Figure 4. During this time, water continued to pour into the basin from the east, down-cutting into the sediments of the Ringold Formation, forming two channels: (1) the Ringold Coulee; and, (2) the Koontz Coulee.

Another significant drop in water level occurred as shown in the block diagram in Figure 5. At this stage, the river cut two channels on either side of Gable Mountain. After the lake completely drained and the Columbia River established its present course, wind erosion became a more dominant factor in sculpturing the landscape. Sediments brought down during the flood were reworked by the wind, especially those in Cold Creek Valley. Here, updraft created by the winds blowing over Rattlesnake Hills picked up the finer grained materials and transported them downwind. The coarser grained materials were slowly moved over the land surface where they accumulated in dunes.



FIGURE 2

BLOCK DIAGRAM SHOWING TOPOGRAPHY DUE TO RILLAGE OF GLACIAL FLOOD WATERS

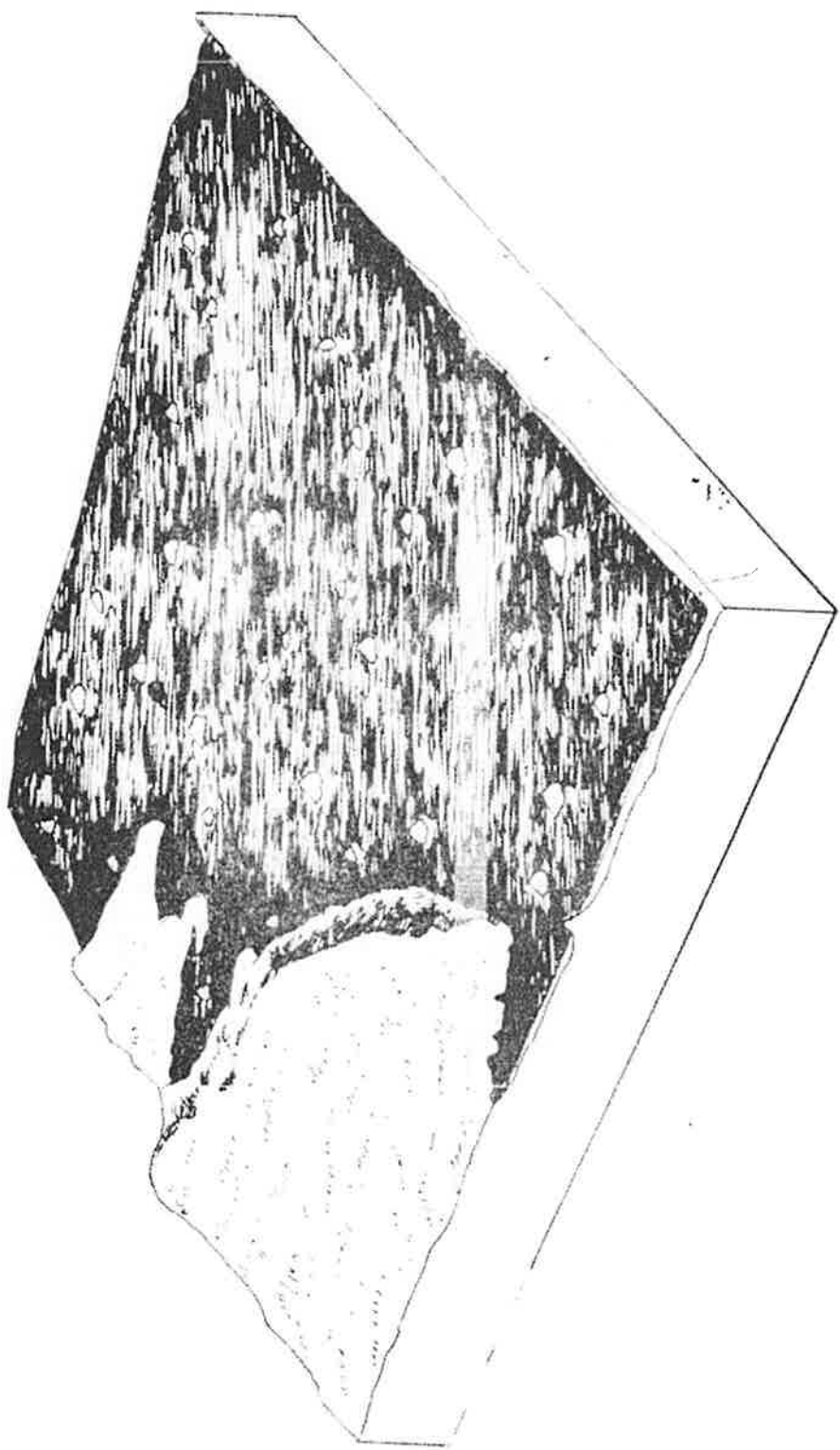


FIGURE 3

BLOCK DIAGRAM SHOWING HAMMORD AREA MUDFLOW BY ICEBURG-LANDING MAPPERS

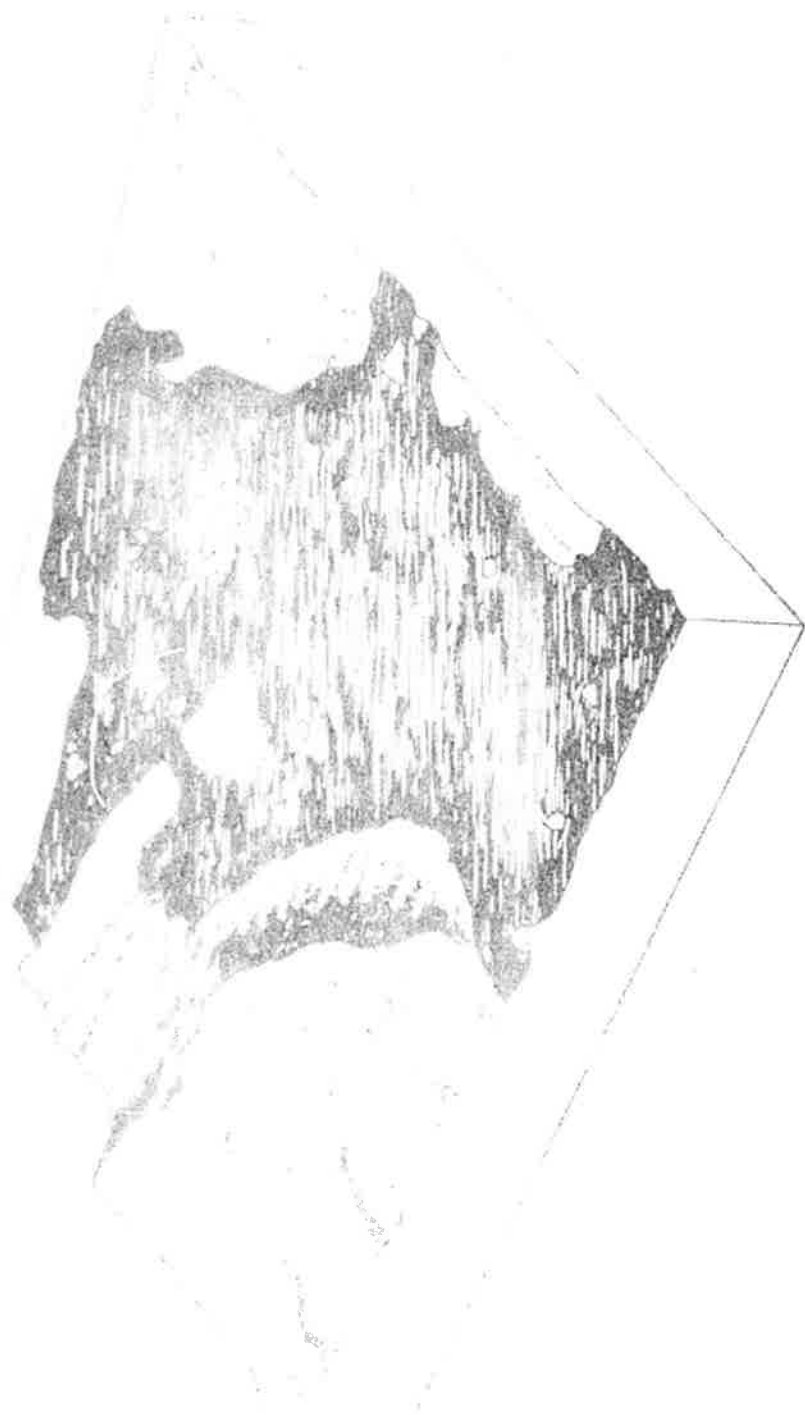
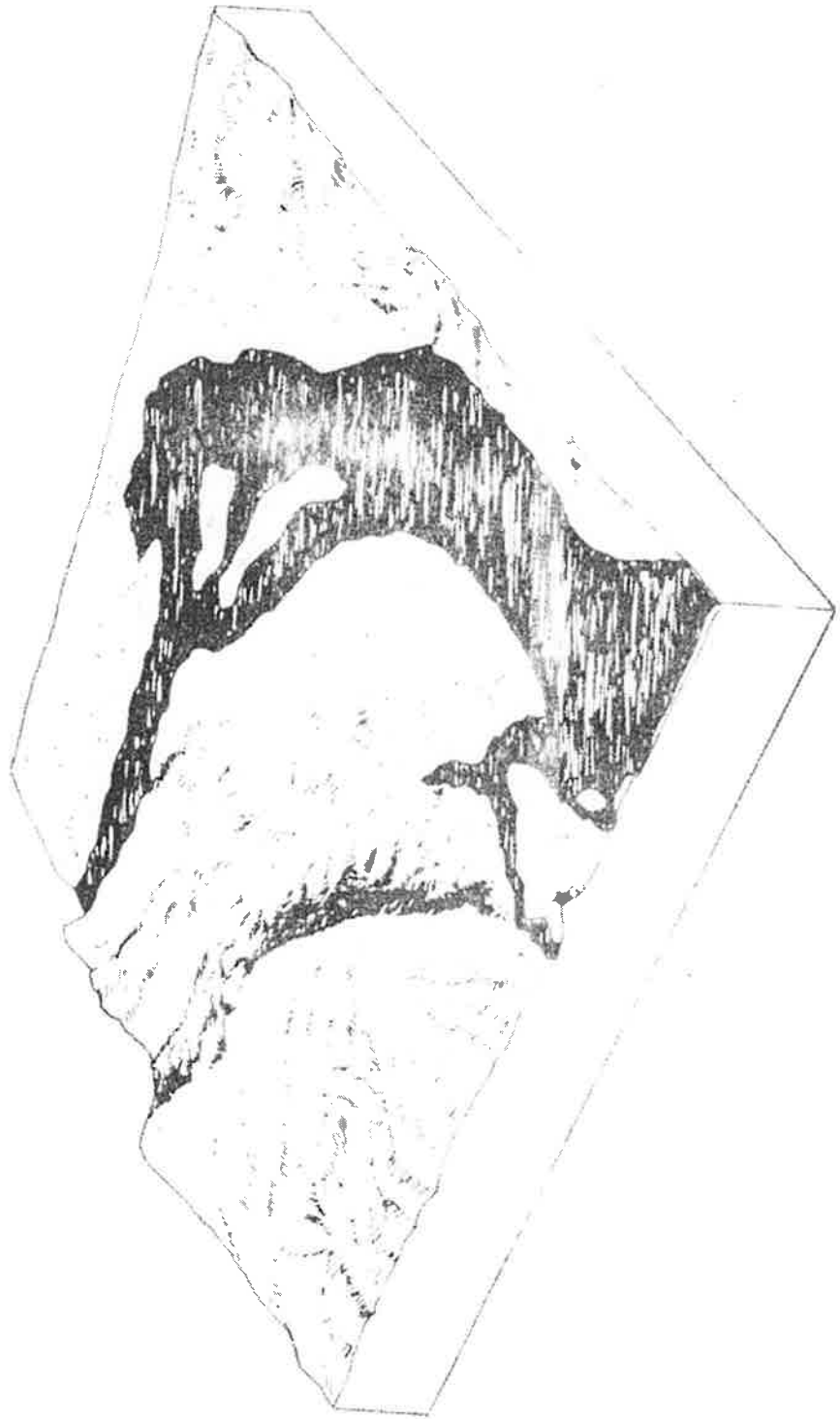


FIGURE 11.—*Sturisoma* sp. (indeterminate) from the Lower Silurian of New York. DRAWN BY E. L. DAVIS.



BLOCK DISMEMBERED AND PREPARED BY THE AUTHOR
FOR MUSEUM EXHIBITION. THE FISH IS A
LATE CRETACEOUS SPECIMEN FROM THE
NEW YORK STATE.

GRAVITY

The gravity field at a point may be represented by the following equation:

$$g = F/m_1 = \sum G m_i / r_i^2 \quad (1)$$

where,

g = gravity field at a point,

F = force of gravity at a point,

m_1 = unit mass,

G = gravitational constant,

m_i = individual mass contributing to the field,

r_i = distance from location of field measurement to m_i .

The gravity field will vary as a function of distance from the individual masses which make up the surface of the earth. It will also vary as a function of the density of earth surface materials, since mass is equal to density times volume. Other parameters that affect field gravity measurements are elevation, tides, latitude, irregular topography, and instrumental drift.⁽⁴⁾ All variations, except those caused by density, can be systematically removed from the original gravity data. If all these variations are removed, the resultant map will reflect the densities of the materials that make up the surface of the earth. This is called a Bouguer Gravity Map. Such a map does not separate the deep density variations from the shallow variations.

To interpret gravity data, it is necessary to remove any effects due to the presence of hills and valleys. These effects are removed using terrain corrections.⁽⁴⁾ Next, shallow density variations must be separated from the deep ones. All methods used to separate these anomalies are subject to error. Some standard techniques used to minimize error are derivative mapping, polynomial surface fitting, wavelength filtering, and visual removal of regional trends.

GRAVITY CORRECTIONS

The standard corrections made to gravity field data so as to detect gravity anomalies caused by shallow density variations are listed below.

1. Corrections that move all field data to a common datum (sea level in this report).
 - a. Free air correction (0.09406 milligal per foot, .308 milligal per meter). This correction is added if the datum is below the elevation of the field data point.
 - b. Bouguer correction ($0.0127 \times$ density per foot - .042 \times density per meter). This correction is subtracted if the datum is below the elevation of the field data point.
2. Corrections that remove variations caused by differences in horizontal location and by differences in time.
 - a. Drift and tidal corrections. This is done by rereading a base station value, plotting the variation of this reading with time, and removing time variation from all data.
 - b. Horizontal location corrections. This is done by calculating the normal variation of gravity along the geoid surface for the field point, then subtracting this value from the observed gravity. The data that were used in this report were corrected using the international formula, which is:

$$g = 978.049 (1+.0052884 \sin^2 \theta - .000059 \sin^2 2\theta) \text{ gal (2)}$$

where,

- g = theoretical gravity value at sea level at the latitude of the field measurement,
 θ = latitude of the field measurement; gal = 1 centimeter per square second.

3. Corrections for irregular terrain. Because the Bouguer correction assumes infinite horizontal sheets for the calculation, existing valleys and hills adjacent to a

gravity station will cause errors in the data. These effects are removed by calculating the effect of each irregularity on a reading and adding it to the gravity value. The density of the material involved was assumed to be 2.87 grams per cubic centimeter. All corrections were made using the Hammer method.⁽⁴⁾

4. Removal of deep-seated density variations. This is more qualitative than all other corrections and is subject to error. In this study, the removal was done using a third order polynomial surface constructed from data points located over the highs shown by Deju and Richard, Plate 5.⁽³⁾ This surface is subtracted from the terrain-corrected data. The residual data should be a representation of the shallow density variations.
5. Removal of other variations. Near-surface density effects can be removed by the gravity-geologic method⁽⁵⁾ if certain conditions are met. These conditions being that the effects are caused by a gently undulating body that is near the surface. It assumes that the effects of this body on each station are approximated by:

$$\Delta g = 0.0127 \times \delta_d \times t \quad (3)$$

where,

Δg = gravity effects,

δ_d = difference in density of the body from the bedrock,

t = thickness of the body in meters.

This correction was made to remove the effect of unsaturated material.

LIMITATIONS

The limitations of the gravity method are due to instrumentation, data gathering, and interpretation errors. The instrument used was a Worden gravity meter that had negligible error. Data gathering and analysis were carefully done, and the geologic data available minimized the interpretation error. There is never

a unique answer in gravity interpretation, but the confidence level of this report's interpretation is high because of the large amount of available geologic data.

The greatest limitation in this study is detailed geologic knowledge of small areas. Anything less than a mile across may be missed. In areas with few data points, anomalies several miles across may be missed.

Finally, the models constructed are of the buried basalt surface. Channels in the Ringold Formation and local variation in the thickness of the basalt interbeds may cause local errors in the model. The channel effects can be minimized, but the interbed effect can only be known by local absolute depth determinations.

DATA BASE

The data used in this report were gathered by Peterson.⁽²⁾ The original data were taken from a contoured Bouguer Gravity Map with station locations and Bouguer values of the stations. The data are accurate to \pm 0.1 milligal. Figure 6 shows the distribution of data points. Deju and Richard⁽³⁾ completed the necessary terrain corrections.

This study took the terrain-corrected data of Deju and Richard⁽³⁾ and placed them on computer cards. These cards contain the (x,y) coordinate of the field point, the Bouguer value, and the terrain-corrected Bouguer value. In addition to these data, a separate field was established for the points to be used to calculate the regional gravity effects. The 1960 Hanford Reservation Water Table Map (Figure 7) was used along with Peterson's field notes to calculate the gravity contribution of the unsaturated material. These data were also placed on computer cards. See Appendix A for a listing of the cards.

DATA REDUCTION

All data used in this study came from cards described in

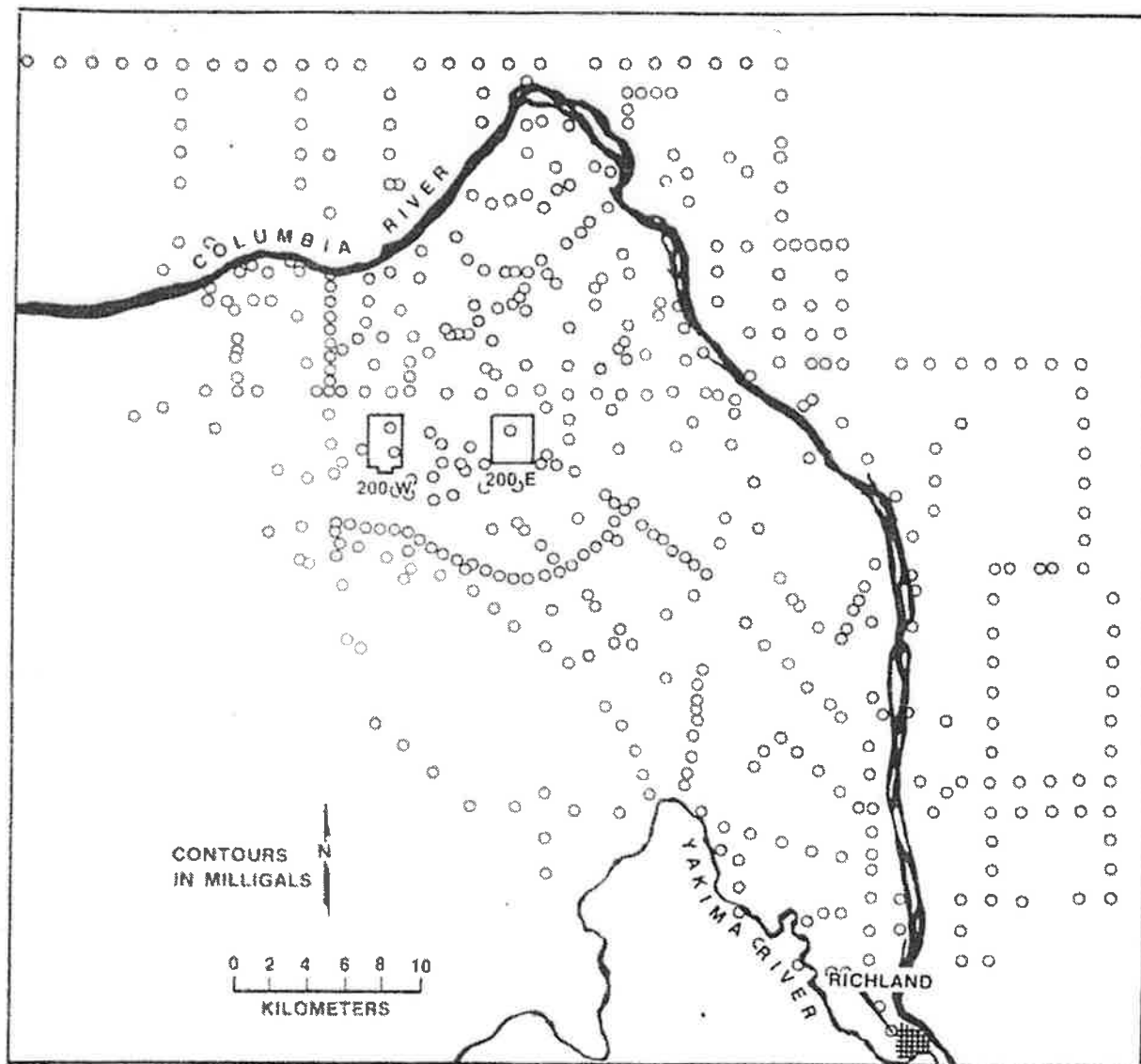


FIGURE 6

LOCATION OF BOUGUER GRAVITY DATA USED IN THIS STUDY

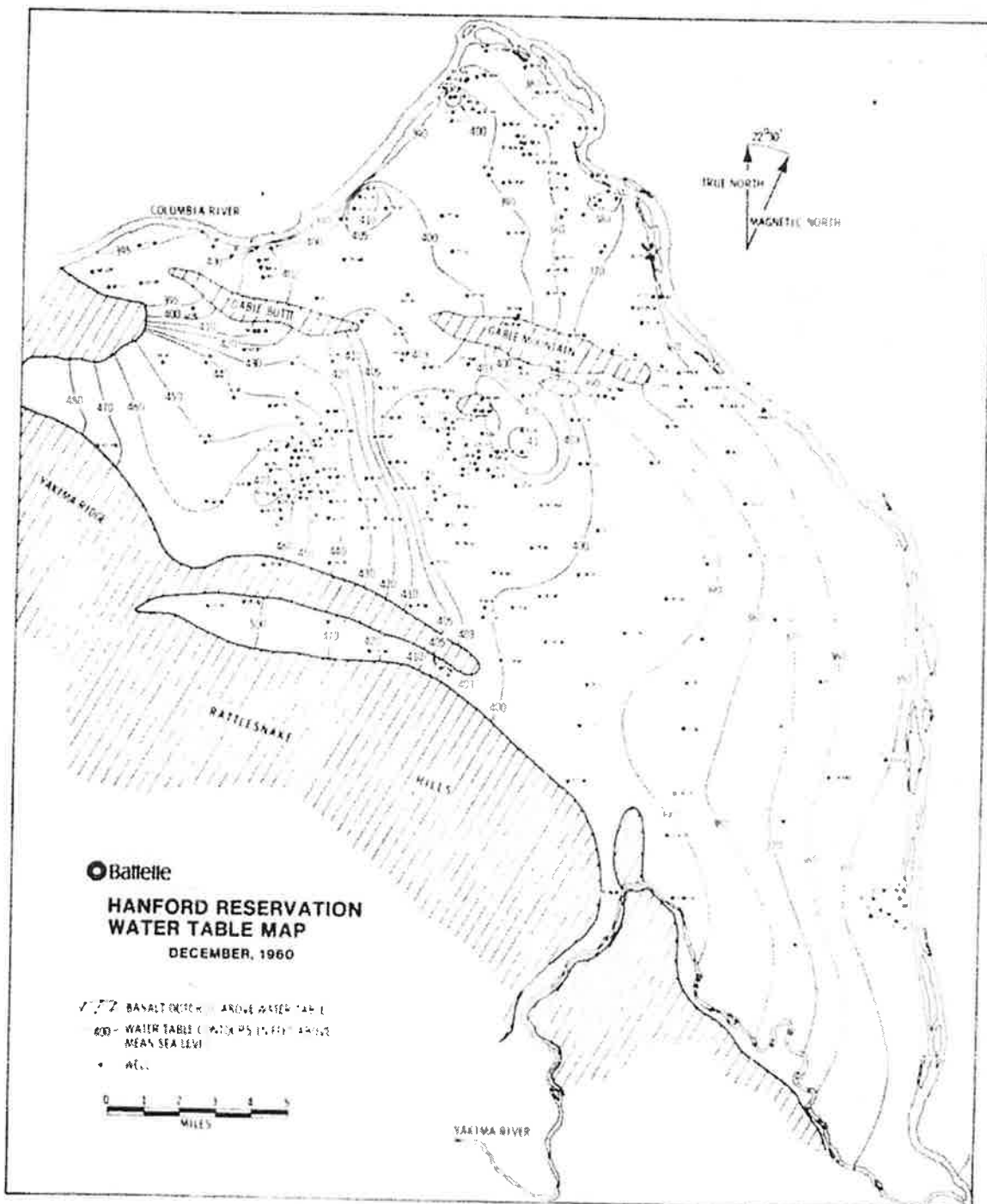


FIGURE 7

1960 HANFORD RESERVATION WATER TABLE MAP

the previous section. Any datum having a low confidence level, such as a value that could not be read from the map or calculated from notes, was eliminated. If the horizontal position appeared in doubt, the point was also eliminated. Only terrain corrections that would change the data by 0.1 milligal or more were considered. Appendix A shows the data points used.

One hundred sixty-six of the data points given in Appendix A were selected to be used to calculate the effect of unsaturated materials on the Bouguer gravity. A correction value was calculated for each of these points in the following manner:

1. The surface elevation was obtained from Peterson's field notes;
2. The water table elevation was obtained from Figure 6; and,
3. The difference in these elevations (t) was used in the following equation:

$$c = .0416 \times \Delta\rho \times t \quad (4)$$

where,

c = the gravity effect of the unsaturated material,

.0416 = a constant assuming the gravity effect is caused by an infinite slab of unsaturated material,

$\Delta\rho$ = the difference in density between the unsaturated material and the basalt surface (1.36 grams per cubic centimeter in this case),

t = the thickness of the unsaturated material in meters.

PROCESSING OF DATA

The three-dimensional model was constructed by the following procedure:

1. The Bouguer data were placed on a grid;
2. The data were contoured (Figure 8);
3. The terrain correction was added to the Bouguer data;
4. The data were placed on a grid;
5. The data were contoured (Figure 9);

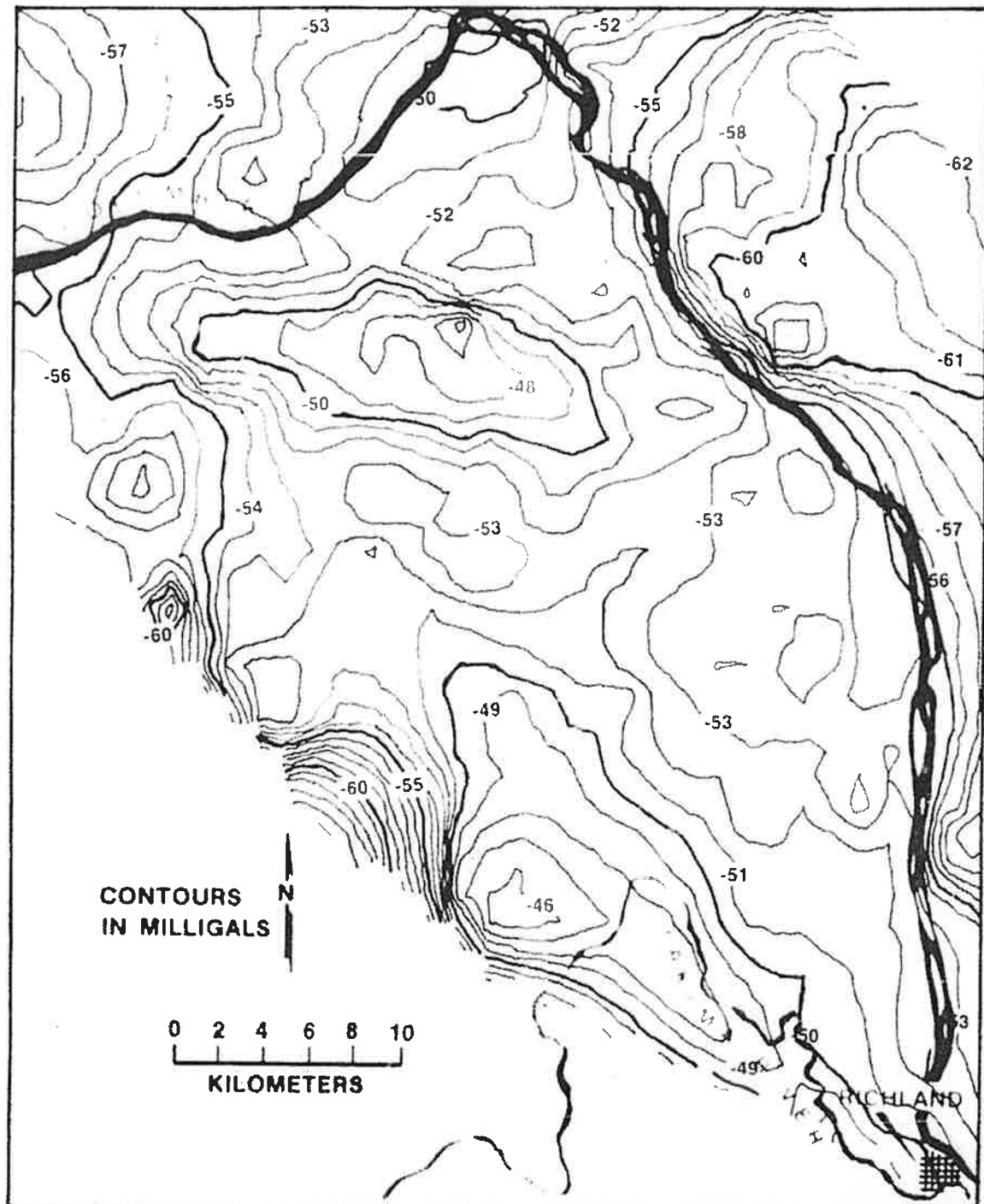


FIGURE 8

499-POINT BOUGUER GRAVITY MAP OF THE HANFORD RESERVATION

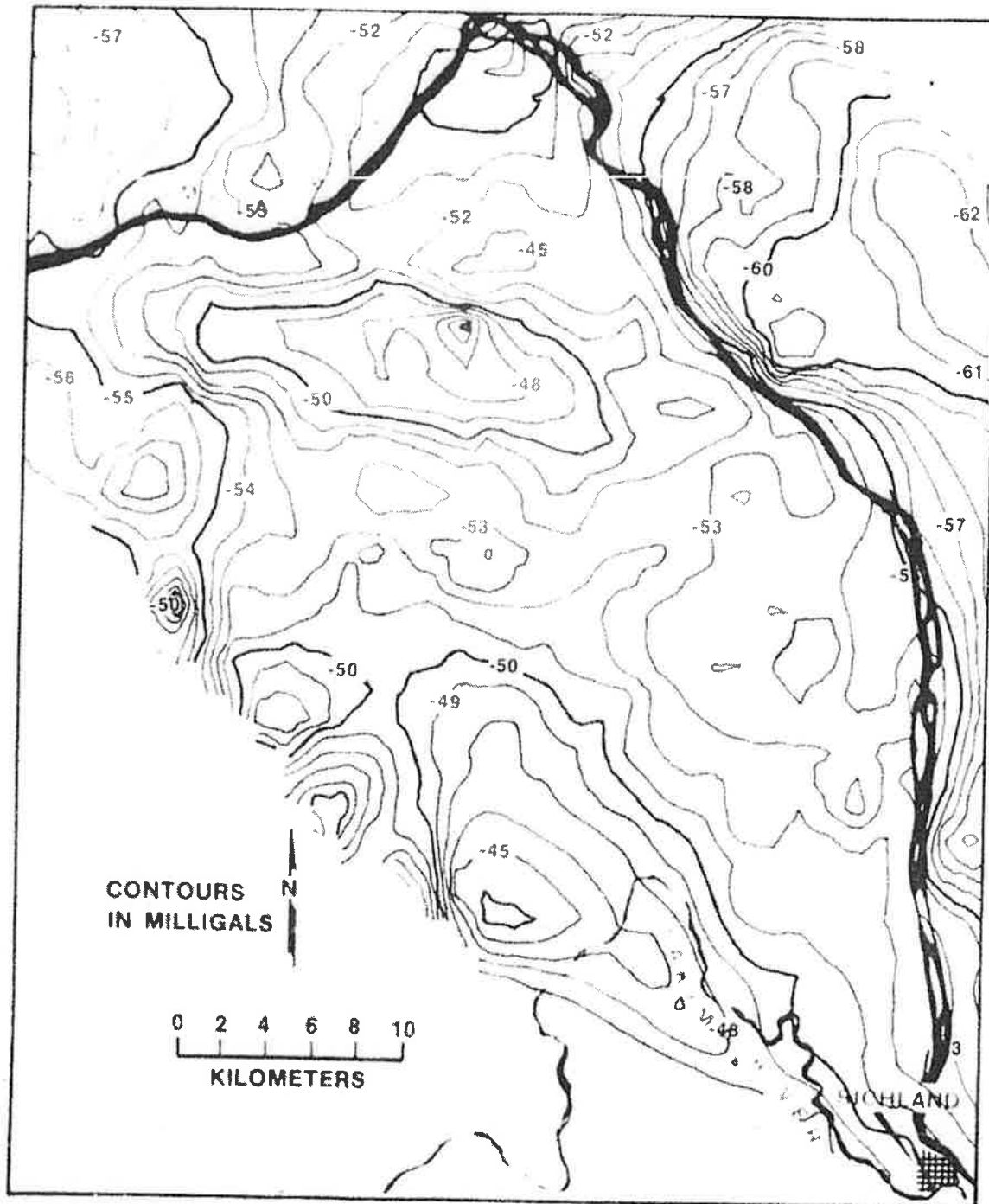


FIGURE 9

499-POINT TERRAIN-CORRECTED BOUGUER GRAVITY MAP
OF THE HANFORD RESERVATION

6. The water table correction was placed on a grid;
7. The data were contoured (Figure 10);
8. The water table correction grid was added to the terrain-corrected Bouguer data;
9. The data were contoured (Figure 11);
10. A regional geology surface was calculated using a third order least squares polynomial of data points on the gravity high shown by Deju and Richard⁽³⁾ (Figure 12);
11. This surface was placed on a grid;
12. The polynomial surface was contoured (Figure 13); and,
13. The polynomial surface was subtracted from Figure 11 to produce a gravity-bedrock map (Figure 14).

All grids used in the calculations covered the area shown by Figure 6. Because water table data were either missing or inadequate beyond the area shown in Figure 7, all contour maps were limited to these boundaries and were constructed on the same scale. Figure 15 shows the data locations for the Bouguer gravity in the above contour maps. Figure 16 displays the polynomial surface points in the above contour maps.

The above process was repeated four times. Each time, the number of data used in the calculation was reduced. The initial data contained 499 points and the final data 88 points. Figures 17 through 22 relate to the 344-point study. This study used the same data to remove the water table effects and regional gravity effects of the 499-point study. Figures 23 through 31 result from the 166-point study. This study used the same data to remove the water table and the data shown in Figure 27 to remove the regional gravity effects. Figures 32 through 41 relate to the 88-point study. This study used all 88 points to remove water table effects and the data shown in Figure 41 to remove the regional gravity effects.

All gravity-bedrock maps were then plotted in three-dimensional perspective viewing each surface from the south, west, north, and east. Appendix B gives these views. All final maps and three-dimensional views were examined to determine:

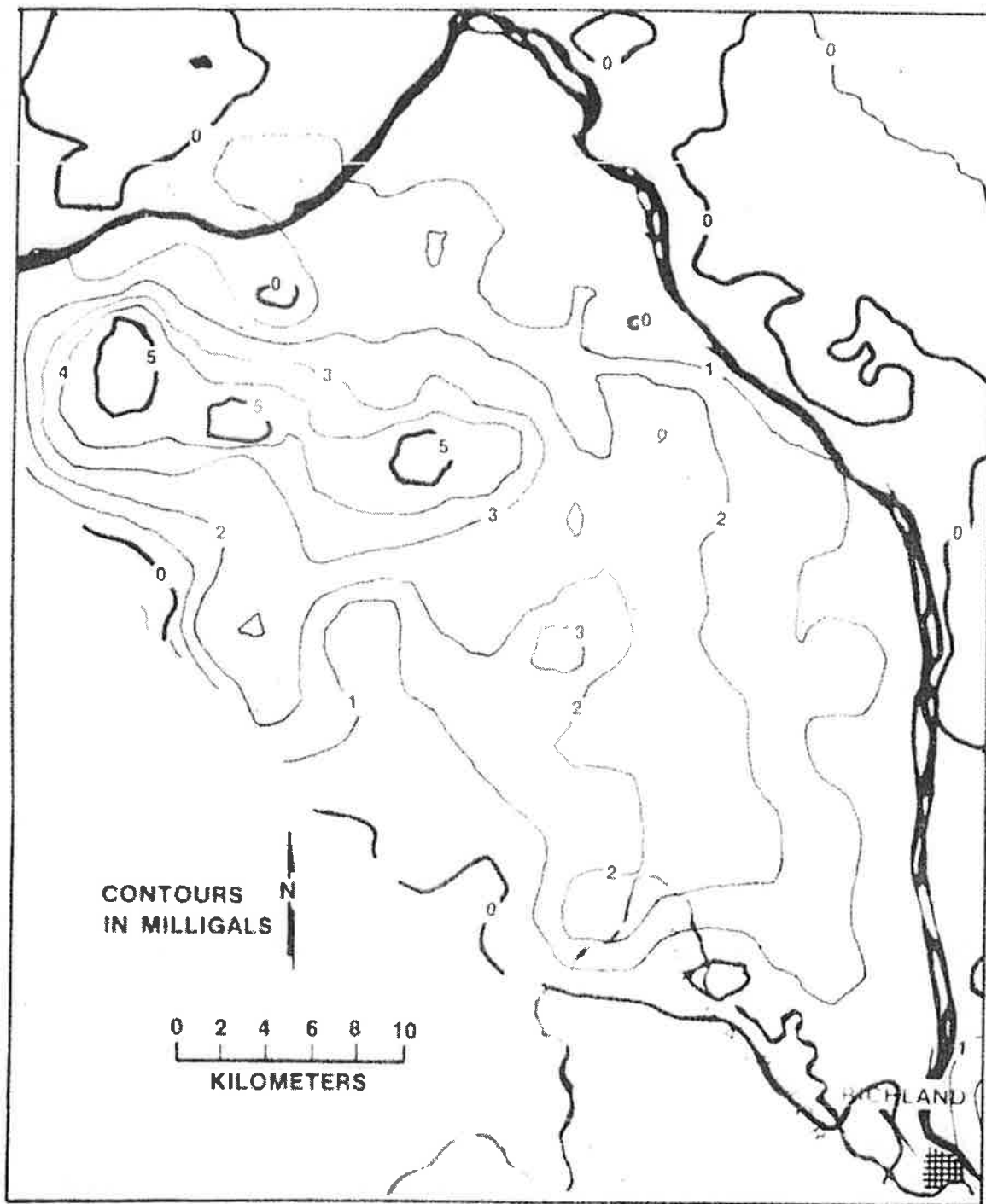


FIGURE 10

166-POINT CORRECTION FOR UNSATURATED MATERIALS
ABOVE THE WATER TABLE

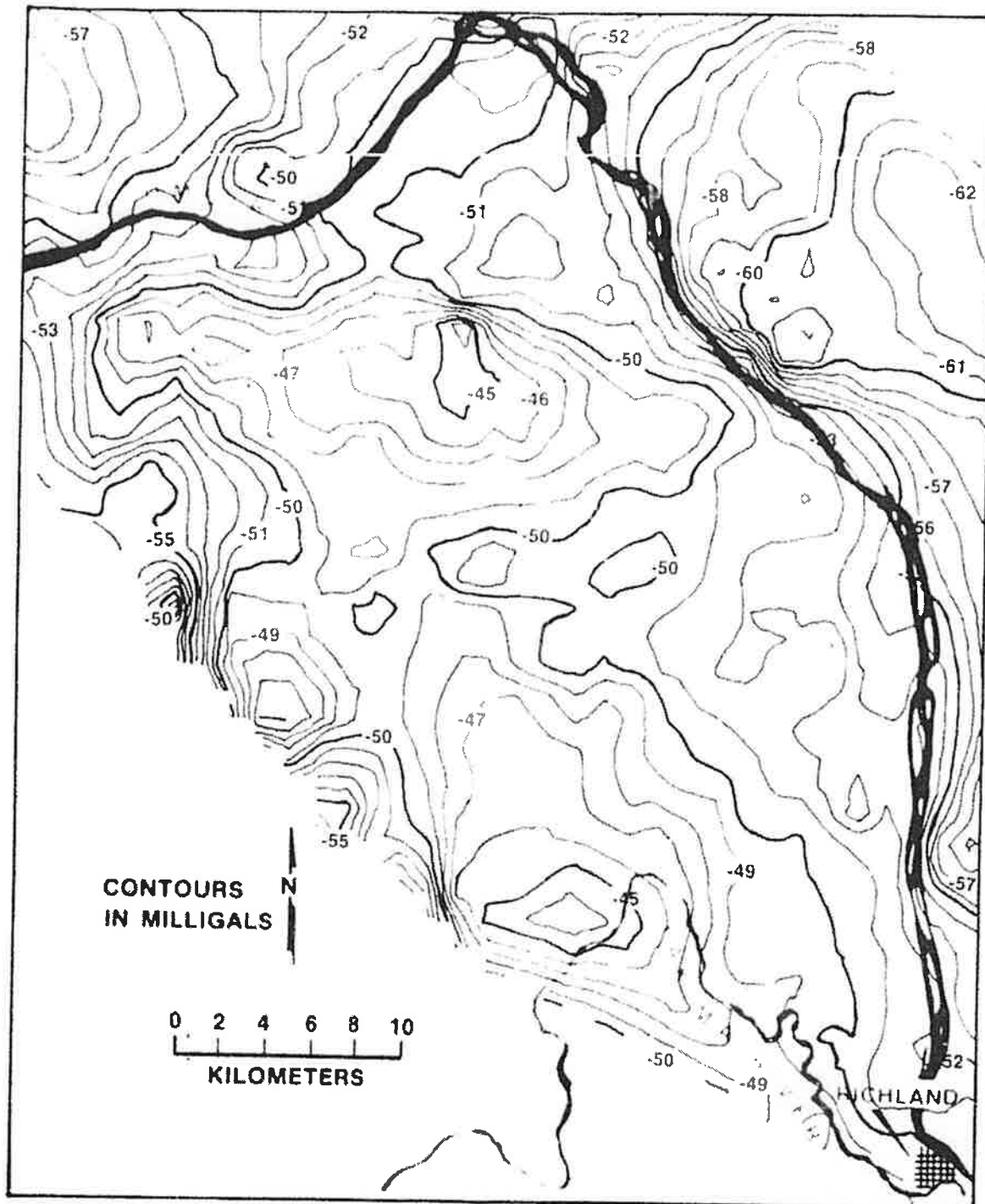


FIGURE 11

499-POINT WATER TABLE AND TERRAIN-CORRECTED
BOUGUER GRAVITY MAP

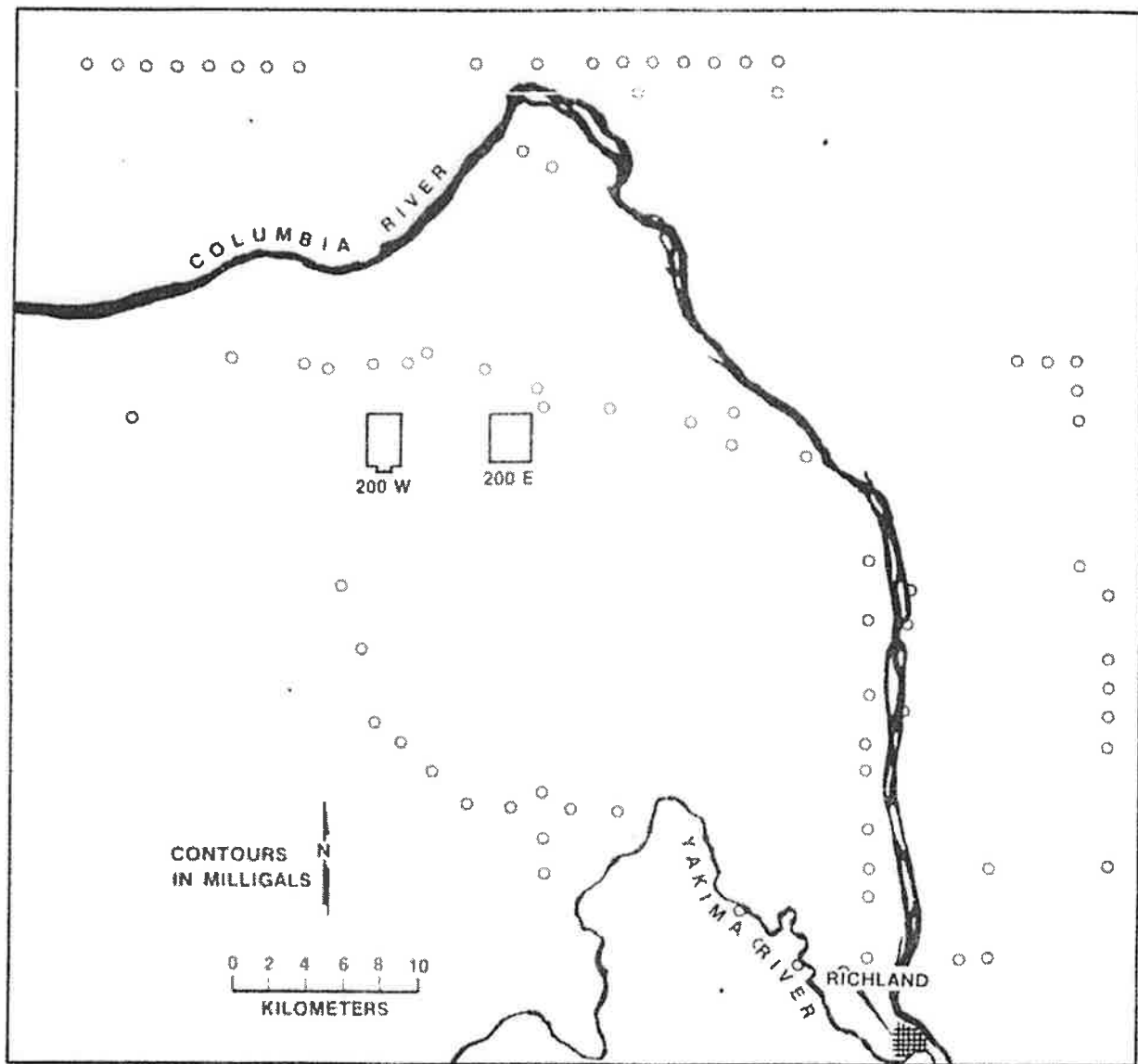


FIGURE 12

LOCATION OF THE DATA USED TO CONSTRUCT THE REGIONAL GRAVITY SURFACE FOR THE 499-POINT THREE-DIMENSIONAL MODEL

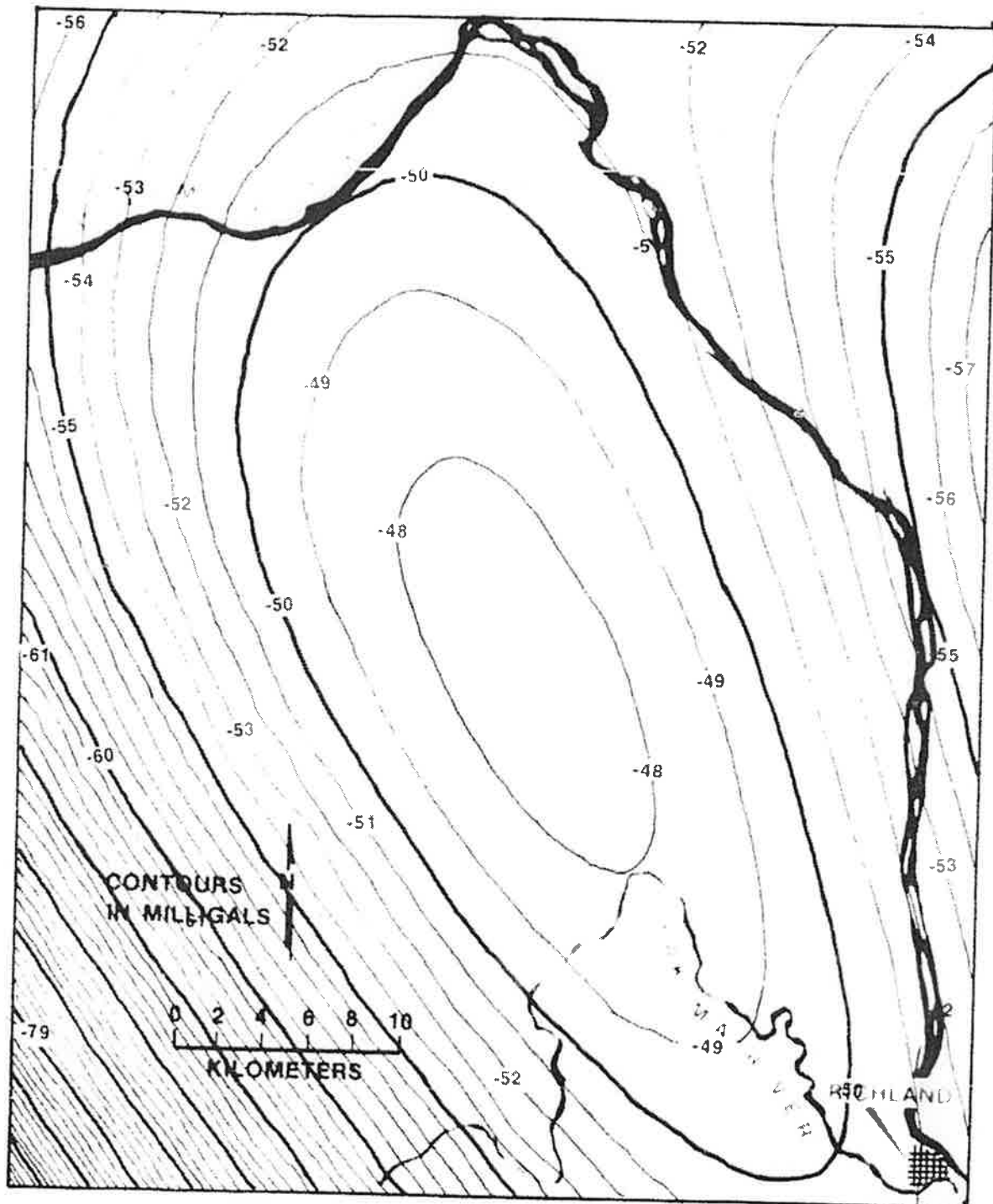


FIGURE 13

REGIONAL GRAVITY SURFACE USED IN THE 499-POINT STUDY

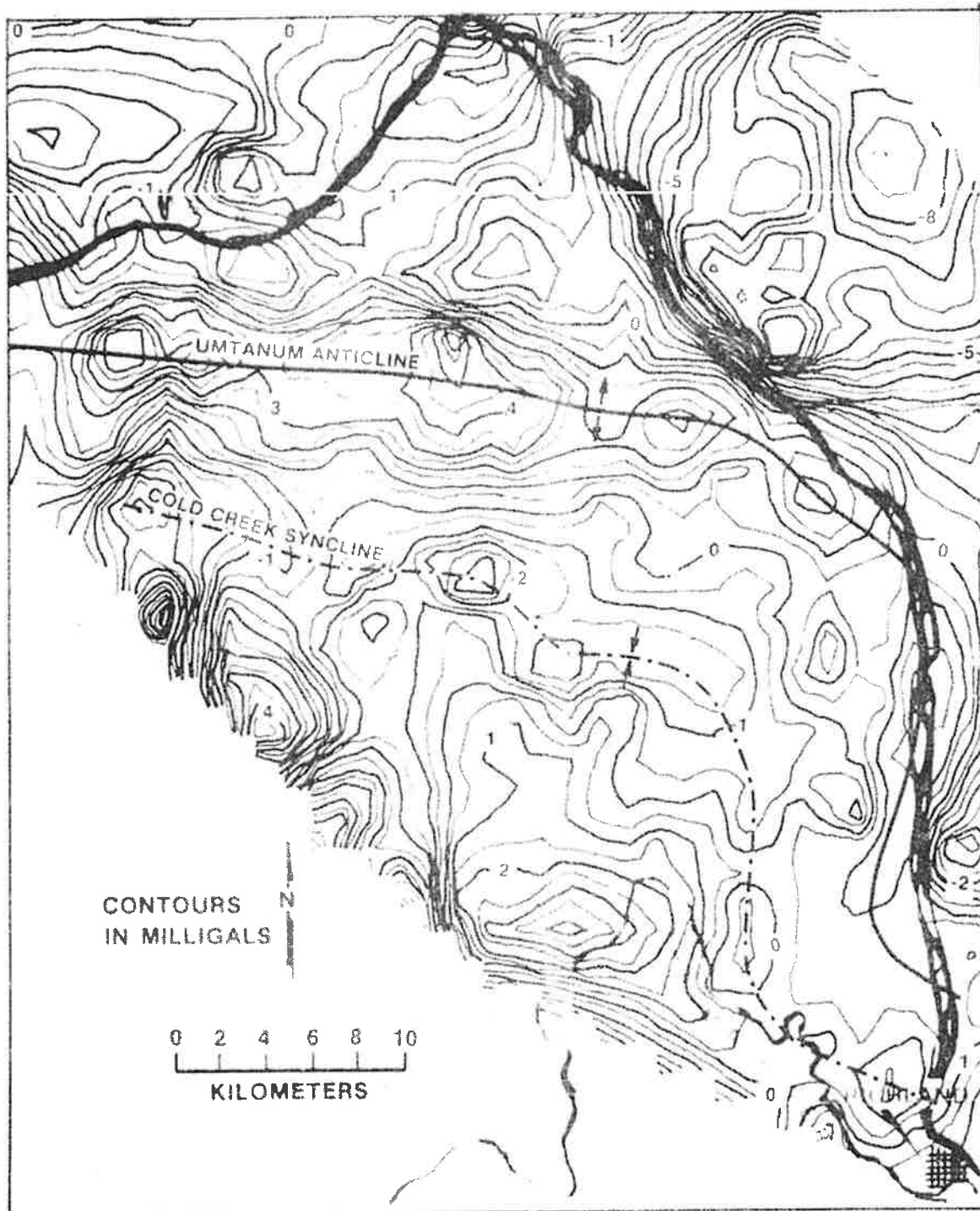


FIGURE 14

499-POINT GRAVITY-BEDROCK MAP CONSTRUCTED BY
SUBTRACTING FIGURE 13 FROM FIGURE 11

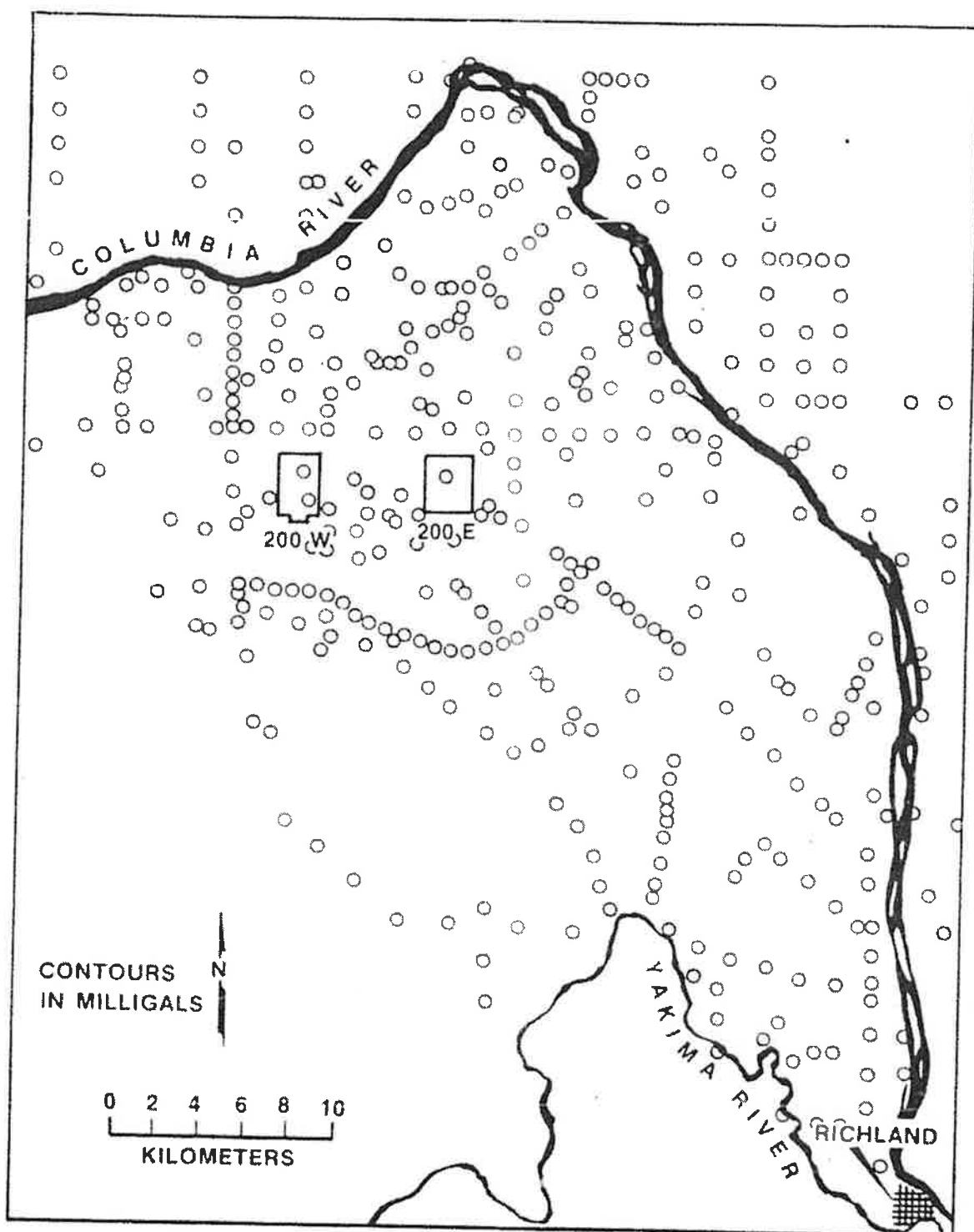


FIGURE 15

GRAVITY POINT LOCATIONS IN THE 499-POINT STUDY
WITHIN THE AREA SHOWN IN FIGURE 14

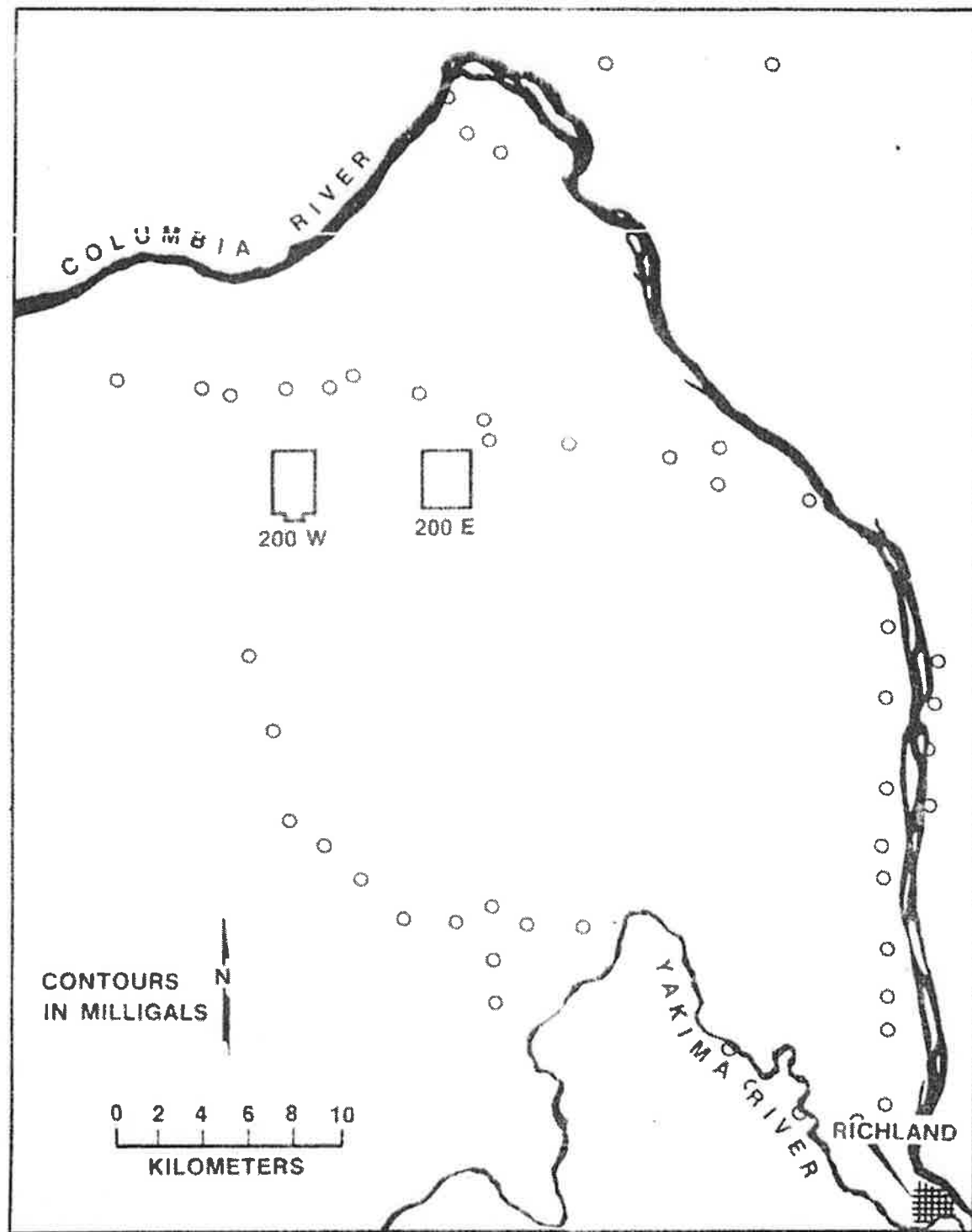


FIGURE 16

GRAVITY STATIONS USED TO CALCULATE THE REGIONAL GRAVITY SURFACE FOR THE 499-POINT STUDY THAT ARE WITHIN THE AREA SHOWN IN FIGURE 13

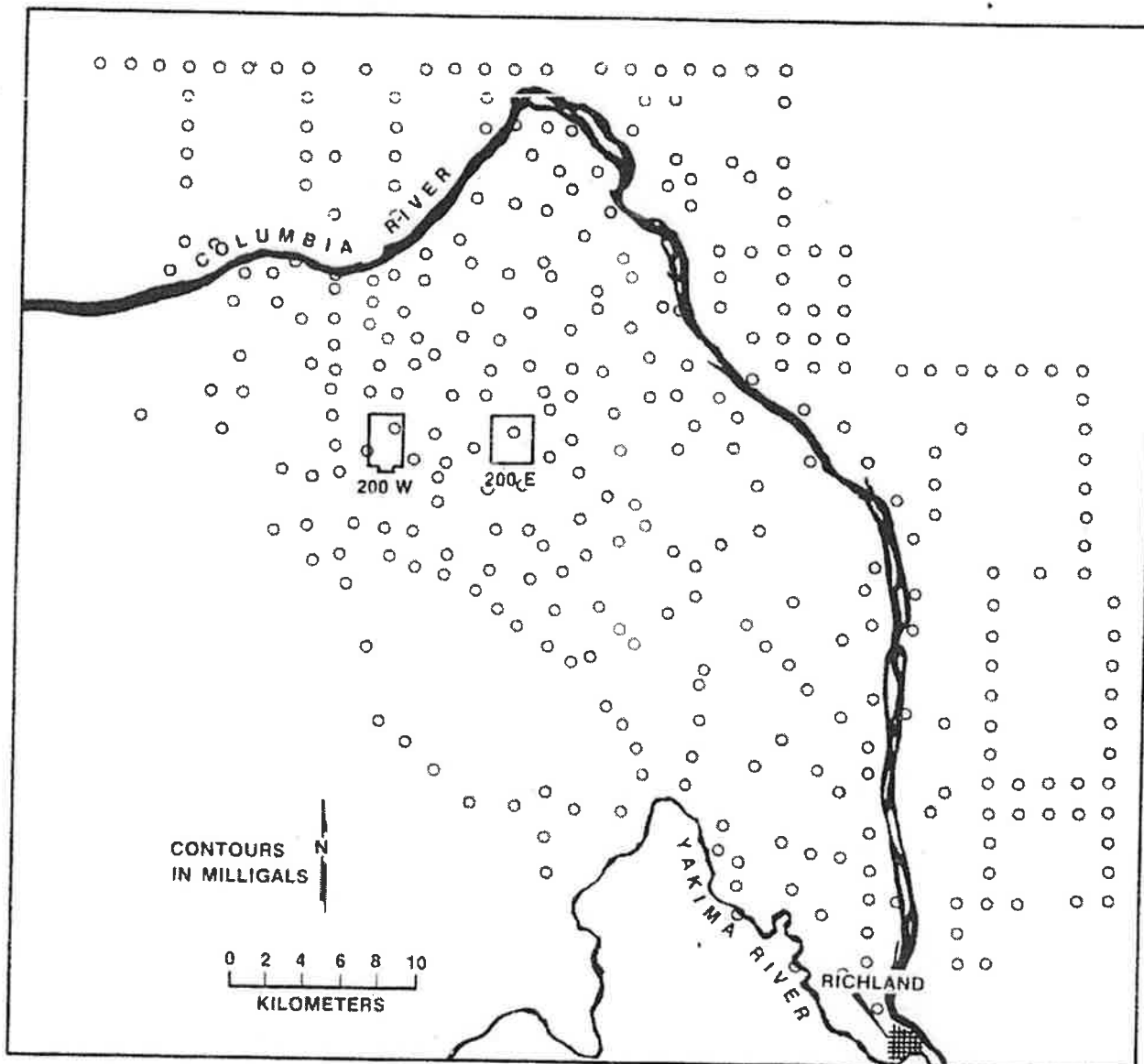


FIGURE 17

LOCATION OF BOUGUER GRAVITY STATIONS USED FOR
THE 344-POINT THREE-DIMENSIONAL MODEL

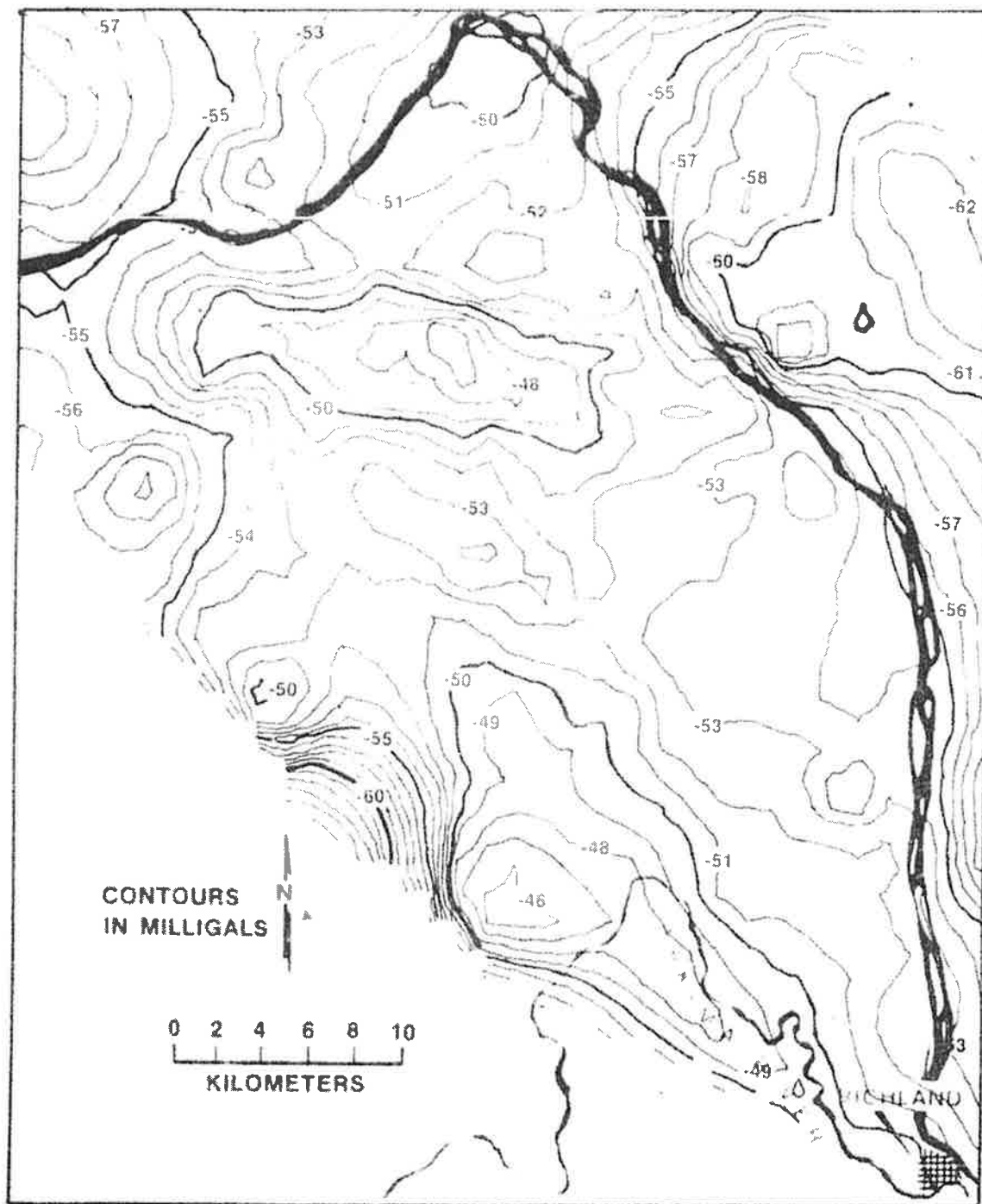


FIGURE 18

344-POINT BOUGUER GRAVITY MAP OF THE HANFORD RESERVATION

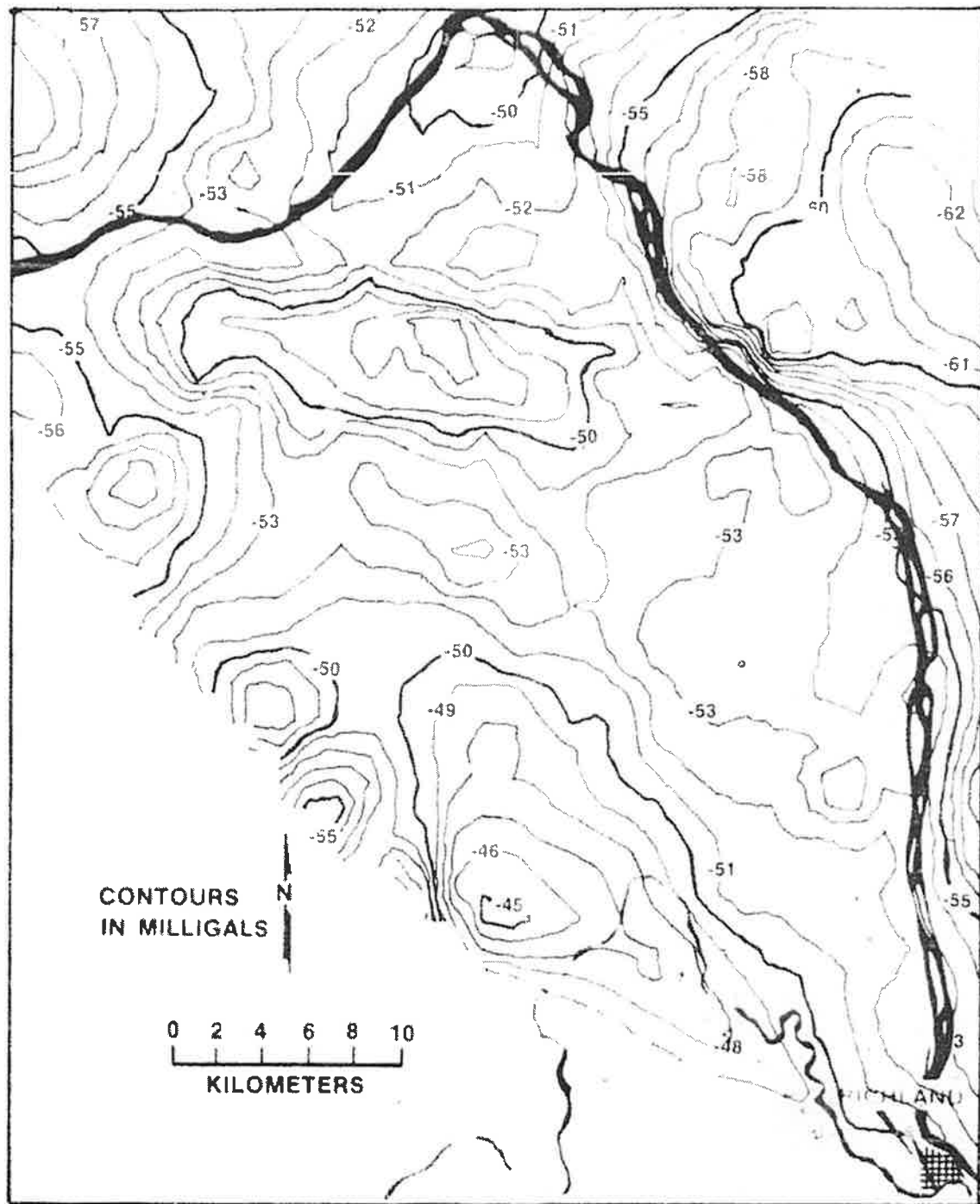


FIGURE 19

344-POINT TERRAIN-CORRECTED BOUGUER GRAVITY MAP
OF THE HANFORD RESERVATION

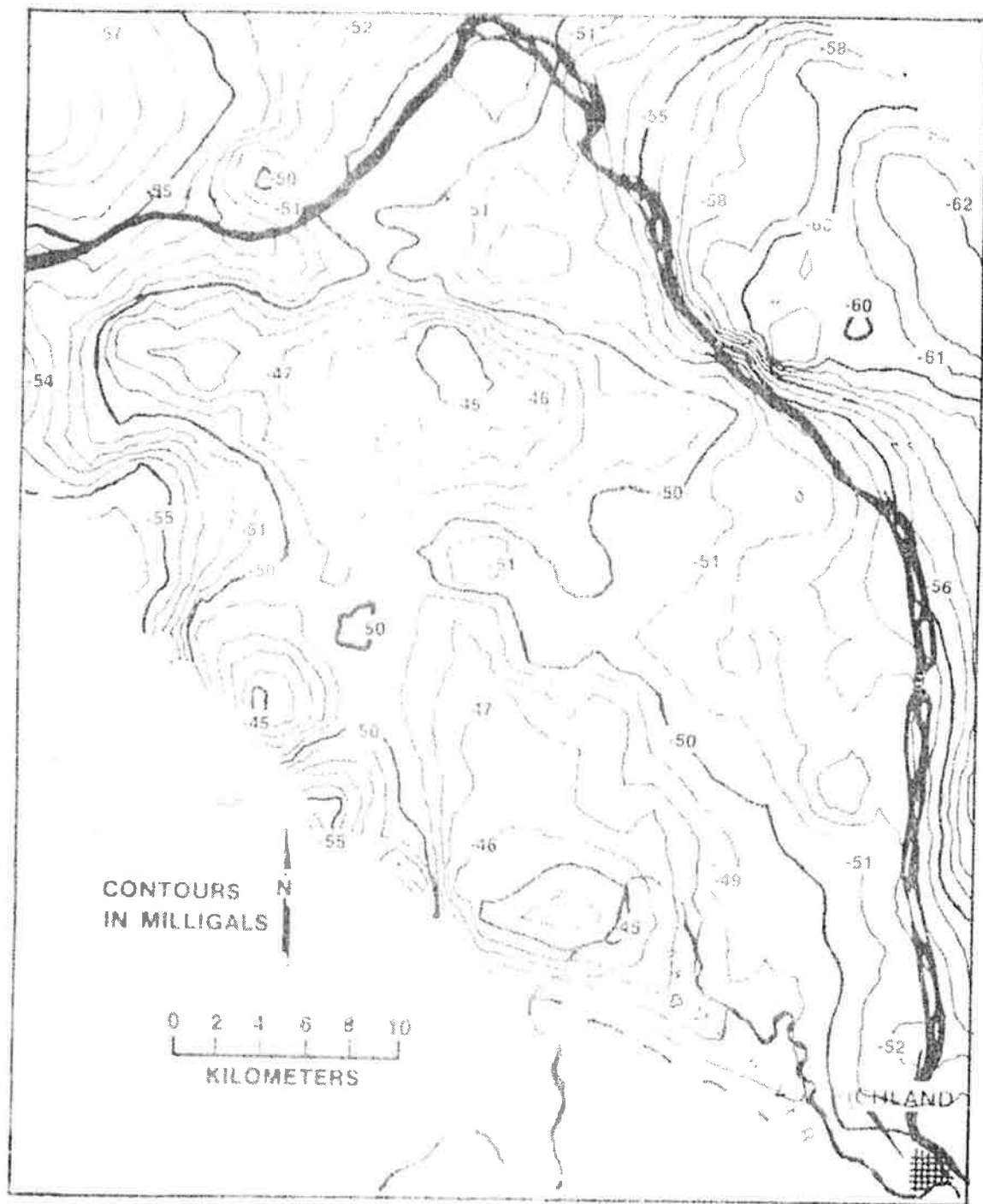


FIGURE 20

344-POINT WATER TABLE AND TERRAIN-CORRECTED BOUGUER
GRAVITY MAP OF THE HANFORD RESERVATION

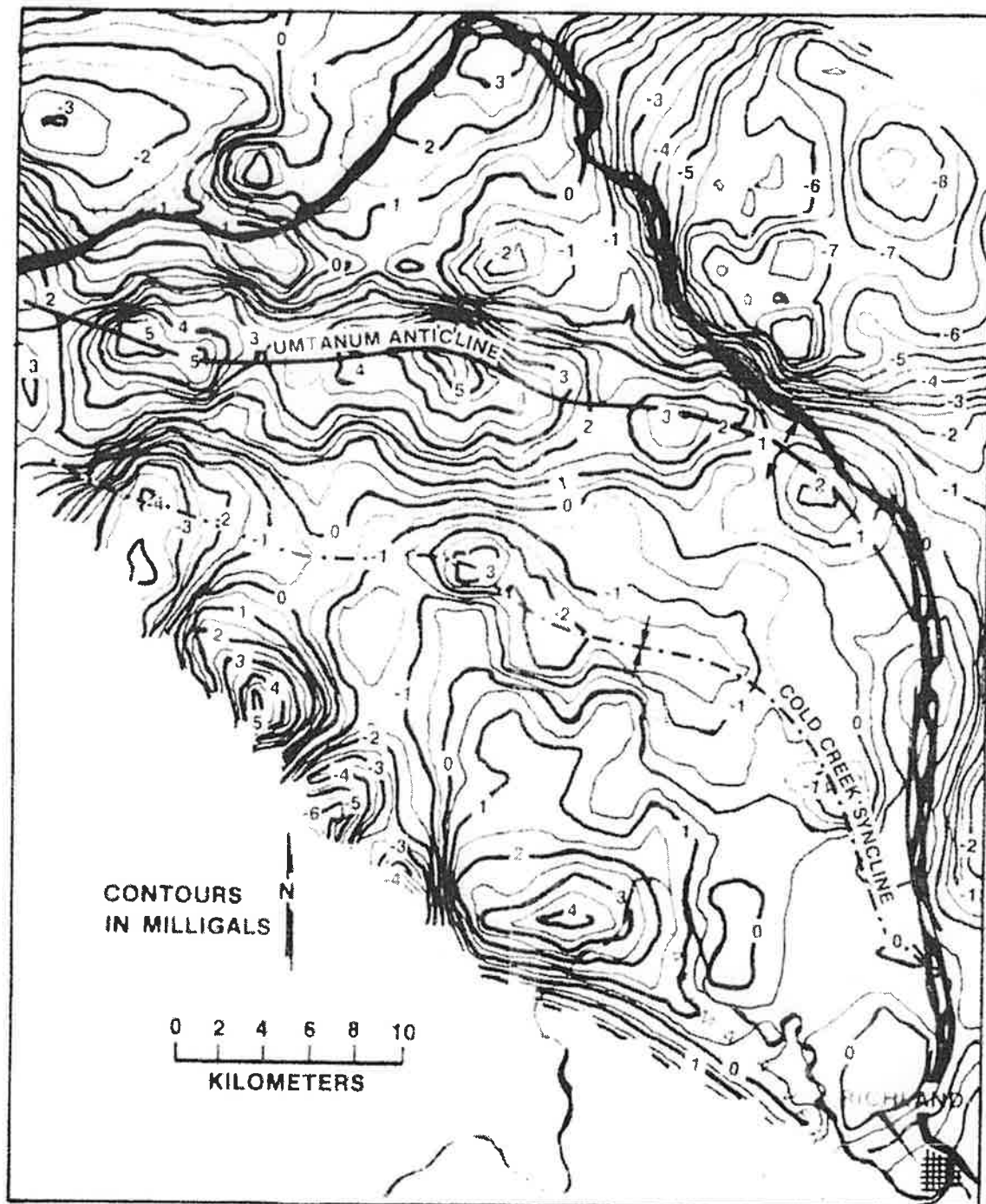


FIGURE 21

344-POINT GRAVITY-BEDROCK MAP CONSTRUCTED BY
SUBTRACTING FIGURE 13 FROM FIGURE 20

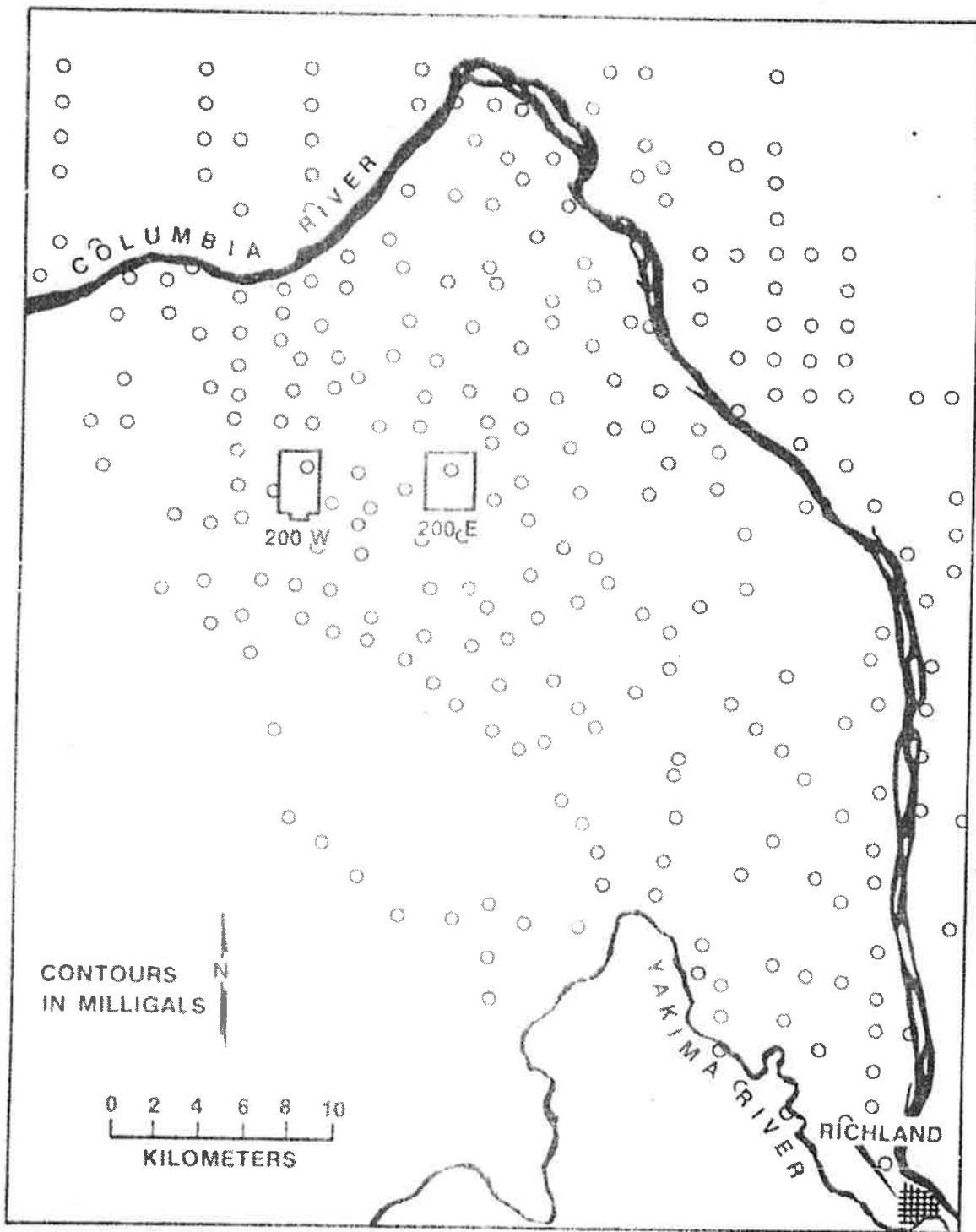


FIGURE 22

GRAVITY POINT LOCATIONS IN THE 344-POINT STUDY
WITHIN THE AREA SHOWN IN FIGURE 20

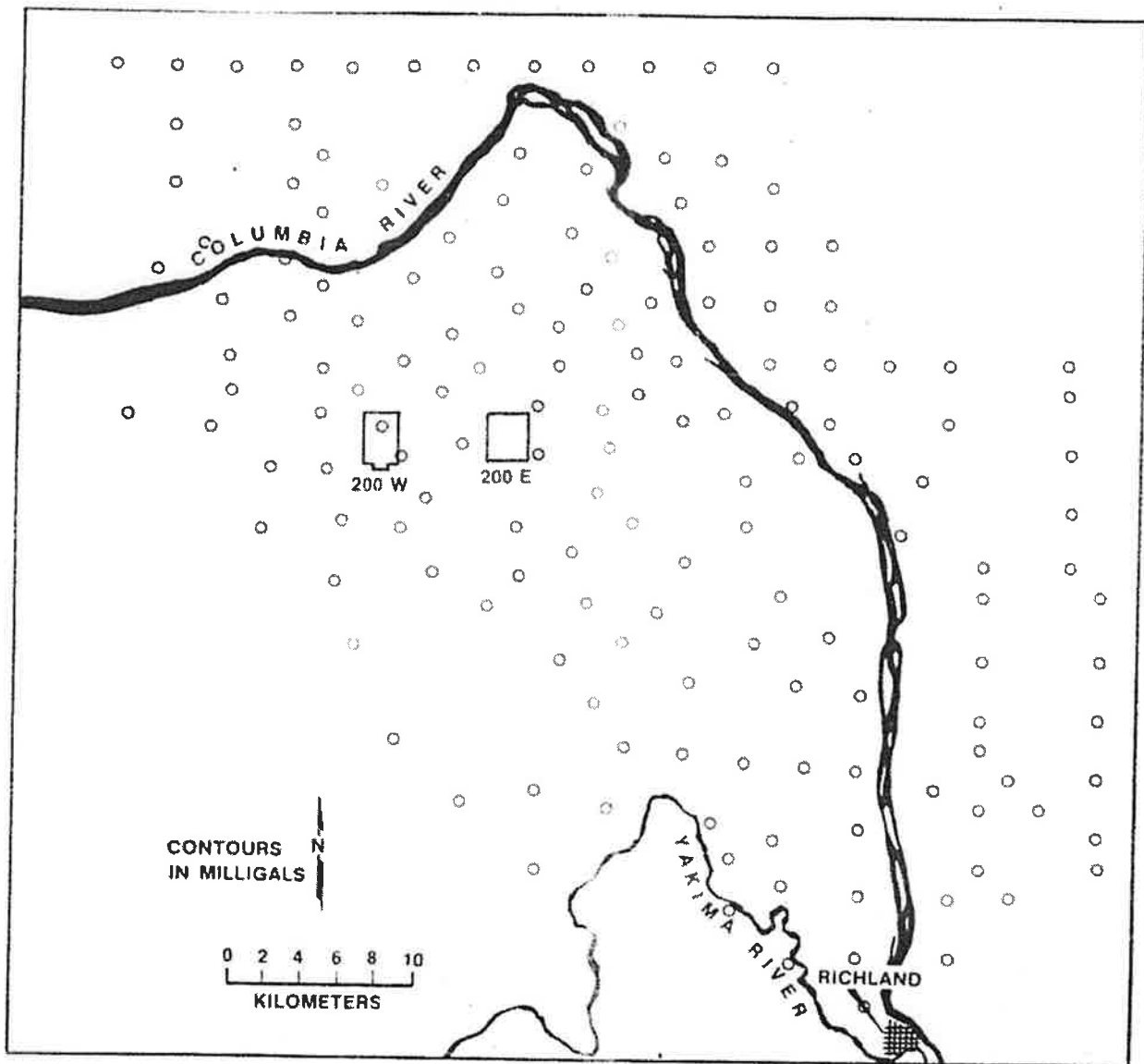


FIGURE 23

LOCATION OF BOUGUER GRAVITY STATIONS USED FOR
THE 166-POINT THREE-DIMENSIONAL MODEL

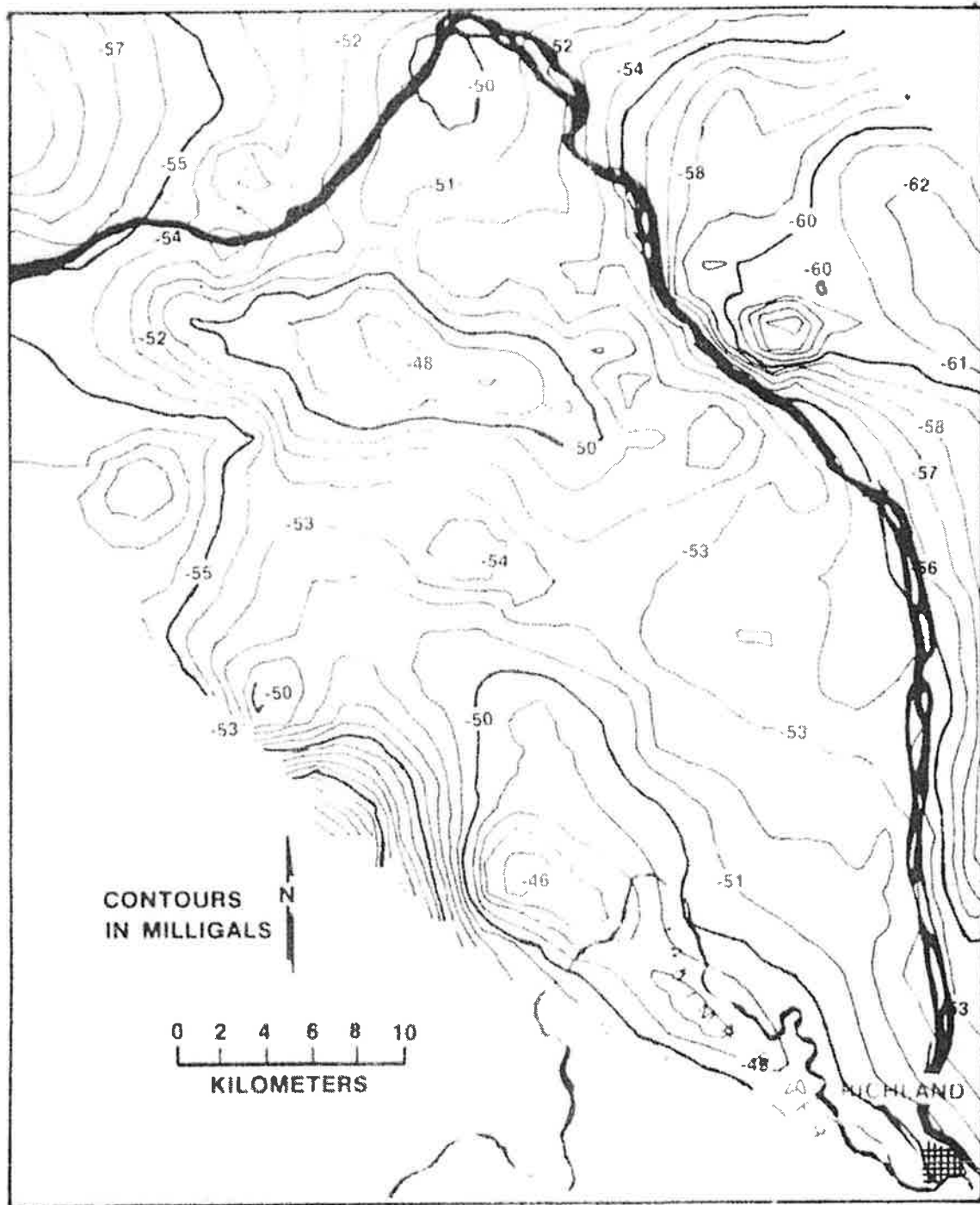


FIGURE 24

166-POINT BOUGUER GRAVITY MAP OF THE HANFORD RESERVATION

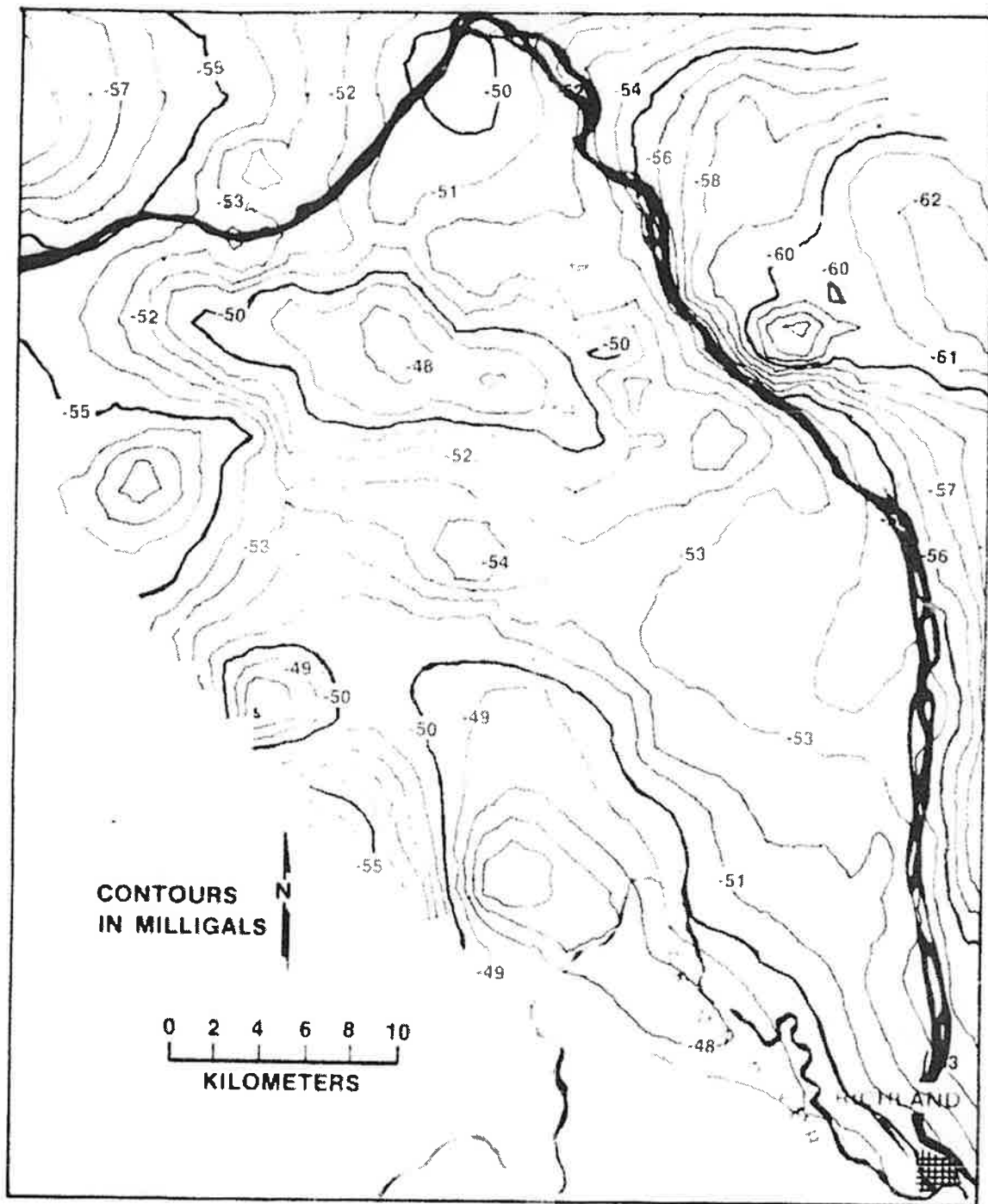


FIGURE 25

166-POINT TERRAIN-CORRECTED BOUGUER GRAVITY MAP
OF THE HANFORD RESERVATION

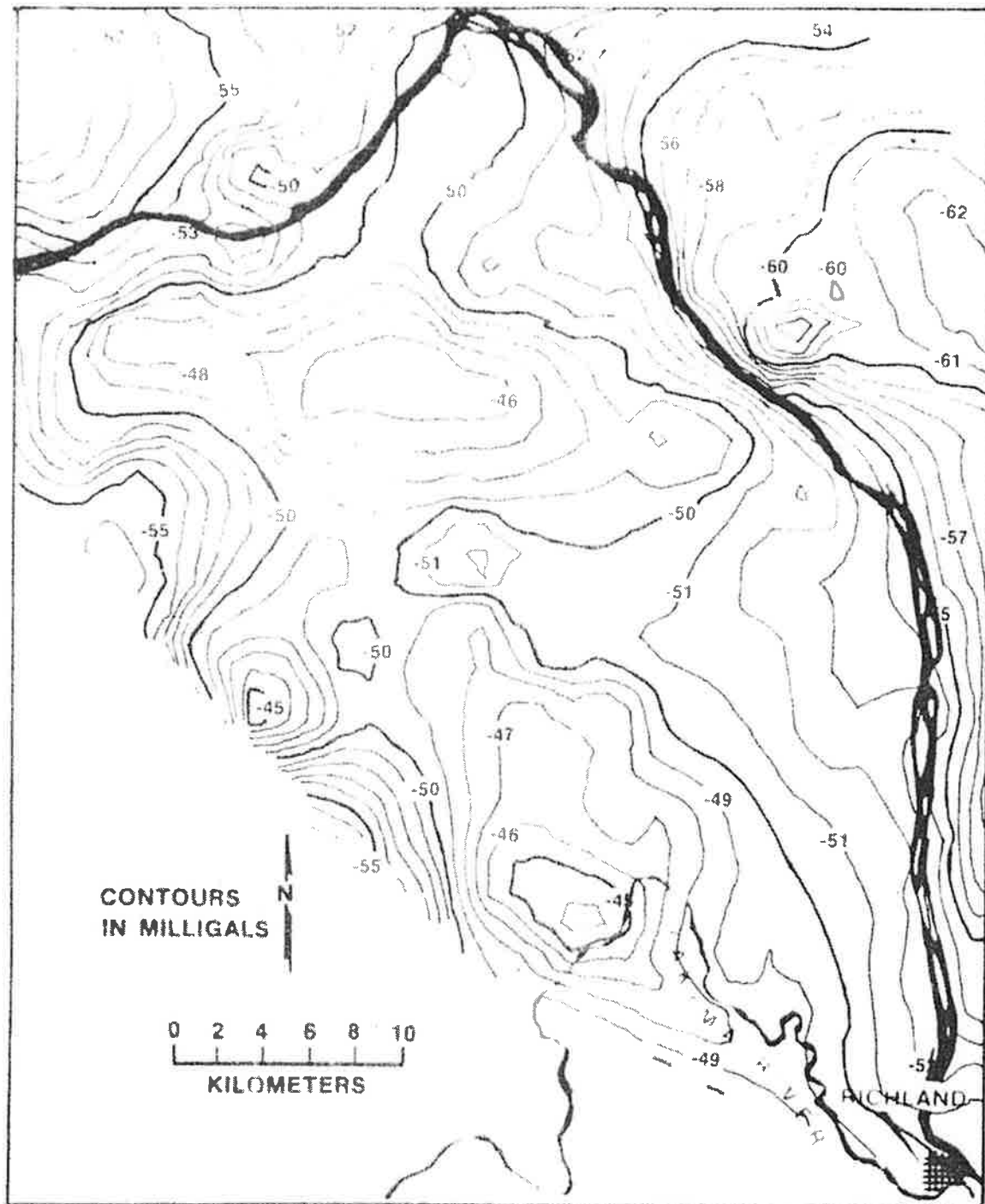


FIGURE 26

166-POINT WATER TABLE AND TERRAIN-CORRECTED BOUGUER GRAVITY MAP OF THE HANFORD RESERVATION

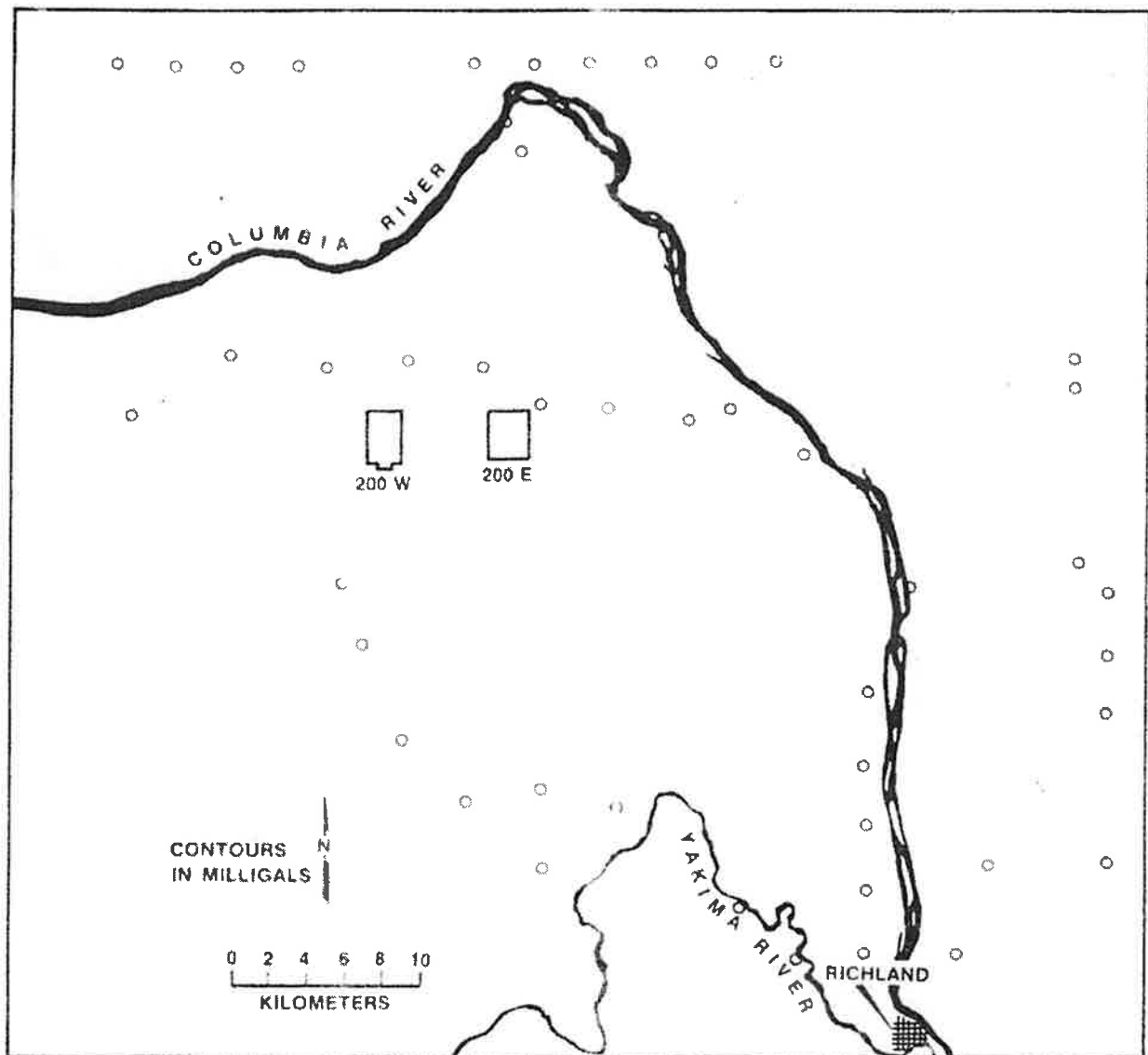


FIGURE 27

LOCATION OF THE DATA USED TO CONSTRUCT THE REGIONAL GRAVITY SURFACE FOR THE 166-POINT THREE-DIMENSIONAL MODEL

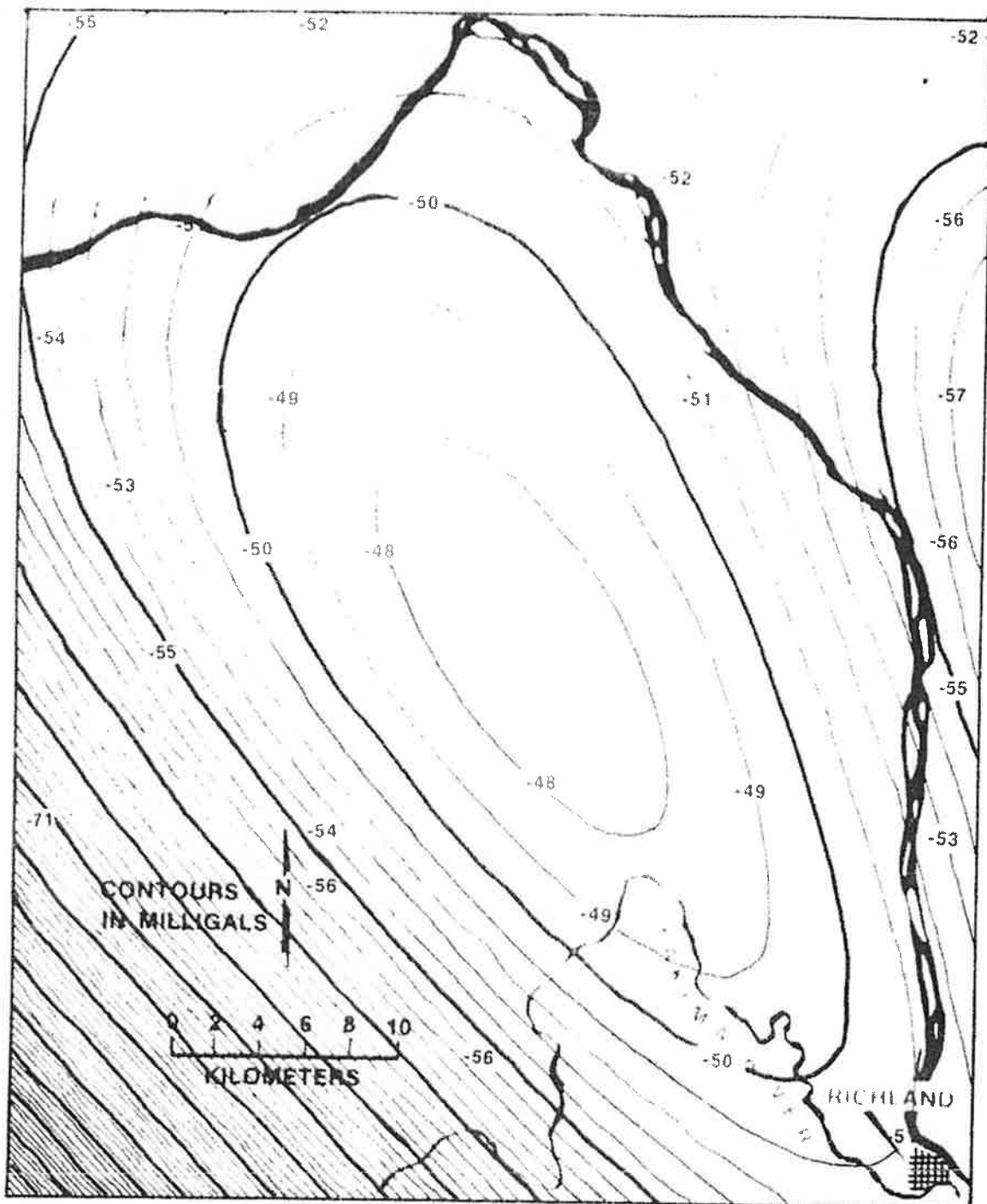


FIGURE 28

REGIONAL GRAVITY SURFACE USED IN THE 166-POINT STUDY

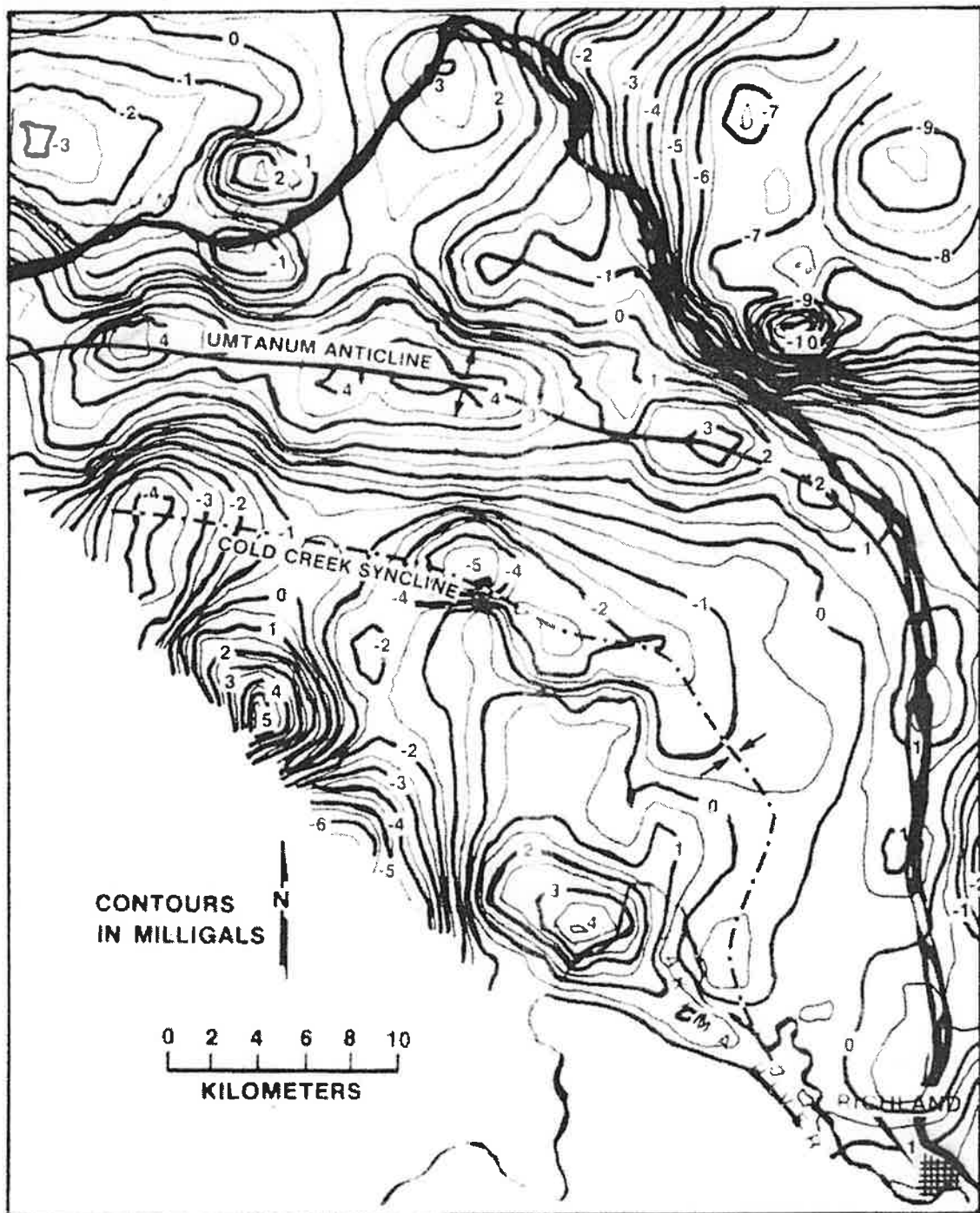


FIGURE 29

166-POINT GRAVITY-BEDROCK MAP CONSTRUCTED BY
SUBTRACTING FIGURE 28 FROM FIGURE 26

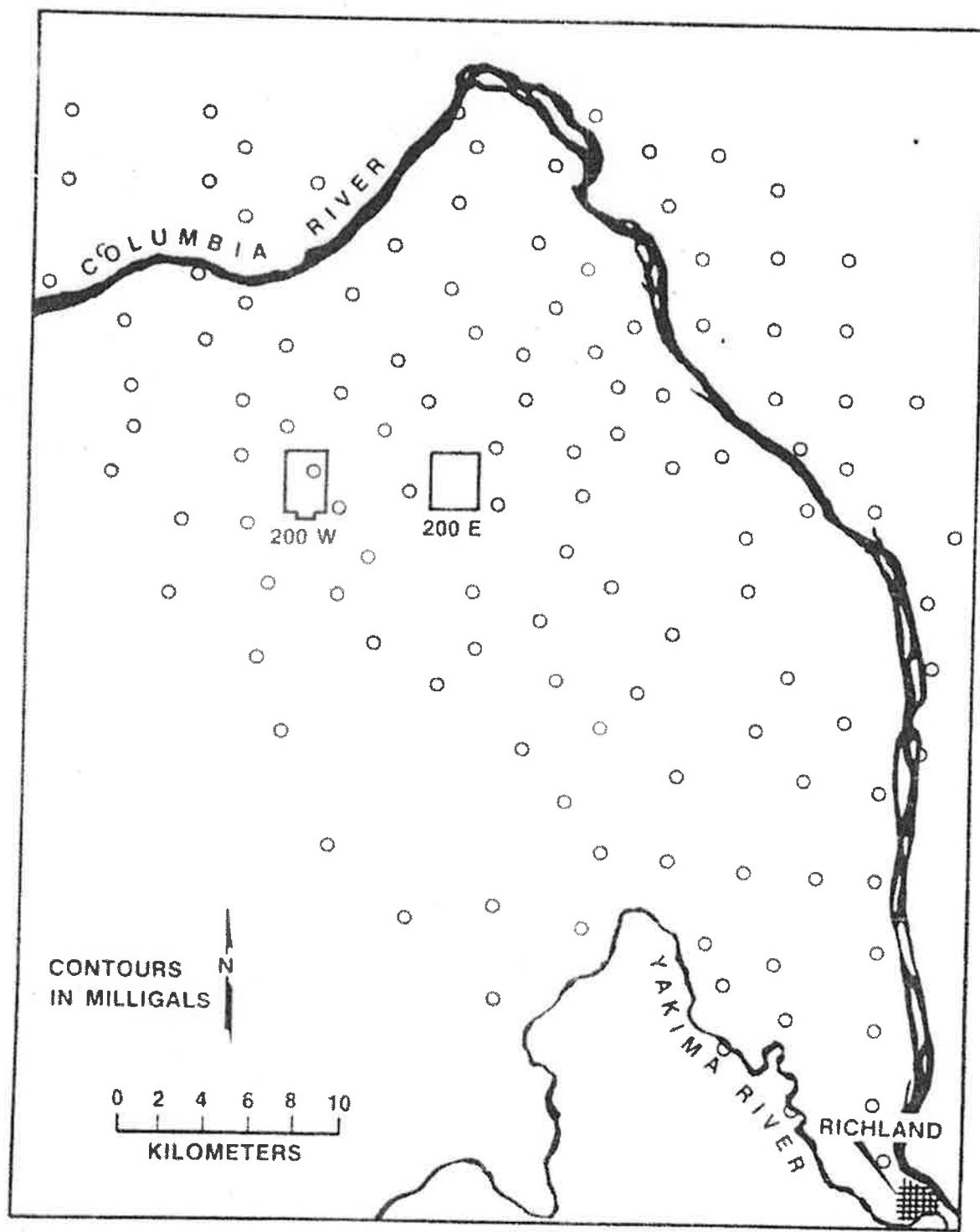


FIGURE 30

GRAVITY STATION LOCATIONS USED IN THE 166-POINT STUDY
THAT ARE WITHIN THE AREA SHOWN IN FIGURE 29

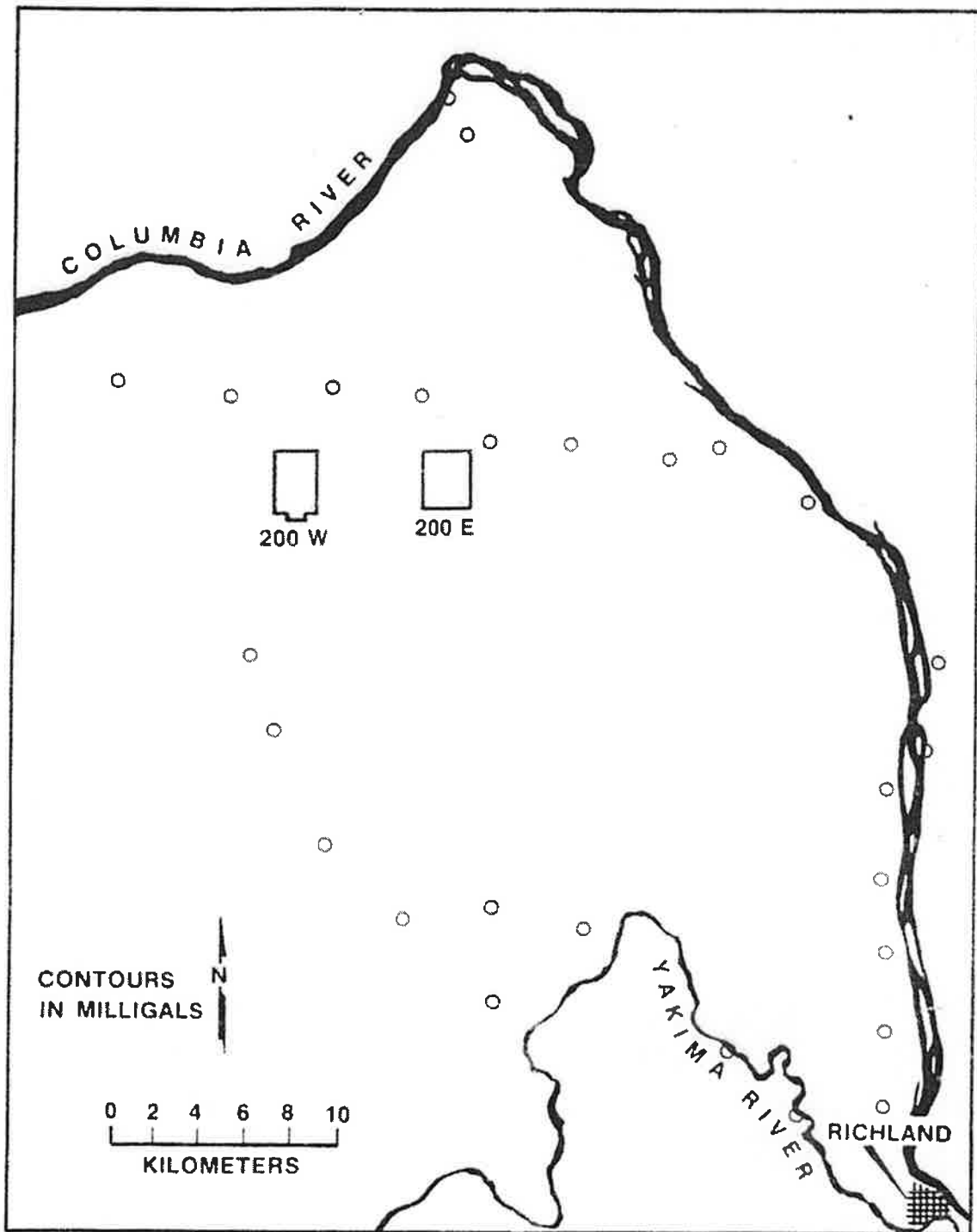


FIGURE 31

GRAVITY STATIONS USED TO CALCULATE THE REGIONAL GRAVITY SURFACE
FOR THE 166-POINT STUDY WITHIN THE AREA OF FIGURE 28

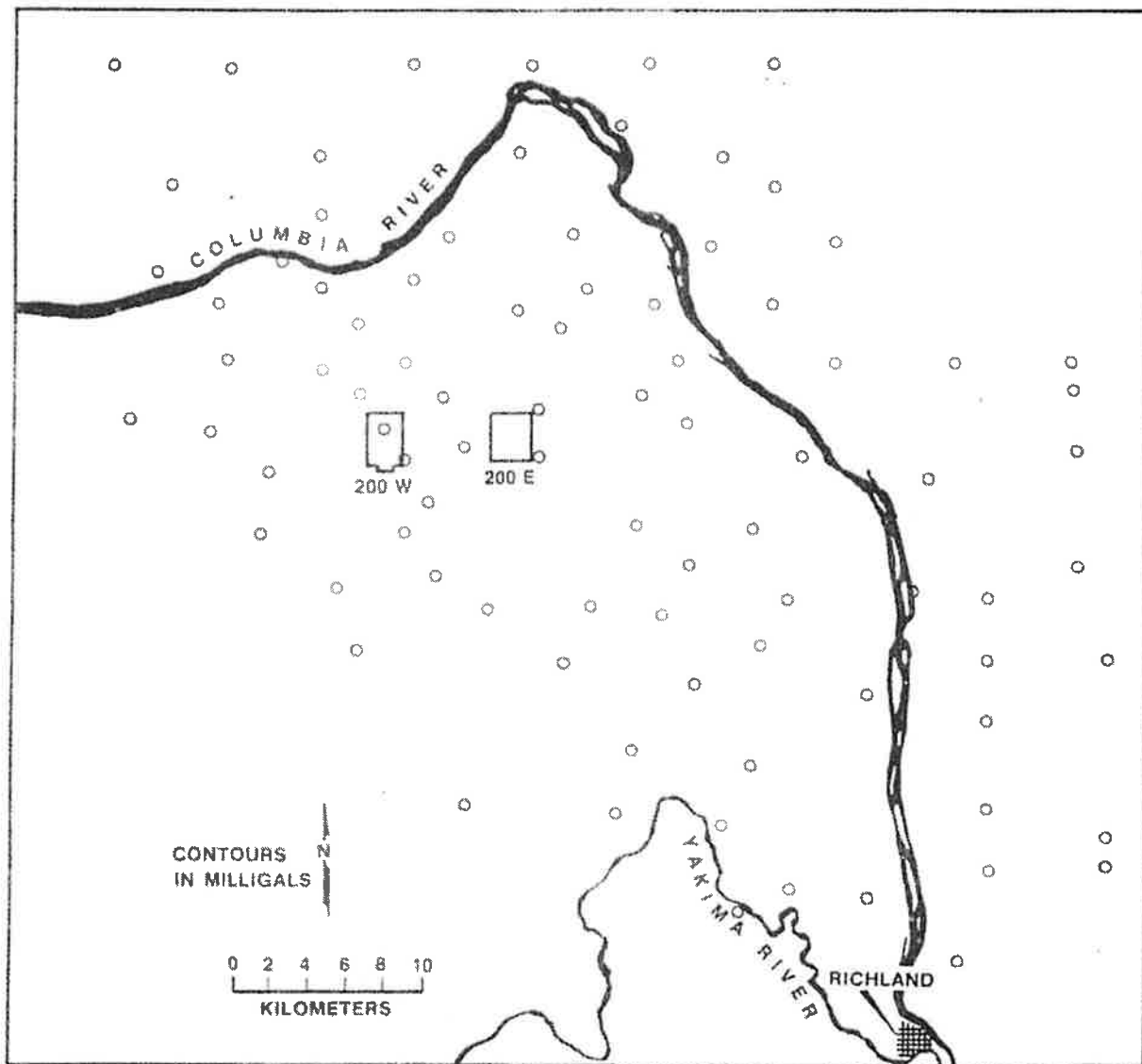


FIGURE 32

LOCATION OF BOUGUER GRAVITY STATIONS USED FOR
THE 88-POINT THREE-DIMENSIONAL MODEL

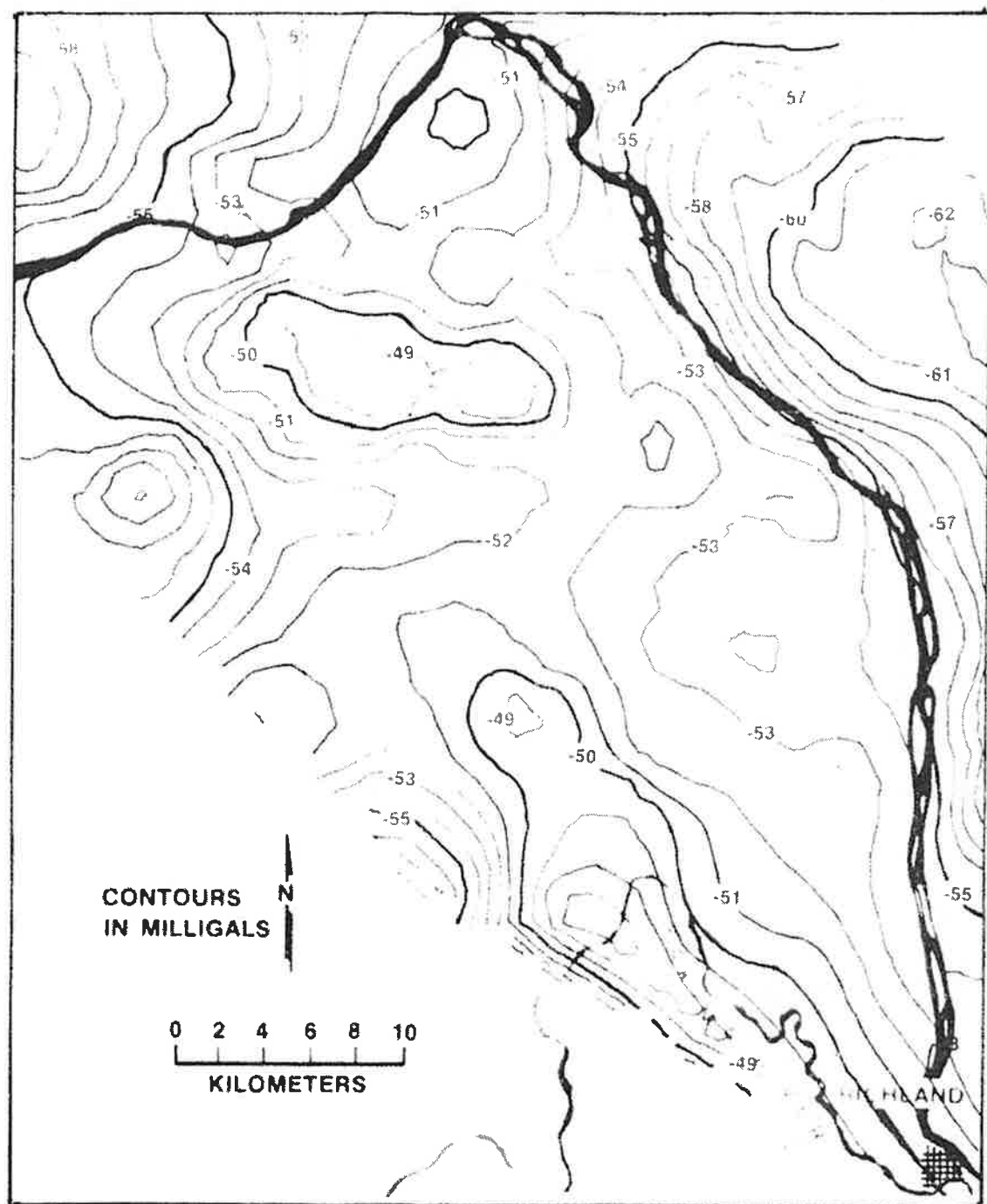


FIGURE 33

88-POINT BOUGUER GRAVITY MAP OF THE HANFORD RESERVATION

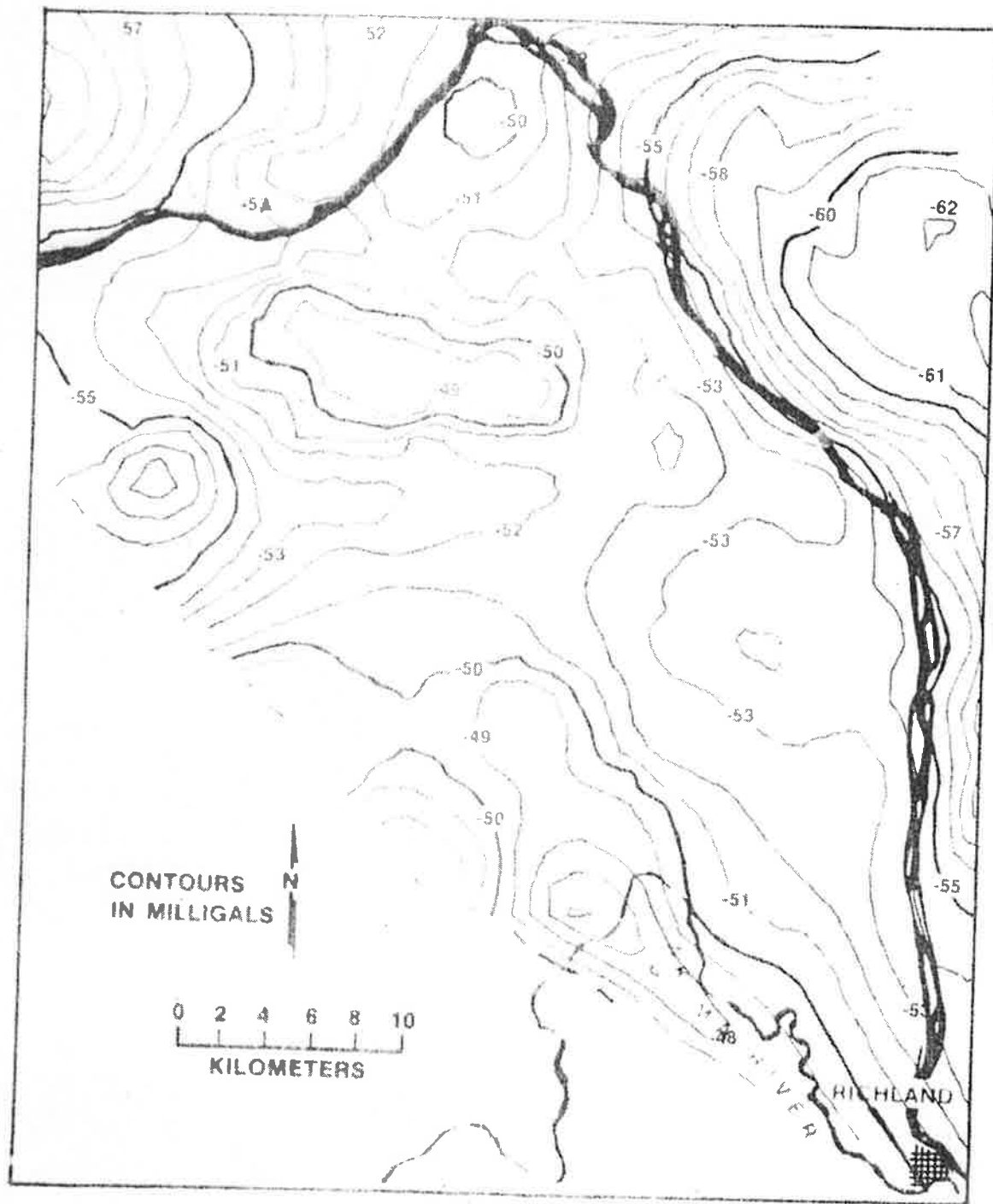


FIGURE 34

88-POINT TERRAIN-CORRECTED BOUGUER GRAVITY MAP
OF THE HANFORD RESERVATION

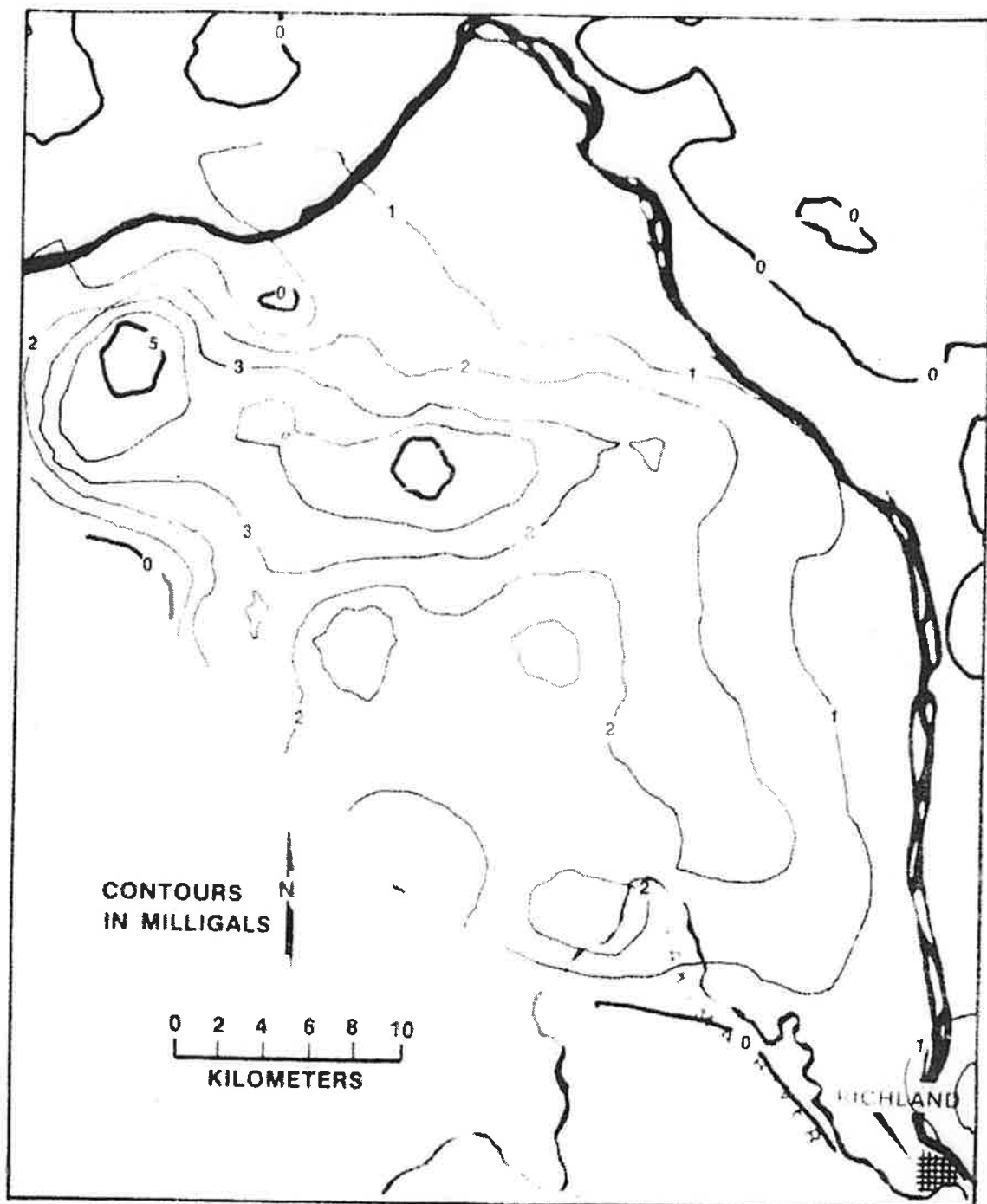


FIGURE 35

88-POINT CORRECTION FOR UNSATURATED MATERIALS
ABOVE THE WATER TABLE

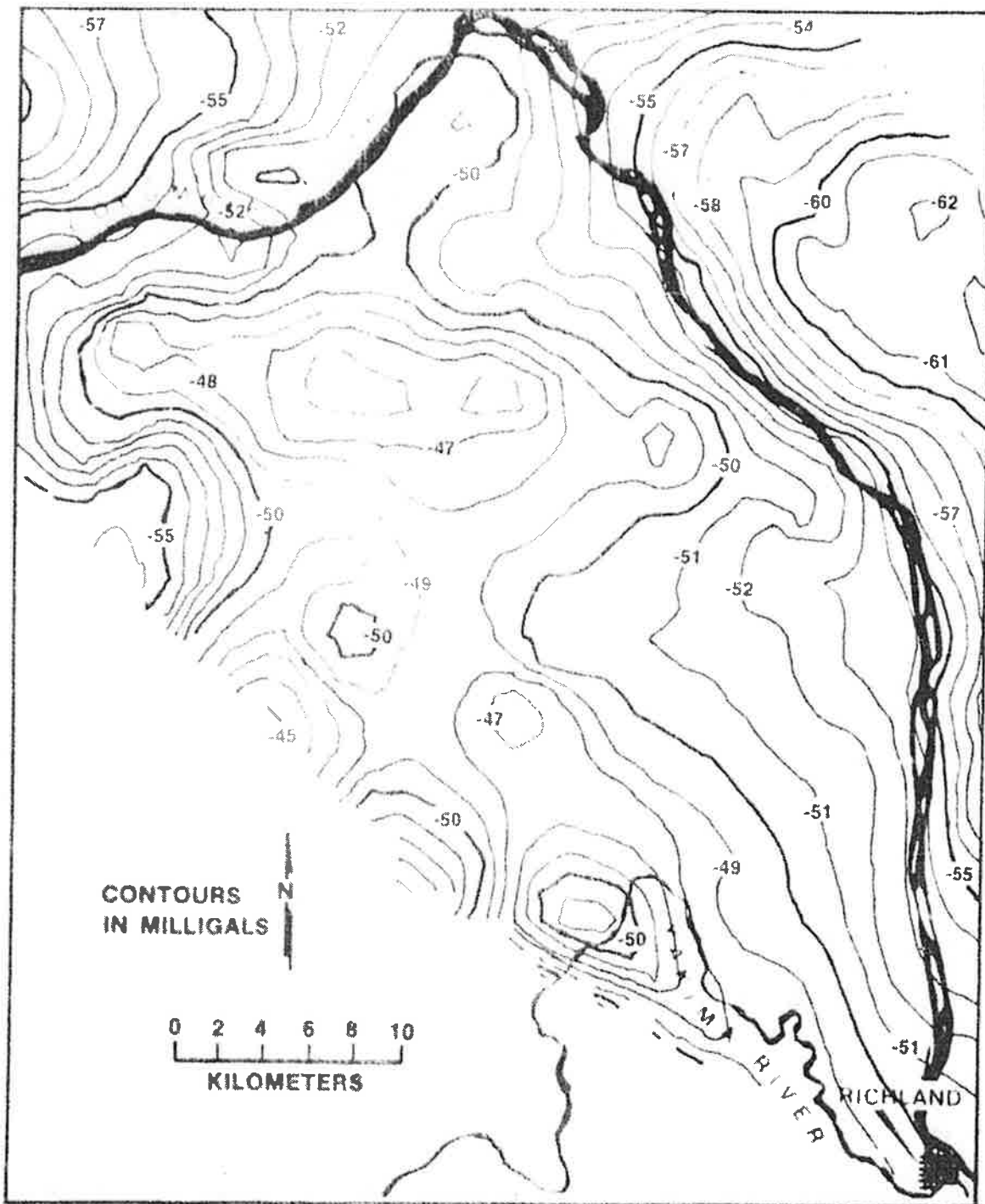


FIGURE 36

88-POINT WATER TABLE AND TERRAIN-CORRECTED BOUGUER
GRAVITY MAP OF THE HANFORD RESERVATION

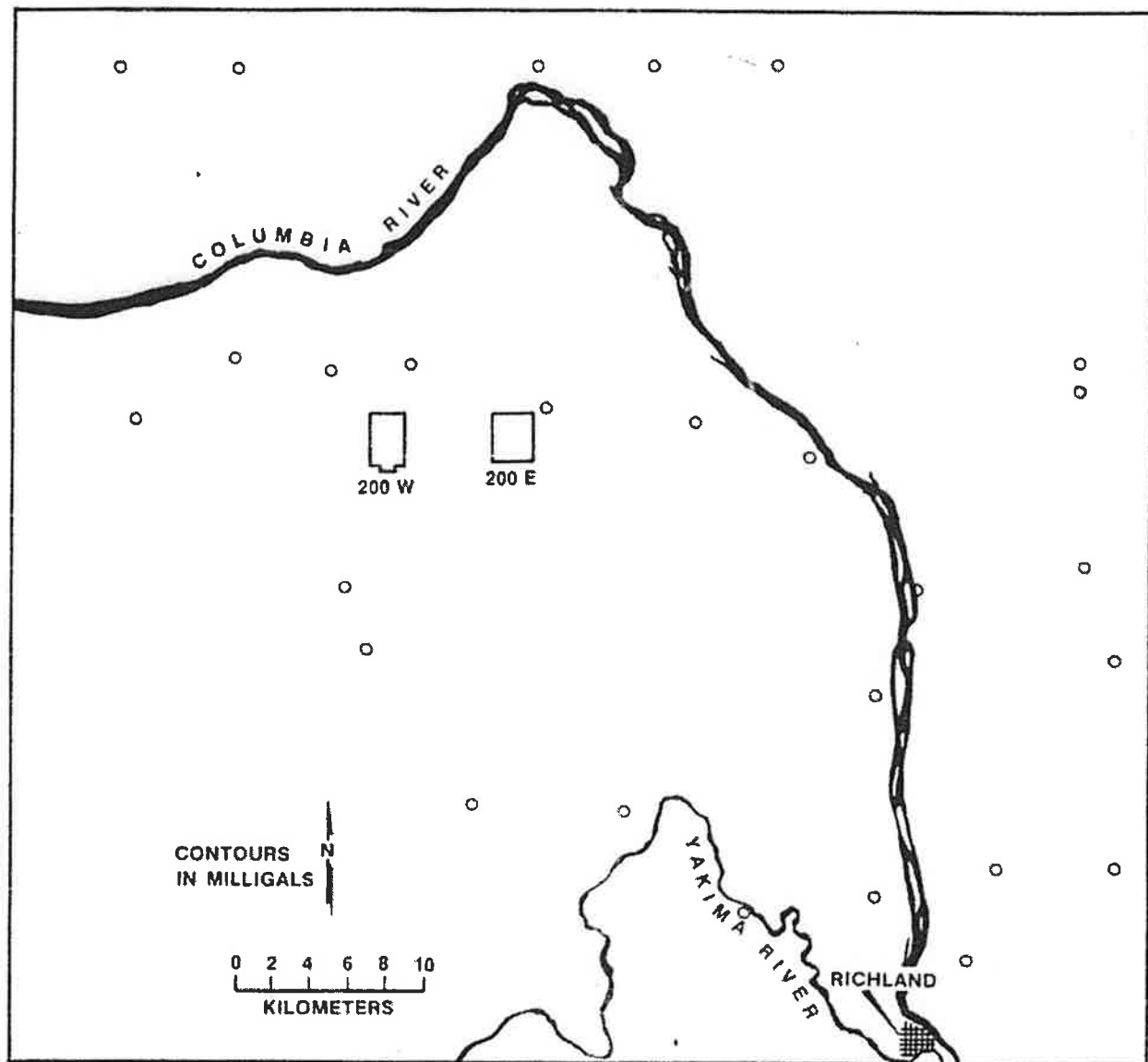


FIGURE 37

LOCATION OF THE DATA USED TO CONSTRUCT THE
REGIONAL GRAVITY SURFACE FOR THE 88-POINT STUDY

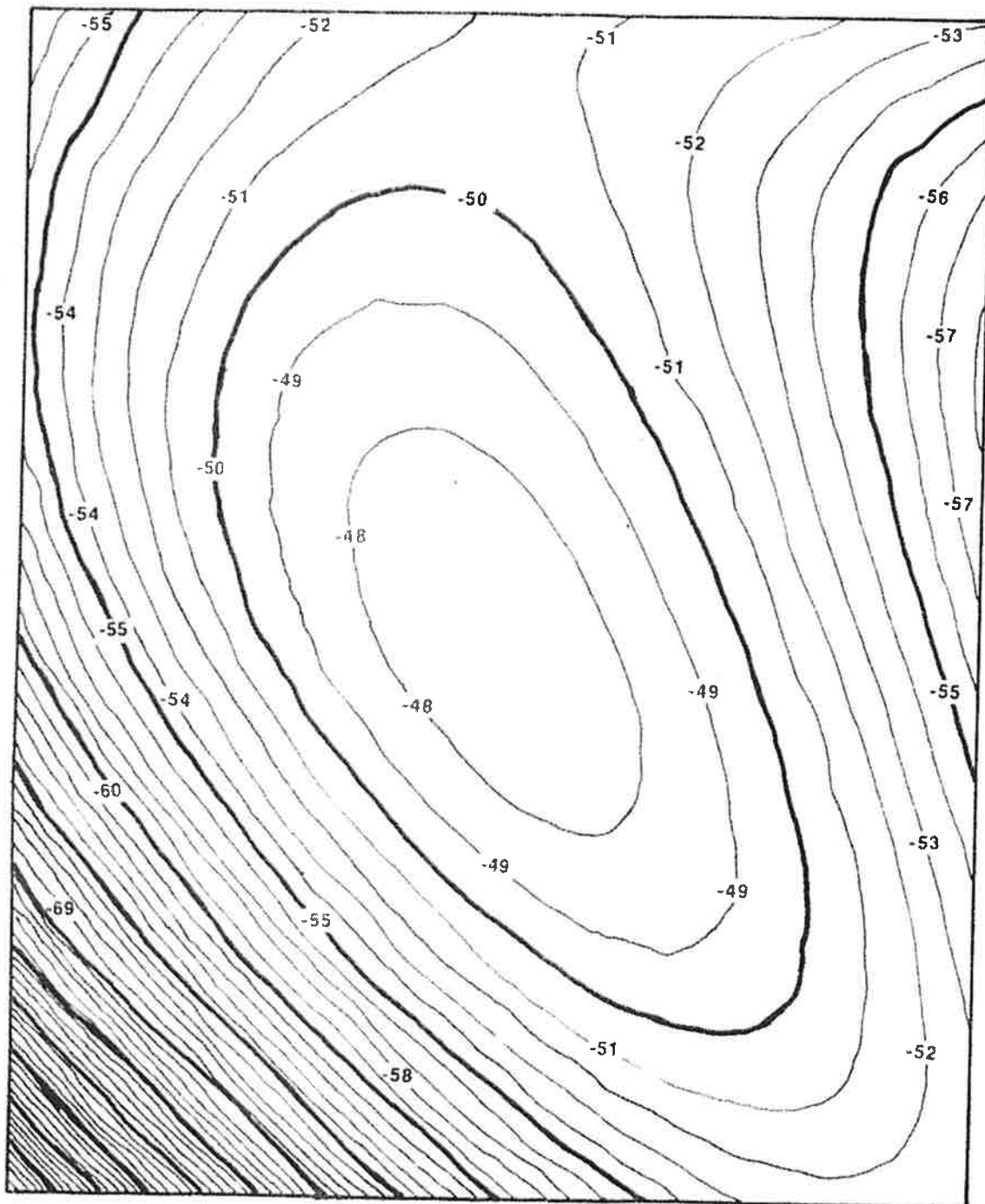


FIGURE 38

REGIONAL GRAVITY SURFACE USED IN THE 88-POINT STUDY

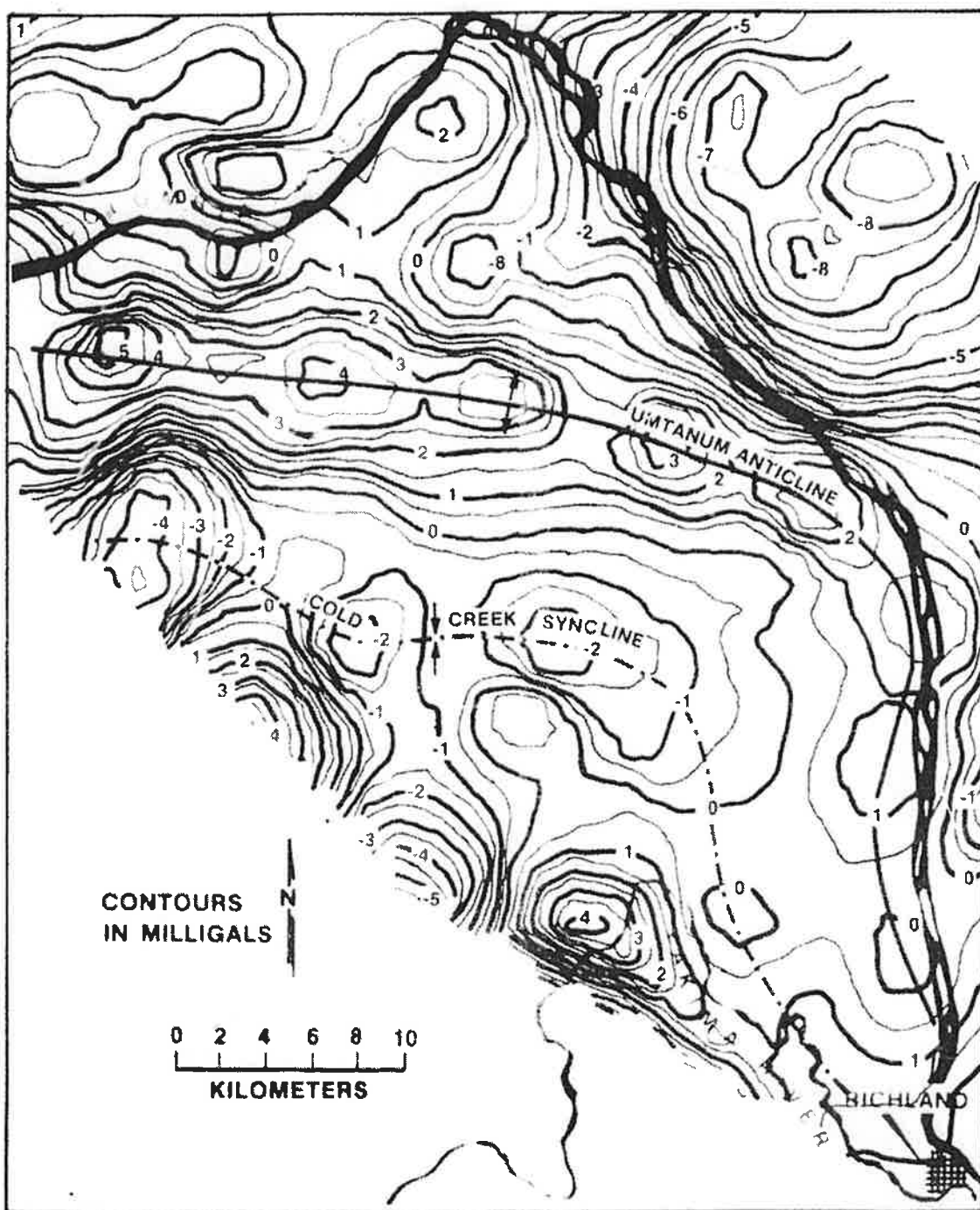


FIGURE 39

88-POINT GRAVITY-BEDROCK MAP CONSTRUCTED BY
SUBTRACTING FIGURE 38 FROM FIGURE 36

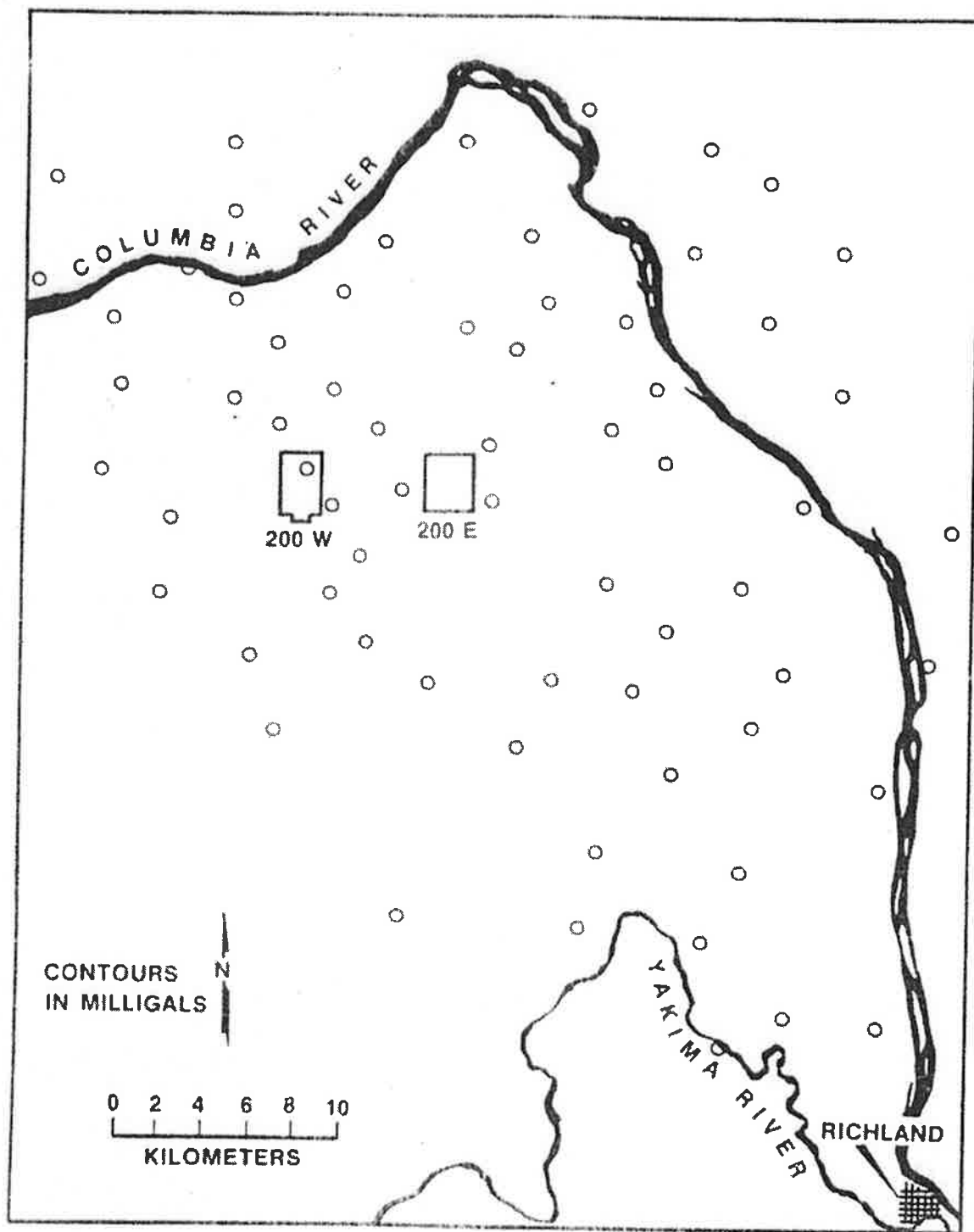


FIGURE 40

GRAVITY STATION LOCATIONS USED IN THE 88-POINT STUDY
THAT ARE WITHIN THE AREA SHOWN IN FIGURE 39

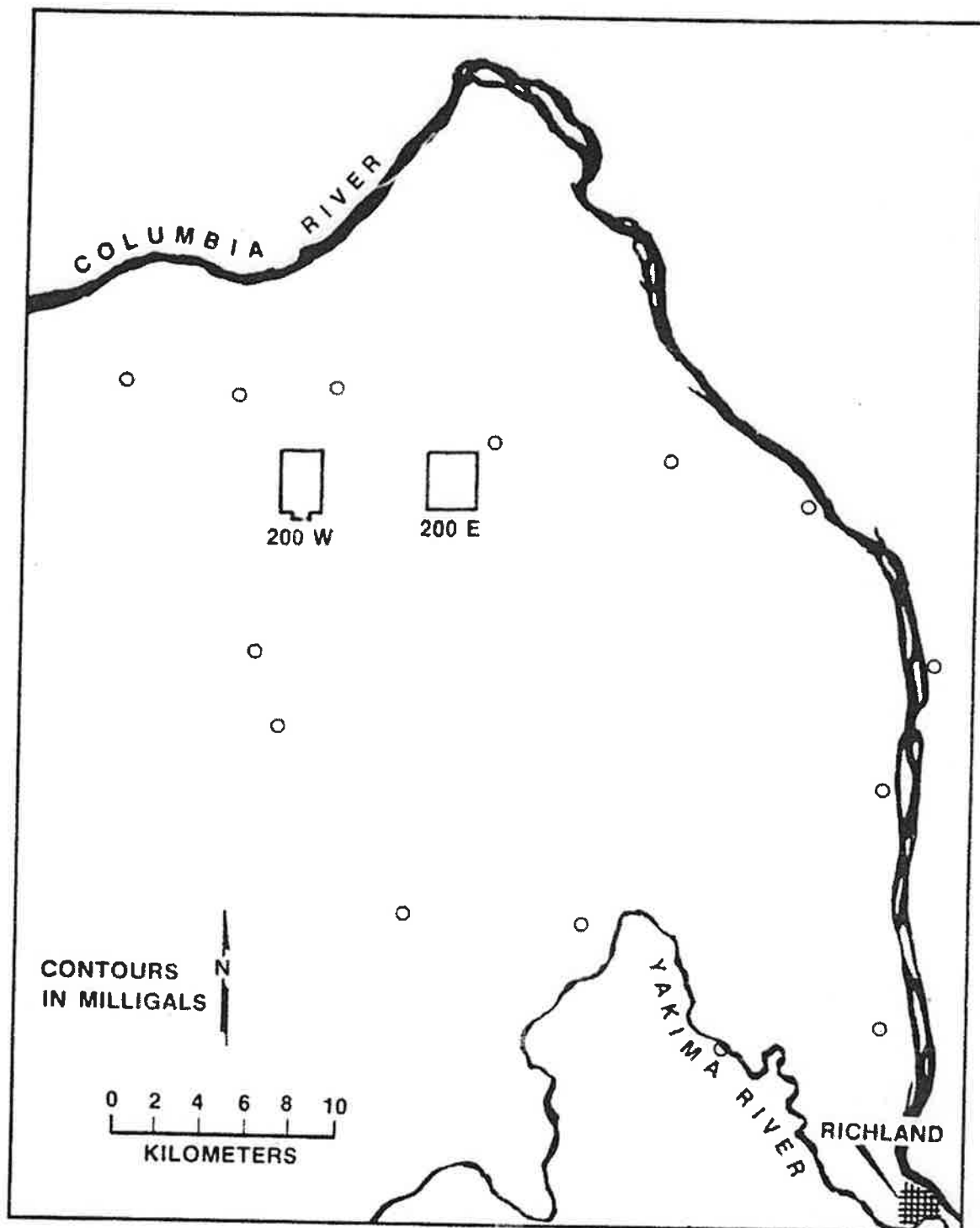


FIGURE 41

GRAVITY STATIONS USED TO CALCULATE THE REGIONAL GRAVITY SURFACE
FOR THE 88-POINT STUDY WITHIN THE AREA OF FIGURE 38

1. The value of this model in defining the bedrock surface;
2. The optimum station density to define the bedrock surface; and,
3. The need for uniform spacing of data points for a bedrock study.

COMPUTER PROGRAMS USED FOR PROCESSING

All contour maps were constructed using the IBM Stampede-OS Version Program on an IBM 360-65 Computer. All output was on the printer and Calcomp Plotter. The three-dimensional models were constructed using the Harvard SYMVU Computer Program on an IBM 360-65 Computer and the output was on a Calcomp Plotter.

INTERPRETATION

RESOLUTION OF DATA

The accuracy of the resultant bedrock models is limited by the distribution of the original data points. Generally, this model will not detail irregularities smaller than the station spacing. Figure 6 shows the original data distribution used to produce the first bedrock model (Figure 14). The station spacing is random with close spacing along roads and coarse spacing elsewhere. Therefore, small features appear related to roads and only large features appear elsewhere. Figures 21, 29, and 39 are bedrock models using a reduced number of data points. Each successive figure more closely approaches gridded data. These figures show the same general structure, but the small details are lost as the close-spaced data points are removed. Without a close-spaced grid, small features cannot be traced with certainty.

Accuracy is also limited by the knowledge of the density of the rock materials. The gravity bedrock maps reflect:

1. The difference in depth to bedrock;
2. The variation in density of the glaciofluvial materials and the Ringold Formation; and,
3. The variation in densities within the basalt sequence.

If the variation in density is macroscopically predictable, then the map will reflect the bedrock surface.

From the density data available, a one-milligal interval should represent approximately 100 feet (30 meters) difference in elevation. Bedrock elevation is reflected by the equation:

$$t = \Delta g / .0416 \Delta \rho \quad (5)$$

where,

t = difference in elevation in meters,

Δg = change in gravity in milligal,

$\Delta \rho$ = density difference between water-saturated materials and basalt.

This equation assumes all corrections related to the post-basalt materials affect gravity as an infinite slab. This assumption is valid over the gravity highs and the lows and does not exceed a 10 percent error on the flanks.

SENSITIVITY

Figures 14, 21, 29, and 39 are models of the basalt surface. The 5-milligal contour reflects a bedrock elevation of about 600 feet (180 meters) above sea level and the contour of -3 milligals reflects a bedrock elevation of about -200 feet (-60 meters) above sea level. Density variations within the post-basalt and inter-basalt materials can produce significant errors in the model. These variations generally will not produce elevation errors exceeding 10 percent of the total elevation difference.

Small gravity highs and lows may be caused by density anomalies within the post-basalt materials or by the result of an irregular distribution of data points. A comparison of Figures 14 to 39 suggests these anomalies reflect data distribution rather than local density anomalies. All anomalies that are smaller than the coarsest station spacing should be interpreted with due caution.

CONCLUSIONS

USEFULNESS OF THE GRAVITY-BEDROCK MODEL

The gravity-bedrock model has improved our understanding of the buried basalt surface. The value is best shown in Appendix B, Figures B-9 through B-24. Umtanum Anticline changes in strike from nearly east-west to nearly north-south. At the same time, it reduces in relief from more than 900 feet (275 meters) above the floor of the Cold Creek Syncline along the western boundary to about 100 feet (30 meters) above on the southeastern corner of the area. If certain assumptions are correct, the models can be used to establish the elevation of the basalt surface. The model is not current over basalt outcrops or north and east of the Columbia River because of the lack of data.

For this model to give a quantitative picture of the buried surface, the following assumptions must be correct:

1. The unsaturated post-basalt materials must have a uniform average density;
2. The saturated materials must have a uniform average density;
3. The basalt must have a uniform average density; and,
4. All average densities must be known.

Each successively deeper horizon is less sensitive to density variations within the body. Within the Hanford reservation, the above assumptions in general are correct. Local large bodies that are either of lower or higher density than that existing within the post-basalts will render the model incorrect. These should produce local errors that frequently occur as small wavelength anomalies. These anomalies of gravity lows can be considered as either a low in the basalt surface or a zone of more porous material in the post-basalt sediments. In either case, it points out a location of potential high ground water flow -- thus useful.

The removal of tidal, drift, terrain-free air, and Bouguer effects are long-proven methods. The regional or deep-seated removal technique best for the specific area is determined by trial and error. The error in this technique cannot be evaluated, but if not correct should do little more than add a slope to the

surface of the resultant model. Checking of basalt depths from well logs indicates the regional surface is correct. The gravity-bedrock method is accurate if the unsaturated material can be considered to be a mathematically infinite slab beneath the station. This assumption can produce up to a 10 percent error in this model at Hanford. As no data were available north and east of the Columbia River, the correction was not made there; thus, making the model incorrect in these locations. For the resulting surface to be a representation of the basalt surface, the same assumption must be correct. The assumptions are valid over the crest and trough of buried folds, but they may have as much as 10 percent error on a fold's flanks.

DETAIL OBTAINED FROM THE MODEL

The gravity model delineates the buried basalt surface better than any previous method. It shows the location of the Umtanum Anticline and the Cold Creek Syncline. These structures turn to the south in the middle of the reservation and reduce in relief as they approach Richland, Washington. The Umtanum Anticline shows sites where breaching of ancestral rivers would be most probable. Figure 29 is considered the surface produced by the best distribution of data. If the depth to basalt is correct at one spot determined from well or seismic data, then the depth can be determined from this model several miles distant by considering a one-milligal difference equal to ~100 feet (30 meters) elevation difference.

The original data collected by Peterson^(1,2) had random horizontal spacing. Four hundred ninety-nine of these points had adequate data to be used in the study. Figure 14 and Figures B-9 through B-12 show the model using all data. The three additional models constructed using fewer data points are shown in Figures 21, 29, and 39 and in Figures B-13 through B-24. Each reduction in data approached gridded data more closely. Detail was lost as the number of data was reduced, but the resultant model more clearly delineates the regional geology. It was difficult to evaluate the minor

details shown in the model with the maximum data. They could have been minor local irregularities or could have been continuous variations that were not found in other localities because of different spacing of the data. Most of the minor irregularities occur along roads. Station spacing was dense. The 166-point study appears to give the best and most predictable results. This means a station spacing of about 1 for every 4 square miles (10 square kilometers) would be optimum if on a grid. Less than half that number would delineate major geologic structures.

SIGNIFICANCE OF THE STUDY

The regional geology shows major folds trending east-west with Saddle Mountains Anticline to the north and Rattlesnake Anticline to the south. This study shows that the Umtanum Anticline and the Cold Creek Syncline are buried under the Pasco Basin. At the general site of Gable Mountain, all of these structures change strike from east-west to north-south. In this flexure, they reduce in magnitude. At Richland, Washington, there is only about 100 feet (30 meters) of relief between the crest of the Umtanum Anticline and the trough of the Cold Creek Syncline. At this point, they appear to merge into the Rattlesnake Anticline and again change in strike to an east-west structure (Figure 29).

APPENDIX A

DATA USED TO CONSTRUCT THE THREE-DIMENSIONAL MODELS

Table A-I lists all data used in the model calculations. The listing includes a record number, the X location, the Y location, and four Z fields. These fields are as follows:

Z_0 = the terrain correction;

Z_1 = the Bouguer value;

Z_2 = the terrain-corrected Bouguer value;

Z_3 = the water table correction; and,

Z_4 = the gravity values used to calculate the regional (or deep-seated) gravity effect.

The X, Y fields are on a scale of 124 units per inch. All figures, except those showing the total station distribution, have the following dimensions:

X_{\min} = 238;

X_{\max} = 1,087;

Y_{\min} = 0;

Y_{\max} = 1,050.

(This produces maps of exactly the same area as shown in Figure 7.)

Any time the number 0.723700E76 appears, it means this station has no data and is ignored in the calculation. An x in the record number indicates these data were used in the 88-point model; and a - means these data were used in the 166-point model; and a + means these data were used in the 344-point model. All data were used in the 499-point model.

TABLE A-1
LISTING OF DATA USED IN MODEL CALCULATIONS

WORLD OF REFERENT						
PREDICATE		PREDICTION				
WORD	REF ID	X	Y	Z	T1	T2
x -> 1	0e5027500f	0.3	0e1069207	0.7	1e2650700f	0.0
2	0.6311003d	0.2	0e1048500f	0.8	-1e5295690f	0.2
3	0.1450030f	0.7	0e2277700f	0.1	-1e5120300f	0.2
4	0.1263750f	0.4	0e2e20700f	0.5	-1e5057400f	0.2
5	0.1068780f	0.6	0e1067500f	0.2	-1e5021000f	0.2
6	0.1155100f	0.5	0e2030400f	0.3	-1e50205694f	0.2
7	0.1155100f	0.5	0e2046000f	0.4	-1e50205694f	0.2
x -> 8	0.5517500f	0.2	0e1067500f	0.4	-1e5274900f	0.2
-> 9	0.5520030f	0.1	0e1066500f	0.6	-1e513032280f	0.2
x -> 10	0.e1e0000f	0.7	0e1065500f	0.4	-1e53451194f	0.2
x -> 11	0.e4e7500f	0.3	0e1065500f	0.4	-1e5246000f	0.2
x -> 12	1.1021750f	0.2	1e1021550f	0.4	0e52011900f	0.2
-> 13	0.4225300f	0.2	0e13e5000f	0.6	1e1901900f	0.2
14	1e7500000	0.2	0e1065001f	0.6	0e5190900f	0.2
+ 15	9e170500f	0.2	1e1065000f	0.4	0e52011900f	0.2
16	1e1626000	0.2	0e1064750f	0.6	1e15713000f	0.2
x -> 17	0.2027400f	0.3	0e1064230f	0.4	0e5490000f	0.2
18	1e-4274730f	0.1	1e1021550f	0.4	1e2531579f	0.2
x -> 19	1e5120500f	0.5	0e1064250f	0.4	1e2802798f	0.3
20	1e137500f	0.3	0e1063750f	0.4	1e2030400f	0.2
+ 21	3e1255000f	0.2	0e1071500f	0.4	1e2442000f	0.2

Table A-I (continued)

RECORD NO.	X	Y	Z	20	21	22	23
- + 22	0.2677590 ^c 0 ^a	0.1043750 ^c 0 ^b	0.1159290 ^c 0 ^d	-0.5688999 ^c 0 ^e	-0.5676416 ^c 0 ^f	-0.5679999 ^c 0 ^g	-0.5679999 ^c 0 ^h
+ 23	0.2027530 ^c 0 ^j	0.1037692 ^c 0 ^k	0.2077510 ^c 0 ^l	-0.5856690 ^c 0 ^m	-0.5829264 ^c 0 ⁿ	-0.5839995 ^c 0 ^o	-0.5839995 ^c 0 ^p
+ 24	0.3620235 ^c 0 ^q	0.0635000 ^c 0 ^r	0.1652000 ^c 0 ^s	-0.5520100 ^c 0 ^t	-0.5501406 ^c 0 ^u	-0.5503307 ^c 0 ^v	-0.5503307 ^c 0 ^w
- + 25	0.3522500 ^c 0 ^x	0.1135000 ^c 0 ^y	0.2683300 ^c 0 ^z	-0.5454500 ^c 0 ^{aa}	-0.5452116 ^c 0 ^{ab}	-0.5452300 ^c 0 ^{ac}	-0.5452300 ^c 0 ^{ad}
- + 26	0.4227041 ^c 0 ^{ae}	0.1925000 ^c 0 ^{af}	0.363	-0.5172510 ^c 0 ^{ag}	-0.5270000 ^c 0 ^{ah}	0.7217931 ^c 0 ^{ai}	0.7217931 ^c 0 ^{aj}
X - + 27	0.3237540 ^c 0 ^{ak}	0.1052720 ^c 0 ^{al}	0.1701650 ^c 0 ^{am}	-0.5705071 ^c 0 ^{an}	-0.5852832 ^c 0 ^{ao}	-0.5853306 ^c 0 ^{ap}	-0.5853306 ^c 0 ^{aq}
28	0.3575000 ^c 0 ^{ar}	0.1557214 ^c 0 ^{as}	0.3277477 ^c 0 ^{at}	-0.5434397 ^c 0 ^{au}	-0.5251752 ^c 0 ^{av}	0.7917515 ^c 0 ^{aw}	0.7917515 ^c 0 ^{ax}
29	0.7197520 ^c 0 ^{ay}	0.1382000 ^c 0 ^{az}	0.2746300 ^c 0 ^{ba}	-0.5143652 ^c 0 ^{bc}	-0.5155928 ^c 0 ^{bd}	0.7217931 ^c 0 ^{be}	0.7217931 ^c 0 ^{bf}
+ 30	0.6185000 ^c 0 ^{bg}	0.1355030 ^c 0 ^{bh}	0.313523350 ^c 0 ^{bi}	-0.5232845 ^c 0 ^{bj}	-0.498614 ^c 0 ^{bk}	0.7237300 ^c 0 ^{bl}	0.7237300 ^c 0 ^{bm}
+ 31	0.6556630 ^c 0 ^{bn}	0.1625252 ^c 0 ^{bo}	0.3675599 ^c 0 ^{bp}	-0.5253030 ^c 0 ^{br}	-0.5165646 ^c 0 ^{bs}	0.7237300 ^c 0 ^{bt}	0.7237300 ^c 0 ^{bu}
+ 32	0.7357610 ^c 0 ^{bu}	0.1916520 ^c 0 ^{bv}	0.4068110 ^c 0 ^{bw}	-0.5118206 ^c 0 ^{bx}	-0.5105167 ^c 0 ^{by}	0.7237300 ^c 0 ^{bz}	0.7237300 ^c 0 ^{ca}
33	0.7775040 ^c 0 ^{cb}	0.1755500 ^c 0 ^{cc}	0.306521350 ^c 0 ^{cd}	-0.5232845 ^c 0 ^{ce}	-0.498614 ^c 0 ^{cf}	0.7237300 ^c 0 ^{cg}	0.7237300 ^c 0 ^{ch}
+ 34	0.7372830 ^c 0 ^{ci}	0.1034750 ^c 0 ^{cj}	0.365077435 ^c 0 ^{ck}	-0.5335350 ^c 0 ^{cl}	-0.5165646 ^c 0 ^{cm}	0.7237300 ^c 0 ^{cn}	0.7237300 ^c 0 ^{co}
+ 35	0.7415750 ^c 0 ^{cp}	0.1615230 ^c 0 ^{cq}	0.3212770 ^c 0 ^{cr}	-0.5232845 ^c 0 ^{cs}	-0.5105167 ^c 0 ^{ct}	0.7237300 ^c 0 ^{cu}	0.7237300 ^c 0 ^{cv}
+ 36	0.6611300 ^c 0 ^{cv}	0.1278300 ^c 0 ^{cw}	0.2037820 ^c 0 ^{cx}	-0.5335350 ^c 0 ^{cy}	-0.5165646 ^c 0 ^{cz}	0.7237300 ^c 0 ^{da}	0.7237300 ^c 0 ^{db}
+ 37	0.3627700 ^c 0 ^{db}	0.1033321 ^c 0 ^{dc}	0.1791525 ^c 0 ^{dd}	-0.5208000 ^c 0 ^{de}	-0.5502000 ^c 0 ^{df}	0.7237300 ^c 0 ^{dg}	0.7237300 ^c 0 ^{dh}
+ 38	0.6177700 ^c 0 ^{di}	0.1277750 ^c 0 ^{dj}	0.21	-0.5063200 ^c 0 ^{dk}	-0.5177500 ^c 0 ^{dl}	0.7237300 ^c 0 ^{dm}	0.7237300 ^c 0 ^{dn}
39	0.7471000 ^c 0 ^{do}	0.1919300 ^c 0 ^{dp}	0.363	-0.5498580 ^c 0 ^{dq}	-0.5576664 ^c 0 ^{dr}	0.7177300 ^c 0 ^{ds}	0.7177300 ^c 0 ^{dt}
- + 40	0.6114700 ^c 0 ^{dt}	0.1076750 ^c 0 ^{du}	0.2127735 ^c 0 ^{dv}	-0.5476634 ^c 0 ^{dw}	-0.5482626 ^c 0 ^{dx}	0.7237300 ^c 0 ^{dy}	0.7237300 ^c 0 ^{dz}
41	0.6742250 ^c 0 ^{ea}	0.1303430 ^c 0 ^{eb}	0.3257647 ^c 0 ^{ec}	-0.5045310 ^c 0 ^{ed}	-0.4951247 ^c 0 ^{ef}	0.7237300 ^c 0 ^{eg}	0.7237300 ^c 0 ^{eh}
+ 42	0.6153930 ^c 0 ^{eh}	0.1703400 ^c 0 ^{ei}	0.2167373 ^c 0 ^{ej}	-0.5462610 ^c 0 ^{ek}	-0.5480457 ^c 0 ^{el}	0.7237300 ^c 0 ^{em}	0.7237300 ^c 0 ^{en}
X - + 43	0.7417100 ^c 0 ^{en}	0.1003424 ^c 0 ^{eo}	0.202	-0.5232845 ^c 0 ^{ep}	-0.5165646 ^c 0 ^{er}	0.7237300 ^c 0 ^{es}	0.7237300 ^c 0 ^{et}
+ 44	0.6177700 ^c 0 ^{et}	0.1170030 ^c 0 ^{eu}	0.2940455 ^c 0 ^{ev}	-0.5476634 ^c 0 ^{ew}	-0.5482626 ^c 0 ^{ex}	0.7237300 ^c 0 ^{ey}	0.7237300 ^c 0 ^{ez}
+ 45	0.6050300 ^c 0 ^{ez}	0.1230000 ^c 0 ^{fa}	0.2620400 ^c 0 ^{fb}	-0.5225648 ^c 0 ^{fc}	-0.5216482 ^c 0 ^{fd}	0.7237300 ^c 0 ^{fe}	0.7237300 ^c 0 ^{fg}
- + 46	0.6427540 ^c 0 ^{fg}	0.1031250 ^c 0 ^{fh}	0.1440000 ^c 0 ^{fi}	-0.5452890 ^c 0 ^{fg}	-0.5528580 ^c 0 ^{fh}	0.7237300 ^c 0 ^{fi}	0.7237300 ^c 0 ^{fg}
47	0.6137600 ^c 0 ^{gi}	0.1101000 ^c 0 ^{gj}	0.2372750 ^c 0 ^{gi}	-0.5476634 ^c 0 ^{gk}	-0.5482626 ^c 0 ^{gl}	0.7237300 ^c 0 ^{gm}	0.7237300 ^c 0 ^{gn}

Table A-1 (continued)
Ounces or milliliters

Table A-1 (continued)

RECORD NO	X	Y	Z	24	22	23	24
+ 74	7.577300F 03	0.9267500C 03	0.1129699C 00	-0.5039999E 02	-0.5028700F 02	0.7237000F 02	0.7237000E 76
75	3.67312540E 03	0.52661315C 03	0.1092100C 00	-0.5259999E 02	-0.5240974E 02	0.7237000C 76	0.7237000E 76
+ 76	9.61736300E 03	0.6229564C 02	0.1126500F 00	-0.5057299E 02	-0.5046184E 02	0.7237000F 76	0.7237000E 76
+ 77	1.6091701C 03	0.5222301C 03	0.11364530E 03	-0.5650103E 02	-0.5535341E 02	0.7237000C 76	0.7237000E 76
78	3.6567263C 03	0.5257100C 04	0.1058159C 00	-0.5127000E 02	-0.5127000E 02	0.7237000C 76	0.7237000E 76
+ 79	3.65125300E 03	0.5246400C 03	0.1058159C 00	-0.5127000E 02	-0.5127000E 02	0.7237000C 76	0.7237000E 76
+ 80	1.62027300C 03	0.5245300C 02	0.11264400C 03	-0.5127000E 02	-0.5127000E 02	0.7237000F 76	0.7237000E 76
+ 81	0.53200000E 03	0.6125170C 03	0.1126771C 00	-0.5127000E 02	-0.5127000E 02	0.7237000C 76	0.7237000E 76
+ 82	1.60507630E 02	0.5097500E 03	0.1058159C 00	-0.5127000E 02	-0.5127000E 02	0.7237000C 76	0.7237000E 76
+ 83	0.46750000E 03	0.5097500E 03	0.1126771C 00	-0.5127000E 02	-0.5127000E 02	0.7237000C 76	0.7237000E 76
+ 84	1.604350170C 03	0.5097500E 03	0.1058159C 00	-0.5127000E 02	-0.5127000E 02	0.7237000C 76	0.7237000E 76
85	3.67007500C 03	0.5097500E 03	0.1126771C 00	-0.5127000E 02	-0.5127000E 02	0.7237000C 76	0.7237000E 76
+ 86	0.46731001C 03	0.5097500E 03	0.1058159C 00	-0.5127000E 02	-0.5127000E 02	0.7237000C 76	0.7237000E 76
+ 87	1.60432500C 03	0.5097500E 03	0.1058159C 00	-0.5127000E 02	-0.5127000E 02	0.7237000C 76	0.7237000E 76
+ 88	1.60432500C 03	0.5097500E 03	0.1058159C 00	-0.5127000E 02	-0.5127000E 02	0.7237000C 76	0.7237000E 76
+ 89	2.50507500E 03	0.5097500E 03	0.1058159C 00	-0.5127000E 02	-0.5127000E 02	0.7237000C 76	0.7237000E 76
90	3.62021001C 03	0.5097500E 03	0.1058159C 00	-0.5127000E 02	-0.5127000E 02	0.7237000C 76	0.7237000E 76
+ 91	1.60432500C 03	0.5097500E 03	0.1058159C 00	-0.5127000E 02	-0.5127000E 02	0.7237000C 76	0.7237000E 76
92	1.605222100C 03	0.5097500E 03	0.1058159C 00	-0.5127000E 02	-0.5127000E 02	0.7237000C 76	0.7237000E 76
93	1.60747100C 03	0.5097500E 03	0.1058159C 00	-0.5127000E 02	-0.5127000E 02	0.7237000C 76	0.7237000E 76
+ 94	3.60575700C 03	0.5097500E 03	0.1058159C 00	-0.5127000E 02	-0.5127000E 02	0.7237000C 76	0.7237000E 76
+ 95	2.623242500C 03	0.5097500E 03	0.1058159C 00	-0.5127000E 02	-0.5127000E 02	0.7237000C 76	0.7237000E 76
+ 96	1.60432500C 03	0.5097500E 03	0.1058159C 00	-0.5127000E 02	-0.5127000E 02	0.7237000C 76	0.7237000E 76
+ 97	0.25275000E 04	0.32749000E 03	0.1058159C 00	-0.5127000E 02	-0.5127000E 02	0.7237000C 76	0.7237000E 76
+ 98	3.62272500C 03	0.30737000E 03	0.1058159C 00	-0.5127000E 02	-0.5127000E 02	0.7237000C 76	0.7237000E 76
+ 99	1.73516290E 02	0.30353000E 03	0.1058159C 00	-0.5127000E 02	-0.5127000E 02	0.7237000C 76	0.7237000E 76

Table A-1 (continued)

Table A-I (continued)

Table A-I (continued)

Ref ID	X	Y	Z	R	T0	T1	T2	T3	T4
152	-0.296782357	0.7	3.0	1.0150092	0.3	0.0	-0.47753906	0.2	0.7330000
x - + 153	3.04535005	0.9	2.7525000	1.4	3.0	4.76000	3.2	-0.43513236	0.2
- + 154	3.07437003	0.2	0.76271007	0.2	3.01367100	0.0	-0.52731007	0.2	0.7330000
155	1.01173400	0.5	3.0137700	0.2	3.01367100	0.1	-0.52731007	0.2	0.7330000
x - + 156	1.01795100	0.2	3.01367100	0.4	3.0472600	0.3	-0.52731007	0.2	0.7330000
157	3.0521000	0.7	3.0287500	0.1	3.0287500	0.0	-0.52731007	0.2	0.7330000
158	1.04727100	0.2	3.0170000	0.3	3.01164200	0.2	-0.52731007	0.2	0.7330000
+ 159	3.0146500	0.4	3.0287500	0.4	3.01367100	0.1	-0.52731007	0.2	0.7330000
+ 160	3.01472000	0.7	3.0120000	0.7	3.0120000	0.2	-0.52731007	0.2	0.7330000
+ 161	3.01472000	0.6	3.01164200	0.2	3.01654400	0.3	-0.52731007	0.2	0.7330000
+ 162	3.01472000	0.2	3.01164200	0.2	3.02650740	0.3	-0.60231002	0.2	0.7330000
- + 163	3.01472000	0.7	3.01770000	0.2	3.01215510	0.1	-0.52431006	0.2	-0.52731007
164	3.01472000	0.1	3.01770000	0.3	3.01770000	0.0	-0.52731007	0.2	0.7330000
+ 165	3.01472000	0.2	3.01770000	0.2	3.01770000	0.0	-0.52731007	0.2	0.7330000
+ 166	3.05117000	0.2	3.01770000	0.2	3.01770000	0.0	-0.52731007	0.2	0.7330000
+ 167	3.04646464	0.2	3.01770000	0.3	3.01770000	0.0	-0.52731007	0.2	0.7330000
+ 168	3.01472000	0.2	3.01770000	0.2	3.01770000	0.0	-0.52731007	0.2	0.7330000
169	1.04717000	0.2	3.01770000	0.2	3.01770000	0.0	-0.52731007	0.2	0.7330000
170	3.01472000	0.2	3.01770000	0.2	3.01770000	0.0	-0.52731007	0.2	0.7330000
171	3.01472000	0.2	3.01770000	0.3	3.01770000	0.1	-0.52731007	0.2	0.7330000
172	3.01472000	0.2	3.01770000	0.3	3.01770000	0.2	-0.52731007	0.2	0.7330000
+ 173	3.0472000	0.2	3.01770000	0.2	3.01770000	0.0	-0.52731007	0.2	0.7330000
174	1.04717000	0.2	3.01770000	0.1	3.01770000	0.0	-0.52731007	0.2	0.7330000
175	3.04646464	0.2	3.01770000	0.1	3.01770000	0.0	-0.52731007	0.2	0.7330000
- 176	3.03260000	0.2	3.01770000	0.2	3.01530000	0.2	-0.52731007	0.2	0.7330000
177	3.01472000	0.2	3.01770000	0.2	3.01530000	0.2	-0.52731007	0.2	0.7330000

Table A-I (continued)

		α	β	γ	$\delta_{\ell\ell}$	ℓ_1	ℓ_2	ℓ_3	ℓ_4
+ 178	3.05377500°	37	3.07887600°	03	0.0°	-0.43092100°	02	-0.43090000°	32
- + 179	2.07557435°	07	0.01545500°	03	0.0°	-0.50505000°	02	-0.50502300°	12
X - + 180	1.02277500°	02	1.07544300°	05	3.077413°	0.0°	-0.53530300°	32	-0.53530300°
181	0.94282530°	07	0.07526200°	03	0.01287100°	0.0°	-0.47857930°	32	-0.47857930°
X - + 182	0.06857530°	37	0.075277500°	02	0.00735163°	0.0°	-0.52503300°	02	-0.52503300°
+ 183	2.01617500°	08	1.07525200°	03	0.0170163°	0.0°	-0.54569500°	32	-0.54569500°
X - + 184	0.01224250°	08	0.07525200°	03	0.0149452°	0.0°	-0.52370912°	32	-0.52370912°
185	1.07421000°	05	0.075277500°	02	0.0°	-0.52370900°	02	-0.52370900°	02
+ 186	0.01113250°	24	0.07527250°	03	0.0°	-0.51511120°	02	-0.51511120°	02
+ 187	0.011063750°	04	0.07527250°	03	0.0°	-0.51503700°	02	-0.51503700°	02
X - + 188	0.012356750°	04	0.07527250°	03	0.0°	-0.51503700°	02	-0.51503700°	02
+ 189	0.01178160°	02	0.07516300°	03	0.02431357°	0.0°	-0.62496900°	02	-0.62496900°
- + 190	0.01047500°	02	0.07516300°	03	0.01207000°	0.0°	-0.62496900°	02	-0.62496900°
191	0.01028750°	05	0.07516300°	03	0.024713°	0.0°	-0.62471300°	02	-0.62471300°
- + 192	0.01052750°	04	0.07516300°	03	0.01207000°	0.0°	-0.62496900°	02	-0.62496900°
X - + 193	0.01070520°	03	0.07516300°	02	0.01207000°	0.0°	-0.62496900°	02	-0.62496900°
+ 194	0.01052750°	02	0.07516300°	03	0.012716°	0.0°	-0.62471300°	02	-0.62471300°
X - + 195	0.01054520°	01	0.07516300°	03	0.012716°	0.0°	-0.62471300°	02	-0.62471300°
+ 196	0.00973250°	02	0.07516300°	04	0.01274510°	0.0°	-0.62474500°	02	-0.62474500°
+ 197	0.00956520°	03	0.07516300°	02	0.022112°	0.0°	-0.62471300°	02	-0.62471300°
- + 198	0.00972500°	05	0.07516300°	03	0.01274510°	0.0°	-0.62474500°	02	-0.62474500°
- + 199	0.00973250°	07	0.07516300°	03	0.01274510°	0.0°	-0.62474500°	02	-0.62474500°
- + 200	0.00956520°	05	0.07516300°	02	0.022112°	0.0°	-0.62471300°	02	-0.62471300°
+ 201	0.00972500°	07	0.07516300°	03	0.01274510°	0.0°	-0.62474500°	02	-0.62474500°
+ 202	0.00973250°	03	0.07516300°	02	0.01274510°	0.0°	-0.62474500°	02	-0.62474500°
203	0.00956520°	03	0.07516300°	02	0.01274510°	0.0°	-0.62474500°	02	-0.62474500°

Table A-I (continued)

RECORD #	X	Y	Z	40	41	42	43	44
+ 204	4.674500E-03	9.712000E-03	9.413250E-03	-0.5375900E-02	-0.5338670E-02	0.17237000E-02	3.72270000E-02	3.72270000E-02
205	3.6125010E-03	8.731615E-03	1.020000E-02	-0.5920000E-02	-0.5920000E-02	0.17237000E-02	3.72270000E-02	3.72270000E-02
206	3.3702570E-03	7.731100E-03	9.025500E-03	-0.5470000E-02	-0.5470000E-02	0.17237000E-02	3.72270000E-02	3.72270000E-02
207	3.645500E-03	6.785200E-03	8.113400E-03	-0.5150000E-02	-0.5150000E-02	0.17237000E-02	3.72270000E-02	3.72270000E-02
x - + 208	3.6162700E-03	5.838300E-03	6.000000E-03	-0.5220000E-02	-0.5220000E-02	0.17237000E-02	3.72270000E-02	3.72270000E-02
+ 209	3.645200E-03	4.881200E-03	3.011636E-03	-0.5050000E-02	-0.5050000E-02	0.17237000E-02	3.72270000E-02	3.72270000E-02
+ 210	3.617300E-03	3.924200E-03	1.011636E-03	-0.5070000E-02	-0.5070000E-02	0.17237000E-02	3.72270000E-02	3.72270000E-02
+ 211	3.617300E-03	3.077300E-03	1.011636E-03	-0.5100000E-02	-0.5100000E-02	0.17237000E-02	3.72270000E-02	3.72270000E-02
212	3.617300E-03	2.230400E-03	6.011636E-03	-0.5330000E-02	-0.5330000E-02	0.17237000E-02	3.72270000E-02	3.72270000E-02
213	3.617300E-03	1.383500E-03	1.011636E-03	-0.5770000E-02	-0.5770000E-02	0.17237000E-02	3.72270000E-02	3.72270000E-02
214	3.617300E-03	5.437600E-04	1.011636E-03	-0.5100000E-02	-0.5100000E-02	0.17237000E-02	3.72270000E-02	3.72270000E-02
215	3.6128130E-03	3.149000E-03	6.011636E-03	-0.5330000E-02	-0.5330000E-02	0.17237000E-02	3.72270000E-02	3.72270000E-02
y - + 216	3.6047250E-03	2.291100E-03	6.011636E-03	-0.5170000E-02	-0.5170000E-02	0.17237000E-02	3.72270000E-02	3.72270000E-02
+ 217	3.6047250E-03	1.447700E-03	6.011636E-03	-0.5050000E-02	-0.5050000E-02	0.17237000E-02	3.72270000E-02	3.72270000E-02
218	3.6047250E-03	5.917500E-04	6.011636E-03	-0.5110000E-02	-0.5110000E-02	0.17237000E-02	3.72270000E-02	3.72270000E-02
219	3.6047250E-03	2.017700E-03	2.017700E-03	-0.5553000E-02	-0.5553000E-02	0.17237000E-02	3.72270000E-02	3.72270000E-02
220	3.6047250E-03	1.171700E-03	1.011636E-03	-0.5020000E-02	-0.5020000E-02	0.17237000E-02	3.72270000E-02	3.72270000E-02
+ 221	3.6047250E-03	3.711700E-03	6.011636E-03	-0.5149000E-02	-0.5149000E-02	0.17237000E-02	3.72270000E-02	3.72270000E-02
+ 222	3.6254510E-03	1.011636E-03	1.011636E-03	-0.5553000E-02	-0.5553000E-02	0.17237000E-02	3.72270000E-02	3.72270000E-02
- + 223	3.6254510E-03	2.671500E-03	1.011636E-03	-0.5470300E-02	-0.5470300E-02	0.17237000E-02	3.72270000E-02	3.72270000E-02
224	3.6254510E-03	1.327500E-03	1.011636E-03	-0.5110000E-02	-0.5110000E-02	0.17237000E-02	3.72270000E-02	3.72270000E-02
x - + 225	3.6254510E-03	1.211500E-03	1.011636E-03	-0.5180000E-02	-0.5180000E-02	0.17237000E-02	3.72270000E-02	3.72270000E-02
226	3.6254510E-03	4.761000E-04	1.011636E-03	-0.5149000E-02	-0.5149000E-02	0.17237000E-02	3.72270000E-02	3.72270000E-02
227	3.6254510E-03	1.111500E-03	1.011636E-03	-0.5050000E-02	-0.5050000E-02	0.17237000E-02	3.72270000E-02	3.72270000E-02
x - + 228	3.6254510E-03	0.7155100E-03	1.011636E-03	-0.5835200E-02	-0.5835200E-02	0.17237000E-02	3.72270000E-02	3.72270000E-02
+ 229	3.6254510E-03	0.2025100E-03	1.011636E-03	-0.5439100E-02	-0.5439100E-02	0.17237000E-02	3.72270000E-02	3.72270000E-02

Table A-I (continued)

5 U 4 P R F F K Y / G R E F FILE									
AFCORD NO	X	Y	Z	X0	Y0	Z0	X1	Y1	Z1
+ 210	0.680500E 03	0.115500E 03	0.12249100E 03	-0.477000E 02	-0.477550E 02	-0.475750E 02	0.723700E 76	0.723700E 76	0.723700E 76
231	0.633500E 03	0.7420100E 03	0.1095E 03	-0.5535E 03	-0.5535E 03	-0.543103E 02	0.722700E 76	0.722700E 76	0.722700E 76
232	0.6555E 03E 02	0.711030E 03	0.114000E 03	-0.523900E 03	-0.523900E 03	-0.519650E 02	0.723700E 76	0.723700E 76	0.723700E 76
- + 233	0.633000E 03	0.6052500E 03	0.513269E 03	-0.54869100E 02	-0.54869100E 02	-0.543861E 02	0.723700E 76	0.723700E 76	0.723700E 76
x - + 234	0.6162500E 03	0.612500E 03	0.612500E 03	-0.43239900E 12	-0.43239900E 12	-0.435455E 02	-0.435455E 02	-0.435455E 02	-0.435455E 02
235	0.522500E 03	0.5990100E 03	0.14728400E 03	-0.56339500E 02	-0.56262700E 02	-0.56262700E 02	0.723700E 76	0.723700E 76	0.723700E 76
- + 236	0.727000E 03	0.6397500E 03	0.6397500E 03	-0.439395E 02	-0.439395E 02	-0.438999E 02	-0.438999E 02	-0.438999E 02	-0.438999E 02
- + 237	0.865500E 03	0.697000E 03	0.697000E 03	-0.51077000E 02	-0.51077000E 02	-0.510644E 02	-0.510644E 02	-0.510644E 02	-0.510644E 02
- + 238	0.755000E 03	0.627500E 03	0.627500E 03	0.52116339E 03	0.52116339E 03	-0.520000E 02	-0.518546E 02	-0.518546E 02	-0.518546E 02
239	0.646100E 03	0.6895000E 03	0.6895000E 03	-0.4887999E 02	-0.4887999E 02	-0.4866699E 02	-0.4866699E 02	-0.4866699E 02	-0.4866699E 02
- x - + 240	1.2235200E 03	0.66592500E 04	0.1429495E 04	-0.5000000E 02	-0.5000000E 02	-0.5055E 02	-0.5055E 02	-0.5055E 02	-0.5055E 02
+ 241	2.122600E 04	0.6887200E 04	0.6887200E 04	-0.6224000E 02	-0.6224000E 02	-0.622000E 02	-0.622000E 02	-0.622000E 02	-0.622000E 02
- + 242	3.1007250E 04	0.6277200E 04	0.6277200E 04	-0.5072000E 02	-0.5072000E 02	-0.507105E 02	-0.507105E 02	-0.507105E 02	-0.507105E 02
- + 243	3.647125E 04	0.6471500E 04	0.6471500E 04	0.7736239E 03	0.7736239E 03	-0.5556435E 02	-0.5556435E 02	-0.5556435E 02	-0.5556435E 02
x - + 244	6.514500E 03	0.6365000E 03	0.6365000E 03	-0.5121000E 02	-0.5121000E 02	-0.512000E 02	-0.512000E 02	-0.512000E 02	-0.512000E 02
x - + 245	3.492500E 03	0.6777200E 03	0.6777200E 03	-0.5070100E 02	-0.5070100E 02	-0.507005E 02	-0.507005E 02	-0.507005E 02	-0.507005E 02
+ 246	9.4112500E 03	0.667700E 03	0.667700E 03	-0.5737350E 02	-0.5737350E 02	-0.5657725E 02	-0.5657725E 02	-0.5657725E 02	-0.5657725E 02
x - + 247	3.215000E 03	0.67676700E 03	0.67676700E 03	-0.565900E 02	-0.565900E 02	-0.551200E 02	-0.551200E 02	-0.551200E 02	-0.551200E 02
+ 248	3.525500E 03	0.66772250E 03	0.66772250E 03	-0.526555E 02	-0.526555E 02	-0.520055E 02	-0.520055E 02	-0.520055E 02	-0.520055E 02
+ 249	2.6452400E 03	0.6666300E 03	0.6666300E 03	-0.505000E 02	-0.505000E 02	-0.502500E 02	-0.502500E 02	-0.502500E 02	-0.502500E 02
+ 250	4.6557700E 03	0.662500E 03	0.662500E 03	-0.505000E 02	-0.505000E 02	-0.502500E 02	-0.502500E 02	-0.502500E 02	-0.502500E 02
+ 251	4.547300E 03	0.66660000E 03	0.66660000E 03	0.2059200E 03	0.2059200E 03	-0.512125E 02	-0.512125E 02	-0.512125E 02	-0.512125E 02
+ 252	3.672500E 03	0.66535700E 03	0.66535700E 03	-0.5420100E 02	-0.5420100E 02	-0.537500E 02	-0.537500E 02	-0.537500E 02	-0.537500E 02
+ 253	3.767500E 03	0.66000000E 03	0.66000000E 03	-0.512125E 02	-0.512125E 02	-0.512125E 02	-0.512125E 02	-0.512125E 02	-0.512125E 02
+ 254	3.1007500E 03	0.66660000E 03	0.66660000E 03	0.2059200E 03	0.2059200E 03	-0.512125E 02	-0.512125E 02	-0.512125E 02	-0.512125E 02
x - + 255	6.514500E 03	0.65592500E 03	0.65592500E 03	-0.522400E 02	-0.522400E 02	-0.5176700E 02	-0.5176700E 02	-0.5176700E 02	-0.5176700E 02

Table A-1 (continued)

Table A-I (continued)

SECOND NO	X	Y	Z	ε1	ε2	ε3	ε4
+ 282	0.5015010111111111	0.0	0.01337203611111111	0.03	0.01337203611111111	0.0	0.01337203611111111
+ 283	0.1026250111111111	0.04	0.01000101111111111	0.03	0.01171531111111111	0.01	0.01567300611111111
284	0.5127530111111111	0.2	0.6051250111111111	0.04	0.01151313011111111	0.03	0.01527017511111111
- + 285	0.7161500111111111	0.3	0.6068500111111111	0.04	0.01644410111111111	0.01	0.01513395911111111
286	0.5116000111111111	0.4	0.6051160111111111	0.04	0.01644410111111111	0.01	0.01513395911111111
x - + 287	0.5012100111111111	0.7	0.6012100111111111	0.03	0.01464530111111111	0.05	0.01464530001111111
+ 288	0.7151000111111111	0.8	0.6068500111111111	0.03	0.01644410111111111	0.01	0.01527000511111111
289	0.5116000111111111	0.9	0.6051160111111111	0.02	0.01644410111111111	0.01	0.01527000511111111
+ 290	0.5116000111111111	0.98	0.6051160111111111	0.04	0.01644410111111111	0.01	0.01527000511111111
291	0.5116000111111111	1.0	0.6051160111111111	0.04	0.01644410111111111	0.01	0.01527000511111111
- + 292	0.5116000111111111	1.05	0.6051160111111111	0.04	0.01644410111111111	0.01	0.01527000511111111
293	0.5116000111111111	1.05	0.6051160111111111	0.02	0.01644410111111111	0.01	0.01527000511111111
+ 294	0.5116000111111111	1.07	0.6051160111111111	0.02	0.01644410111111111	0.01	0.01527000511111111
295	0.5116000111111111	1.1	0.6051160111111111	0.04	0.01644410111111111	0.01	0.01527000511111111
x - + 296	0.5116000111111111	1.1	0.6051160111111111	0.04	0.01644410111111111	0.01	0.01527000511111111
297	0.5116000111111111	1.15	0.6051160111111111	0.03	0.01644410111111111	0.01	0.01527000511111111
298	0.5116000111111111	1.15	0.6051160111111111	0.04	0.01644410111111111	0.01	0.01527000511111111
- + 299	0.5116000111111111	1.15	0.6051160111111111	0.04	0.01644410111111111	0.01	0.01527000511111111
x - + 300	0.5116000111111111	1.15	0.6051160111111111	0.04	0.01644410111111111	0.01	0.01527000511111111
+ 301	0.5116000111111111	1.15	0.6051160111111111	0.04	0.01644410111111111	0.01	0.01527000511111111
302	0.5116000111111111	1.15	0.6051160111111111	0.04	0.01644410111111111	0.01	0.01527000511111111
+ 303	0.5116000111111111	1.15	0.6051160111111111	0.04	0.01644410111111111	0.01	0.01527000511111111
304	0.5116000111111111	1.15	0.6051160111111111	0.04	0.01644410111111111	0.01	0.01527000511111111
- + 305	0.5116000111111111	1.15	0.6051160111111111	0.04	0.01644410111111111	0.01	0.01527000511111111
+ 306	0.5116000111111111	1.15	0.6051160111111111	0.04	0.01644410111111111	0.01	0.01527000511111111
307	0.5116000111111111	1.15	0.6051160111111111	0.04	0.01644410111111111	0.01	0.01527000511111111

Table A-I (continued)

RECORD NO	X	Y	Z	10	21	27	23	24
308	0.4367510E-02	0.5692500E-03	0.3494195E-03	-0.527000E-02	-0.5230417E-02	0.7237000E-74	0.7237000E-74	0.7237000E-74
x - + 309	0.5149000E-02	0.5692500E-03	0.317494E-03	-0.52223300E-02	-0.5146525E-02	0.7237000E-74	0.7237000E-74	0.7237000E-74
- + 310	0.1047000E-06	0.5677500E-03	0.5415167E-03	-0.556900E-02	-0.5710617E-02	0.7237000E-76	0.7237000E-76	0.7237000E-76
x - + 311	0.3650000E-02	0.5675000E-03	0.307440E-03	-0.56395E-02	-0.556900E-02	0.7237000E-76	0.7237000E-76	0.7237000E-76
312	0.7252500E-03	0.5675000E-03	0.631	-0.52245E-03	-0.5146525E-03	0.7237000E-76	0.7237000E-76	0.7237000E-76
+ 313	0.1231000E-04	0.5635900E-03	0.62	-0.637599E-03	-0.567500E-02	0.7237000E-76	0.7237000E-76	0.7237000E-76
314	0.732530E-02	0.5651000E-03	0.624390E-03	-0.51899E-02	-0.5146525E-02	0.7237000E-76	0.7237000E-76	0.7237000E-76
315	0.7277500E-03	0.5632500E-03	0.417395E-03	-0.507000E-02	-0.507000E-02	0.7237000E-76	0.7237000E-76	0.7237000E-76
+ 316	0.7552510E-03	0.5659900E-03	0.405100E-03	-0.517594E-02	-0.517594E-02	0.7237000E-76	0.7237000E-76	0.7237000E-76
+ 317	0.854740E-04	0.55335700E-03	0.62	-0.426129E-02	-0.426129E-02	0.7237000E-76	0.7237000E-76	0.7237000E-76
+ 318	0.649300E-03	0.5562500E-03	0.60	-0.435599E-02	-0.435599E-02	0.7237000E-76	0.7237000E-76	0.7237000E-76
319	0.6495610E-03	0.5547800E-03	0.391414E-03	-0.425099E-02	-0.425099E-02	0.7237000E-76	0.7237000E-76	0.7237000E-76
320	0.711500E-02	0.55527439E-03	0.60	-0.577000E-02	-0.577000E-02	0.7237000E-76	0.7237000E-76	0.7237000E-76
321	0.6610700E-02	0.5557000E-03	0.44950574E-03	-0.52245E-02	-0.52245E-02	0.7237000E-76	0.7237000E-76	0.7237000E-76
+ 322	0.7647200E-03	0.55597000E-03	0.63	-0.525639E-02	-0.525639E-02	0.7237000E-76	0.7237000E-76	0.7237000E-76
323	0.5357610E-03	0.54697500E-03	0.2133394E-03	-0.420313E-02	-0.416666E-02	0.7237000E-76	0.7237000E-76	0.7237000E-76
324	0.51430010E-02	0.54626000E-03	0.4233794E-03	-0.512090E-02	-0.507776E-02	0.7237000E-76	0.7237000E-76	0.7237000E-76
- + 325	0.6450000E-03	0.54647500E-03	0.132239E-03	-0.533649E-02	-0.5294700E-02	0.7237000E-76	0.7237000E-76	0.7237000E-76
+ 326	1.05217500E-02	0.56465000E-03	0.3130399E-03	-0.5230100E-02	-0.516886E-02	0.7237000E-76	0.7237000E-76	0.7237000E-76
327	0.4370000E-03	0.54339000E-03	0.5472119E-03	-0.5245900E-02	-0.523116E-02	0.7237000E-76	0.7237000E-76	0.7237000E-76
328	0.6460000E-03	0.54275300E-03	0.63	-0.528995E-02	-0.528995E-02	0.7237000E-76	0.7237000E-76	0.7237000E-76
329	0.6662500E-02	0.5420000E-03	0.474500E-03	-0.527099E-02	-0.527099E-02	0.7237000E-76	0.7237000E-76	0.7237000E-76
+ 330	0.4740000E-03	0.54125000E-03	0.564125E-03	-0.523595E-02	-0.519465E-02	0.7237000E-76	0.7237000E-76	0.7237000E-76
331	0.5557500E-03	0.52875000E-03	0.512500E-03	-0.512500E-02	-0.506060E-02	0.7237000E-76	0.7237000E-76	0.7237000E-76
332	0.56450000E-03	0.51775000E-03	0.3432390E-03	-0.513675E-02	-0.510567E-02	0.7237000E-76	0.7237000E-76	0.7237000E-76
+ 333	0.1000720E-04	0.5377500E-03	0.62	-0.547025E-02	-0.547025E-02	0.7237000E-76	0.7237000E-76	0.7237000E-76

Table A-I (continued)

RECD N	X	V	W	Z ₁	Z ₂	Z ₃	Z ₄
+ 334	0.409000e-03	0.5250000e-03	0.6280690e-03	-0.5309490e-03	-0.6717192e-03	0.723700e-03	0.6721700e-03
x - + 335	0.618250e-03	0.5350100e-03	0.69	-0.5320000e-03	-0.6527000e-03	0.723700e-03	0.6721700e-03
- + 336	0.113250e-03	0.5327500e-03	0.64	-0.6200000e-03	-0.6730000e-03	0.723700e-03	0.6721700e-03
337	0.1151750e-03	0.5337500e-03	0.69	-0.6270700e-03	-0.6730000e-03	0.723700e-03	0.6721700e-03
+ 338	0.1154500e-03	0.5327500e-03	0.62	-0.6276990e-03	-0.6730000e-03	0.723700e-03	0.6721700e-03
339	0.1154500e-03	0.5337500e-03	0.69	-0.6289990e-03	-0.6730000e-03	0.723700e-03	0.6721700e-03
x - + 340	0.1211750e-03	0.5311700e-03	0.62	-0.6289990e-03	-0.6730000e-03	0.723700e-03	0.6721700e-03
341	0.645100e-03	0.523500e-03	0.73	0.1715700e-03	0.11	-0.6289990e-03	0.723700e-03
342	0.52290e-03	0.5337500e-03	0.63	0.1685100e-03	0.11	-0.6289990e-03	0.723700e-03
+ 343	0.127790e-02	0.5320100e-03	0.62	0.5173670e-03	0.11	-0.6289990e-03	0.723700e-03
344	0.5275400e-03	0.5232000e-03	0.73	0.3117500e-03	0.11	-0.6289990e-03	0.723700e-03
+ 345	0.5275400e-03	0.5200000e-03	0.63	0.3168400e-03	0.11	-0.6289990e-03	0.723700e-03
+ 346	0.673780e-03	0.5202500e-03	0.63	0.1693400e-03	0.11	-0.5186350e-02	0.6723700e-02
347	0.2112e-03e-03	0.5232000e-03	0.62	0.3117500e-03	0.11	-0.5236490e-02	0.6723700e-02
+ 348	0.1446e-03e-03	0.5232000e-03	0.63	0.3168400e-03	0.11	-0.5186350e-02	0.6723700e-02
349	0.674030e-03	0.5232000e-03	0.63	0.2031600e-03	0.11	-0.5236490e-02	0.6723700e-02
x - + 350	0.64370e-03	0.5232000e-03	0.62	0.2031600e-03	0.11	-0.5236490e-02	0.6723700e-02
351	0.61560e-03	0.5232000e-03	0.63	0.2031600e-03	0.11	-0.5236490e-02	0.6723700e-02
352	0.62290e-03	0.5232000e-03	0.62	0.2031600e-03	0.11	-0.5236490e-02	0.6723700e-02
353	0.61660e-03	0.5232000e-03	0.63	0.2031600e-03	0.11	-0.5236490e-02	0.6723700e-02
354	0.61660e-03	0.5232000e-03	0.62	0.2031600e-03	0.11	-0.5236490e-02	0.6723700e-02
- + 355	0.6412e-03	0.5232000e-03	0.63	0.2031600e-03	0.11	-0.5236490e-02	0.6723700e-02
+ 356	0.6412e-03	0.5232000e-03	0.62	0.2031600e-03	0.11	-0.5236490e-02	0.6723700e-02
x - + 357	0.6412e-03	0.5232000e-03	0.63	0.2031600e-03	0.11	-0.5236490e-02	0.6723700e-02
x - + 358	0.1451250e-03	0.5337500e-03	0.63	0.2031600e-03	0.11	-0.5236490e-02	0.6723700e-02
+ 359	0.651300e-03	0.5232000e-03	0.64	0.2031600e-03	0.11	-0.5236490e-02	0.6723700e-02

Table A-I (continued)

RECORDED NO	X	Y	Z	T0	T1	T2	T3	T4	T5
+ 360	0.8177509	0.4	0.5015000	0.3	0.0	-0.653559e-006	0.2	0.7234000	0.6
- + 361	0.1263257	1.6	0.3025000	0.1	1.0	-0.6250000	0.2	-0.6450497	0.2
- + 362	0.4136000	0.4	0.5014000	0.1	1.0	-0.6250000	0.2	-0.6450497	0.2
- + 363	0.7040000	0.2	0.6002000	0.1	1.0	-0.6030000	0.2	-0.6730000	0.2
X - + 364	0.6922150	0.1	0.5015000	0.1	1.0	-0.6250000	0.2	-0.6450497	0.2
365	0.6512230	0.1	0.6497700	0.1	1.0	-0.6250000	0.2	-0.6450497	0.2
366	0.6512230	0.1	0.6497700	0.1	1.0	-0.6250000	0.2	-0.6450497	0.2
Y - + 367	0.6750000	0.1	0.6497700	0.1	1.0	-0.6250000	0.2	-0.6450497	0.2
368	0.6512230	0.1	0.6497700	0.1	1.0	-0.6250000	0.2	-0.6450497	0.2
Y - + 369	0.6512230	0.1	0.6497700	0.1	1.0	-0.6250000	0.2	-0.6450497	0.2
- + 370	0.6750000	0.1	0.6497700	0.1	1.0	-0.6250000	0.2	-0.6450497	0.2
X - + 371	0.6750000	0.1	0.6497700	0.1	1.0	-0.6250000	0.2	-0.6450497	0.2
- + 372	0.6175260	0.6	0.6162930	0.1	1.0	-0.6250000	0.2	-0.6450497	0.2
- + 373	0.6775000	0.1	0.6497700	0.1	1.0	-0.6250000	0.2	-0.6450497	0.2
+ 374	0.6175260	0.6	0.6162930	0.1	1.0	-0.6250000	0.2	-0.6450497	0.2
- + 375	0.6775000	0.1	0.6497700	0.1	1.0	-0.6250000	0.2	-0.6450497	0.2
376	0.6505000	0.2	0.6496500	0.1	1.0	-0.6250000	0.2	-0.6450497	0.2
+ 377	0.1263257	0.6	0.6677700	0.1	1.0	-0.6250000	0.2	-0.6450497	0.2
- + 378	0.6765000	0.2	0.6497500	0.1	1.0	-0.6250000	0.2	-0.6450497	0.2
+ 379	0.6765000	0.2	0.6496500	0.1	1.0	-0.6250000	0.2	-0.6450497	0.2
+ 380	0.6136000	0.6	0.6453000	0.1	1.0	-0.6250000	0.2	-0.6450497	0.2
- + 381	0.6516500	0.2	0.6497500	0.1	1.0	-0.6250000	0.2	-0.6450497	0.2
382	0.6516500	0.2	0.6497500	0.1	1.0	-0.6250000	0.2	-0.6450497	0.2
383	0.6516500	0.2	0.6497500	0.1	1.0	-0.6250000	0.2	-0.6450497	0.2
- + 384	0.6735000	0.2	0.6496500	0.1	1.0	-0.6250000	0.2	-0.6450497	0.2
X - + 385	0.6516500	0.2	0.6497500	0.1	1.0	-0.6250000	0.2	-0.6450497	0.2

Table A-I (continued)

DUMPER FILE

RECORD NO.	X	Y	Z	41	42	43	44
+ 386	3.663600E 03	0.446500E 03	0.447500E 00	-0.490000E 02	-0.495240E 02	0.723700E 02	0.723700E 02
x - + 387	0.417600E 62	0.445500E 03	1.265590E 11	-0.502000E 02	-0.475401E 02	-0.575000E 02	-0.575000E 01
+ 388	3.765500E 37	0.426200E 03	0.311634E 01	-0.510000E 02	-0.497636E 02	0.237000E 02	0.237000E 01
x - + 389	0.126240E 34	0.452500E 03	1.04	-0.637000E 02	-0.637000E 02	-0.637000E 02	-0.637000E 02
x - + 390	0.113600E 04	0.432500E 03	2.03	-0.615100E 02	-0.615100E 02	-0.615100E 02	-0.615100E 02
+ 391	0.112500E 03	0.431760E 03	3.03	-0.539959E 02	-0.539959E 02	-0.539959E 02	-0.539959E 02
- + 392	3.102075E 04	2.417000E 03	1.04	-0.514000E 02	-0.514000E 02	-0.514000E 02	-0.514000E 02
x - + 393	0.648200E 07	0.424700E 03	1.61-2.56E 01	-0.481694E 02	-0.481694E 02	-0.481694E 02	-0.481694E 02
- + 394	3.624760E 03	0.427600E 03	3.03	-0.527450E 02	-0.527450E 02	-0.527450E 02	-0.527450E 02
395	0.758300E 01	0.413670E 01	0.3	0.116725E 01	-0.520000E 02	-0.520000E 02	-0.520000E 02
x - + 396	0.62745020E 02	0.607400E 03	2.03	-0.525100E 02	-0.525100E 02	-0.525100E 02	-0.525100E 02
- + 397	3.638259E 04	0.405250E 03	0.63	-0.530000E 02	-0.530000E 02	-0.530000E 02	-0.530000E 02
+ 398	4.126350E 04	0.493750E 02	1.00	-0.622640E 02	-0.622640E 02	-0.622640E 02	-0.622640E 02
+ 399	3.61135150E 04	0.4000E 03	2.03	-0.514000E 02	-0.514000E 02	-0.514000E 02	-0.514000E 02
x - + 400	1.134725E 06	0.765250E 02	0.43	-0.530000E 02	-0.530000E 02	-0.530000E 02	-0.530000E 02
401	0.922500E 02	0.259250E 03	0.00	-0.524000E 02	-0.524000E 02	-0.524000E 02	-0.524000E 02
402	0.677270E 02	0.447270E 03	1.03	-0.524000E 02	-0.524000E 02	-0.524000E 02	-0.524000E 02
- + 403	0.724600E 03	0.677500E 03	0.63	0.324000E 02	-0.533427E 02	-0.533427E 02	-0.533427E 02
404	3.86275700E 02	0.403000E 03	2.02	-0.514000E 02	-0.514000E 02	-0.514000E 02	-0.514000E 02
+ 405	0.1647500E 04	0.877400E 02	1.67-2.62E 01	-0.508000E 02	-0.508000E 02	-0.508000E 02	-0.508000E 02
406	3.10108500E 04	0.1712500E 01	1.01	-0.531100E 02	-0.531100E 02	-0.531100E 02	-0.531100E 02
+ 407	3.674500E 04	0.417400E 03	2.03	-0.545000E 02	-0.545000E 02	-0.545000E 02	-0.545000E 02
- + 408	3.6777500E 04	0.721500E 03	3.03	-0.605000E 02	-0.605000E 02	-0.605000E 02	-0.605000E 02
+ 409	3.140400E 04	0.174500E 01	1.01	-0.531100E 02	-0.531100E 02	-0.531100E 02	-0.531100E 02
x - + 410	0.115750E 04	0.349750E 03	0.00	-0.615000E 02	-0.615000E 02	-0.615000E 02	-0.615000E 02
411	0.227000E 03	0.369500E 02	0.112095E 01	-0.517000E 02	-0.517000E 02	-0.517000E 02	-0.517000E 02

Table A-1 (continued)

+ 412	0.6200000e+02	0.0	0.121560e+03	0.0	-0.5170000e+02	-0.5170000e+02	0.0	0.723700e+02	0.0	0.723700e+02	0.0	0.723700e+02
+ 413	0.6213333e+01	0.1	0.354500e+01	0.1	0.10100e+01	0.0	-0.630964e+01	0.0	-0.5290e+01	0.0	-0.5290e+01	0.0
+ 414	0.6243700e+02	0.4	0.3632500e+02	0.4	0.25000e+02	0.0	-0.528114e+02	0.0	-0.528114e+02	0.0	-0.528114e+02	0.0
415	0.6252700e+02	0.5	0.251500e+02	0.5	0.121220e+02	0.0	-0.513000e+02	0.0	-0.513000e+02	0.0	-0.513000e+02	0.0
+ 416	0.6272500e+02	0.5	0.35000e+02	0.5	0.0	0.0	-0.6170000e+02	0.0	-0.5282000e+02	0.0	-0.5282000e+02	0.0
+ 417	0.6282200e+02	0.6	0.3617000e+02	0.6	0.0	0.0	-0.5254000e+02	0.0	-0.5254000e+02	0.0	-0.5254000e+02	0.0
* + 418	0.6310000e+02	0.7	0.3427000e+02	0.7	0.0	0.0	-0.5176000e+02	0.0	-0.5176000e+02	0.0	-0.5176000e+02	0.0
+ 419	0.6326200e+02	0.6	0.242400e+02	0.6	0.0	0.0	-0.5170000e+02	0.0	-0.5170000e+02	0.0	-0.5170000e+02	0.0
x - + 420	0.6370000e+02	0.6	0.3575000e+02	0.6	0.0	0.0	-0.5170000e+02	0.0	-0.5170000e+02	0.0	-0.5170000e+02	0.0
- + 421	0.6375000e+02	0.7	0.3575000e+02	0.7	0.0	0.0	-0.5170000e+02	0.0	-0.5170000e+02	0.0	-0.5170000e+02	0.0
+ 422	0.6375000e+02	0.7	0.33372500e+02	0.7	0.0	0.0	-0.5170000e+02	0.0	-0.5170000e+02	0.0	-0.5170000e+02	0.0
423	0.6427500e+02	0.7	0.3370000e+02	0.7	0.0	0.0	-0.5170000e+02	0.0	-0.5170000e+02	0.0	-0.5170000e+02	0.0
- + 424	0.64372500e+02	0.7	0.3310000e+02	0.7	0.0	0.0	-0.5170000e+02	0.0	-0.5170000e+02	0.0	-0.5170000e+02	0.0
x - + 425	0.6457000e+02	0.7	0.3510000e+02	0.7	0.0	0.0	-0.5170000e+02	0.0	-0.5170000e+02	0.0	-0.5170000e+02	0.0
- + 426	0.6500000e+02	0.8	0.3164500e+03	0.8	0.0	0.0	-0.5210000e+02	0.0	-0.5170000e+02	0.0	-0.5170000e+02	0.0
- + 427	0.6504700e+02	0.8	0.3152500e+03	0.8	0.0	0.0	-0.5170000e+02	0.0	-0.5170000e+02	0.0	-0.5170000e+02	0.0
+ 428	0.6512700e+02	0.7	0.3170000e+03	0.7	0.0	0.0	-0.5170000e+02	0.0	-0.5170000e+02	0.0	-0.5170000e+02	0.0
+ 429	0.6547000e+02	0.5	0.3117500e+03	0.5	0.0	0.0	-0.5170000e+02	0.0	-0.5170000e+02	0.0	-0.5170000e+02	0.0
+ 430	0.6746000e+02	0.7	0.3157000e+03	0.7	0.0	0.0	-0.5170000e+02	0.0	-0.5170000e+02	0.0	-0.5170000e+02	0.0
- + 431	0.6772700e+02	0.6	0.3070000e+03	0.6	0.0	0.0	-0.5170000e+02	0.0	-0.5170000e+02	0.0	-0.5170000e+02	0.0
+ 432	0.68202500e+02	0.6	0.3045000e+03	0.6	0.0	0.0	-0.5170000e+02	0.0	-0.5170000e+02	0.0	-0.5170000e+02	0.0
+ 433	0.6910000e+02	0.6	0.3072500e+03	0.6	0.0	0.0	-0.5170000e+02	0.0	-0.5170000e+02	0.0	-0.5170000e+02	0.0
434	0.6950000e+02	0.6	0.3045000e+03	0.6	0.0	0.0	-0.5170000e+02	0.0	-0.5170000e+02	0.0	-0.5170000e+02	0.0
435	0.6987000e+02	0.6	0.3052500e+03	0.6	0.0	0.0	-0.5170000e+02	0.0	-0.5170000e+02	0.0	-0.5170000e+02	0.0
+ 436	0.7112400e+02	0.4	0.3032500e+03	0.4	0.0	0.0	-0.5170000e+02	0.0	-0.5170000e+02	0.0	-0.5170000e+02	0.0
* + 437	0.7150000e+02	0.4	0.3032500e+03	0.4	0.0	0.0	-0.5170000e+02	0.0	-0.5170000e+02	0.0	-0.5170000e+02	0.0

Table A-I (continued)

RECORD NO.	X	Y	Z	Z1	Z2	Z3	Z4	
+ 438	0.8110000	0.3	0.3002500	0.3	0.15007300E-00	-0.49290994E-02	-0.4914125E-02	0.127000E-06
+ 439	0.9745000	0.3	0.2650100	0.3	0.0	-0.517000E-02	-0.517000E-02	0.127000E-06
- + 440	0.1087500	0.4	0.2441500	0.3	0.61360594	0.0	-0.530000E-02	-0.758657E-02
- + 441	0.7732700	0.2	0.2650100	0.3	0.35463500	0.0	-0.602000E-02	-0.676663E-02
- + 442	0.6260250	0.3	0.2442500	0.3	0.7350100	0.0	-0.64570521	-0.64570500E-02
- + 443	0.6063300	0.3	0.2441500	0.3	0.0	-0.64565941	-0.64565994	0.0
X - + 444	0.6241000	0.3	0.2650100	0.3	0.64544821	0.0	-0.64565941	0.0
- + 445	0.6207800	0.4	0.2441500	0.3	0.0	-0.730000E-02	-0.41424826	-0.14649597
+ 446	0.6242250	0.3	0.2762200	0.3	0.0	-0.62465261	0.0	-0.62465261
- + 447	0.6272700	0.3	0.2752200	0.3	0.0	-0.64460002	-0.3645462800	0.0
- + 448	0.6149500	0.3	0.2752200	0.3	0.0	-2.054800E-02	-0.3645462800	0.0
+ 449	0.6242000	0.4	0.2762200	0.3	0.0	-0.602000E-02	-0.602000E-02	-0.602000E-02
- + 450	0.6167250	0.2	0.6174250	0.3	0.21944396	0.0	-0.650000E-02	0.0
- + 451	0.6111200	0.3	0.27427250	0.3	0.0	-0.575000E-02	-0.674850E-02	-0.575000E-02
X - + 452	0.61136100	0.2	0.62157200	0.2	0.0	-0.650000E-02	-0.650000E-02	-0.650000E-02
+ 453	0.61654250	0.2	0.62727250	0.2	0.28686500	0.0	-0.645000E-02	-0.645000E-02
- + 454	0.61274100	0.3	0.62712100	0.3	0.0	-0.645000E-02	-0.645000E-02	-0.645000E-02
X - + 455	0.61741500	0.2	0.62712100	0.2	0.43074074	0.0	-0.645000E-02	-0.645000E-02
X - + 456	0.6062300	0.3	0.62550100	0.3	0.0	-0.62550100	-0.62550100	0.0
- + 457	0.6167500	0.2	0.62251000	0.2	0.0	-0.505000E-02	-0.505000E-02	-0.505000E-02
- + 458	0.60501750	0.2	0.6227000	0.2	0.0	-0.510000E-02	-0.510000E-02	-0.510000E-02
X - + 459	0.61741500	0.2	0.62550100	0.2	0.0	-0.645000E-02	-0.645000E-02	-0.645000E-02
+ 460	0.61136100	0.2	0.62550100	0.2	0.0	-0.645000E-02	-0.645000E-02	-0.645000E-02
- + 461	0.6062300	0.3	0.6248200	0.3	0.0	-0.645000E-02	-0.645000E-02	-0.645000E-02
- + 462	0.61915000	0.2	0.62345000	0.2	0.0	-0.505000E-02	-0.505000E-02	-0.505000E-02
- + 463	0.61649250	0.2	0.62345000	0.2	0.0	-0.510000E-02	-0.510000E-02	-0.510000E-02

Table A-I (continued)

REF ID	Y	Z1	Z2	Z3	Z4	Z5	Z6	Z7	Z8	Z9
+ 464	0.5445000E 02	0.2267500E 04	3.2	-0.1419999E 02	-0.4210000E 32	0.7379300E 76	0.219300	72		
465	3.2007567E 04	1.2267300E 05	0.2	-0.1220000E 05	-0.5120000E 97	0.7379300E 76	0.219300	72		
+ 466	0.5785000E 03	0.2124000E 04	3.2	-0.1220000E 05	-0.5120000E 97	0.7379300E 76	0.219300	72		
- + 467	0.8155000E 02	0.1924000E 03	1.3	-0.1220000E 05	-0.5120000E 97	0.7379300E 76	0.219300	72		
X - + 468	0.1712750E 04	0.1924000E 03	0.2	-0.1405000E 23	-0.4920000E 32	-0.1371000E 97	0.7379300E 76	0.219300	72	
X - + 469	0.111362500E 04	0.2124000E 03	3.2	-0.1380000E 05	-0.5120000E 97	0.7379300E 76	0.219300	72		
+ 470	0.6107810E 14	0.7124000E 05	0.2	-0.1259450E 03	-0.5120000E 97	0.7379300E 76	0.219300	72		
- + 471	0.2662030E 04	0.2124000E 03	0.2	-0.1380000E 05	-0.5120000E 97	0.7379300E 76	0.219300	72		
+ 472	0.6107810E 14	0.1124000E 03	0.2	-0.1259450E 03	-0.5120000E 97	0.7379300E 76	0.219300	72		
X - + 473	0.1231510E 05	0.1224000E 03	0.2	-0.1380000E 05	-0.5120000E 97	0.7379300E 76	0.219300	72		
+ 474	0.1423750E 04	0.1324000E 03	0.2	-0.1259450E 03	-0.5120000E 97	0.7379300E 76	0.219300	72		
X - + 475	0.11136750E 14	0.1124000E 03	0.2	-0.1380000E 05	-0.5120000E 97	0.7379300E 76	0.219300	72		
+ 476	0.1231500E 04	0.1324000E 03	0.2	-0.1259450E 03	-0.5120000E 97	0.7379300E 76	0.219300	72		
- + 477	0.1113600E 04	0.1224000E 03	0.2	-0.1380000E 05	-0.5120000E 97	0.7379300E 76	0.219300	72		
+ 478	0.11135750E 04	0.1124000E 03	0.2	-0.1380000E 05	-0.5120000E 97	0.7379300E 76	0.219300	72		
+ 479	0.1103350E 04	0.1224000E 03	0.2	-0.1259450E 03	-0.5120000E 97	0.7379300E 76	0.219300	72		
+ 480	0.1103350E 04	0.1124000E 03	0.2	-0.1380000E 05	-0.5120000E 97	0.7379300E 76	0.219300	72		
481	0.11135750E 04	0.1224000E 03	0.2	-0.1259450E 03	-0.5120000E 97	0.7379300E 76	0.219300	72		
+ 482	0.11135750E 04	0.1124000E 03	0.2	-0.1380000E 05	-0.5120000E 97	0.7379300E 76	0.219300	72		
+ 483	0.1113500E 04	0.1224000E 03	0.2	-0.1259450E 03	-0.5120000E 97	0.7379300E 76	0.219300	72		
484	0.11135750E 04	0.1124000E 03	0.2	-0.1380000E 05	-0.5120000E 97	0.7379300E 76	0.219300	72		
X - + 485	0.14712500E 02	0.1113000E 03	0.2	-0.1380000E 05	-0.5120000E 97	-0.4637999E 02	-0.4637999E 02	0.6525000E 01	0.6525000E 01	
486	0.14712500E 02	0.1113000E 03	0.2	-0.1380000E 05	-0.5120000E 97	-0.4637999E 02	-0.4637999E 02	0.6525000E 01	0.6525000E 01	
487	0.1113500E 04	0.1124000E 03	0.2	-0.1259450E 03	-0.5120000E 97	0.7379300E 76	0.219300	72		
+ 488	0.11135750E 04	0.1124000E 03	0.2	-0.1380000E 05	-0.5120000E 97	0.7379300E 76	0.219300	72		
+ 489	0.11135750E 04	0.1124000E 03	0.2	-0.1380000E 05	-0.5120000E 97	0.7379300E 76	0.219300	72		

Table A-I (continued)

APPENDIX B

PERSPECTIVE STUDIES OF THE HANFORD RESERVATION GRAVITY STUDIES

Three-dimensional perspective views of the various gravity studies of the Hanford reservation were constructed using the Harvard SYMVU Computer Program on an IBM 360-65 Computer. The figures show three stages of progress in the gravity studies. These are:

1. The Peterson-Bouguer gravity map;
2. The Deju and Richard residual gravity map; and,
3. The current gravity-bedrock maps.

Each set of data is viewed from the south, west, north, and east, respectively. All views are at an altitude of 25 degrees above the horizontal.

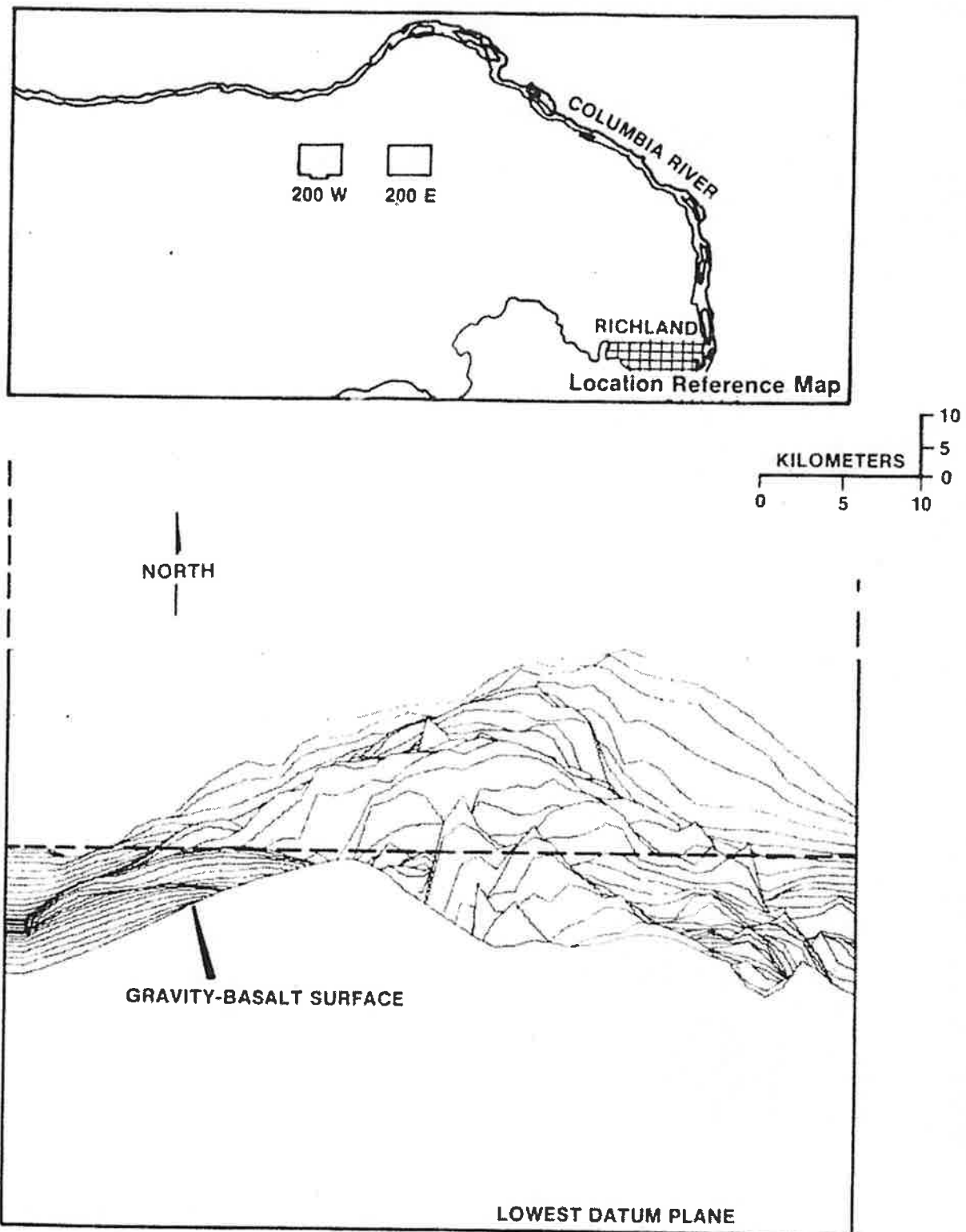


FIGURE B-1

HANFORD RESERVATION PETERSON-BOUGUER GRAVITY MAP, SOUTH VIEW

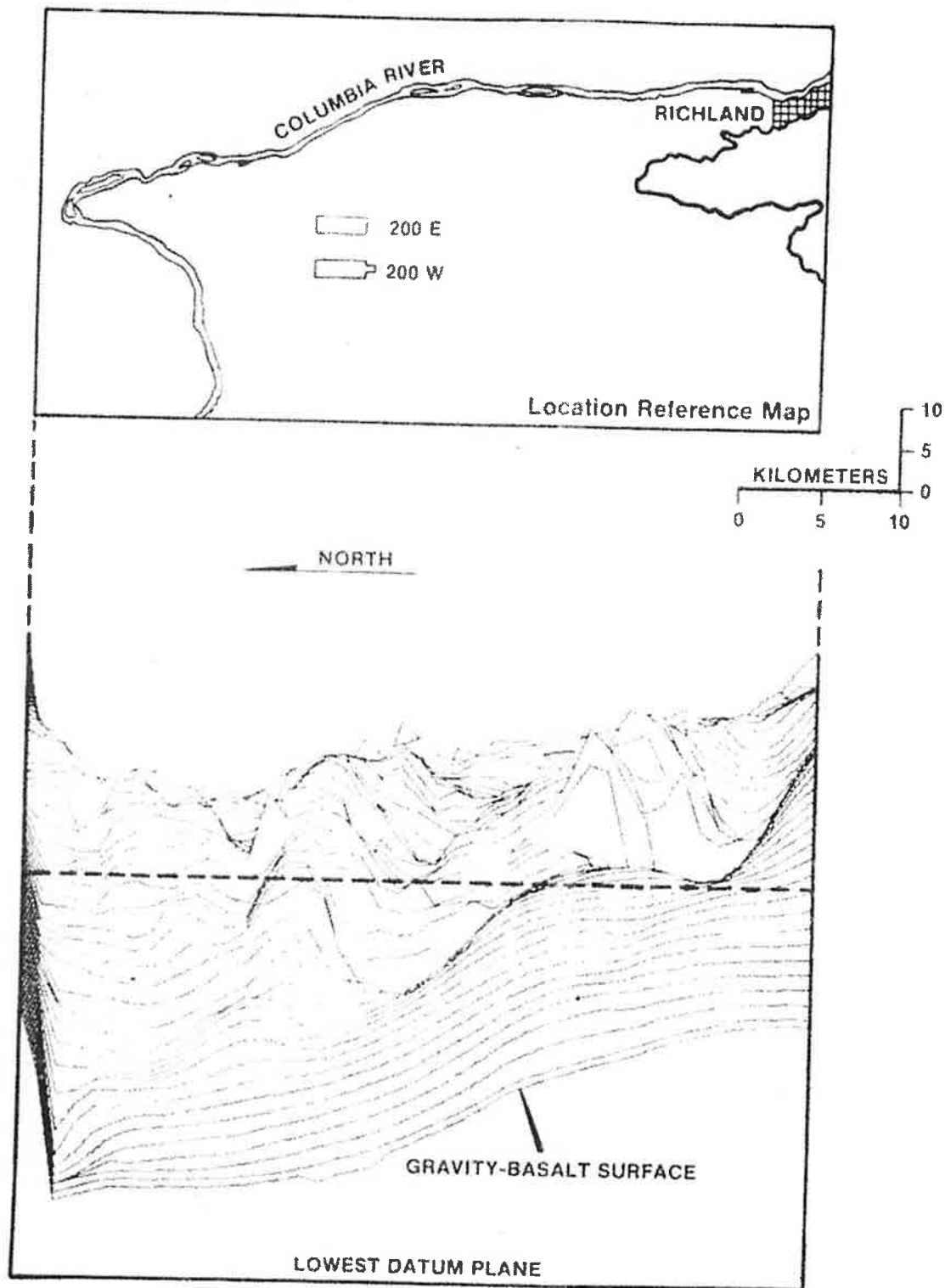


FIGURE B-2

HANFORD RESERVATION PETERSON-BOUGUER GRAVITY MAP, WEST VIEW

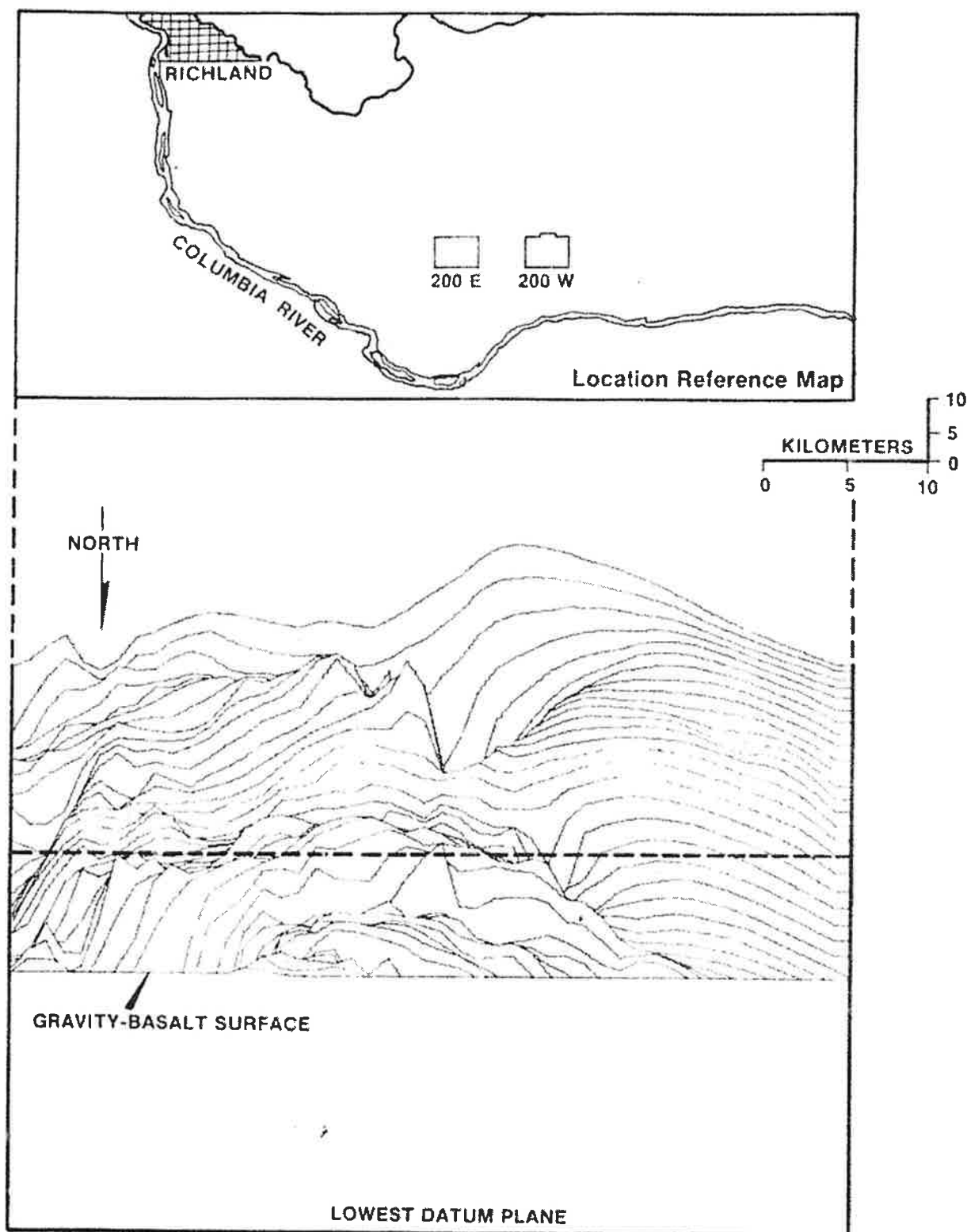


FIGURE B-3

HANFORD RESERVATION PETERSON-BOUGUER GRAVITY MAP, NORTH VIEW

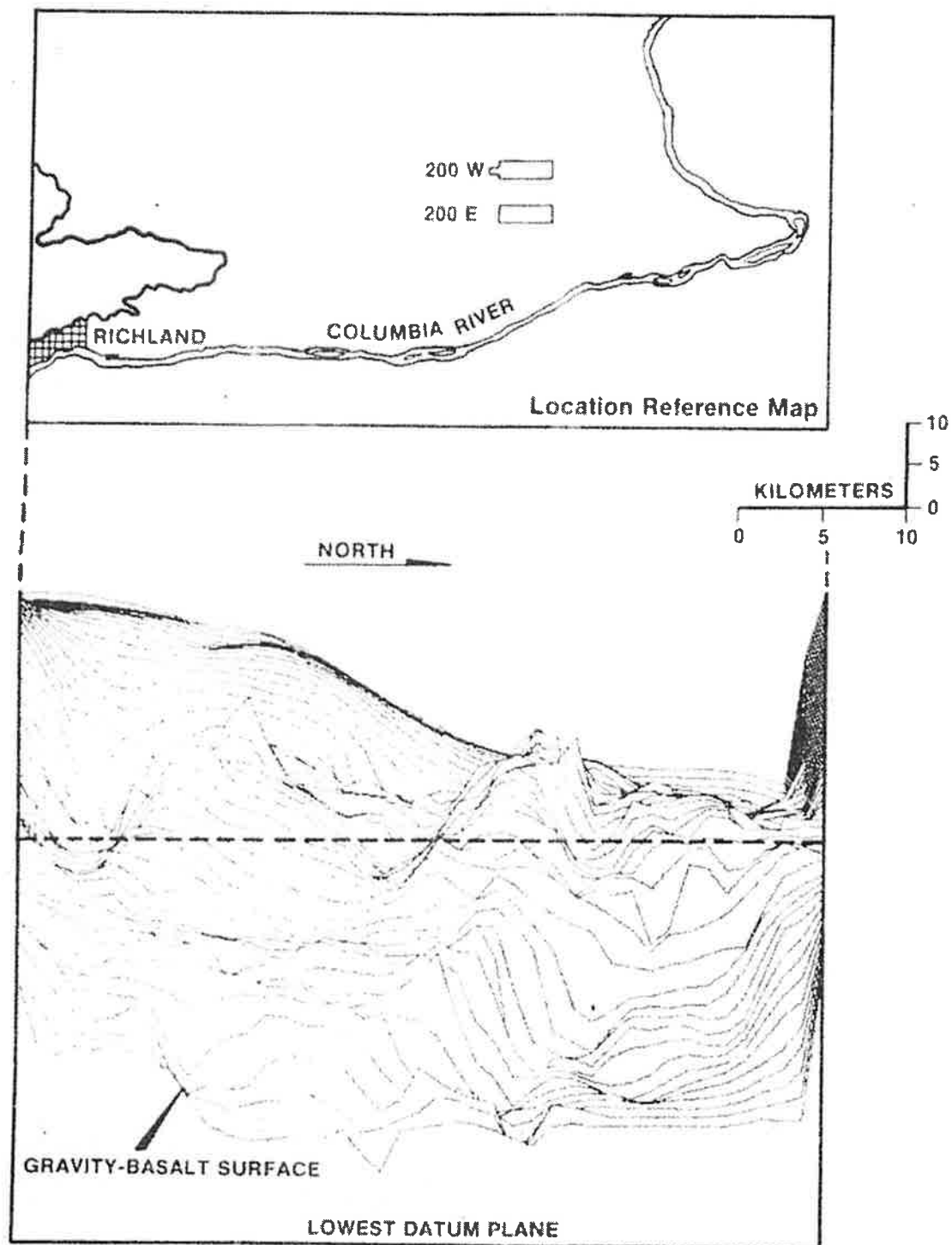


FIGURE B-4

HANFORD RESERVATION PETERSON-BOUGUER GRAVITY MAP, EAST VIEW

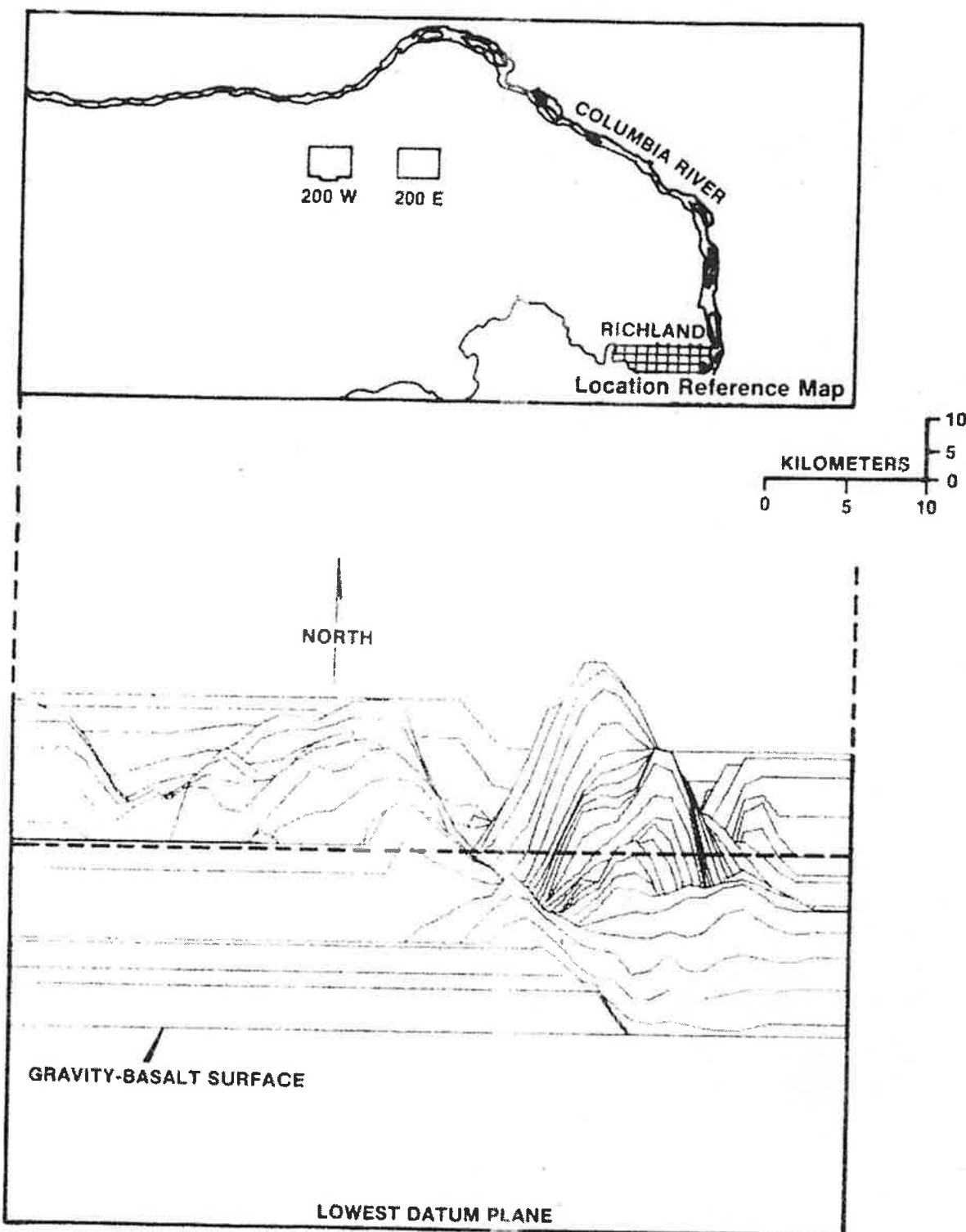


FIGURE B-5

HANFORD RESERVATION DEJU AND RICHARD RESIDUAL GRAVITY MAP, SOUTH VIEW

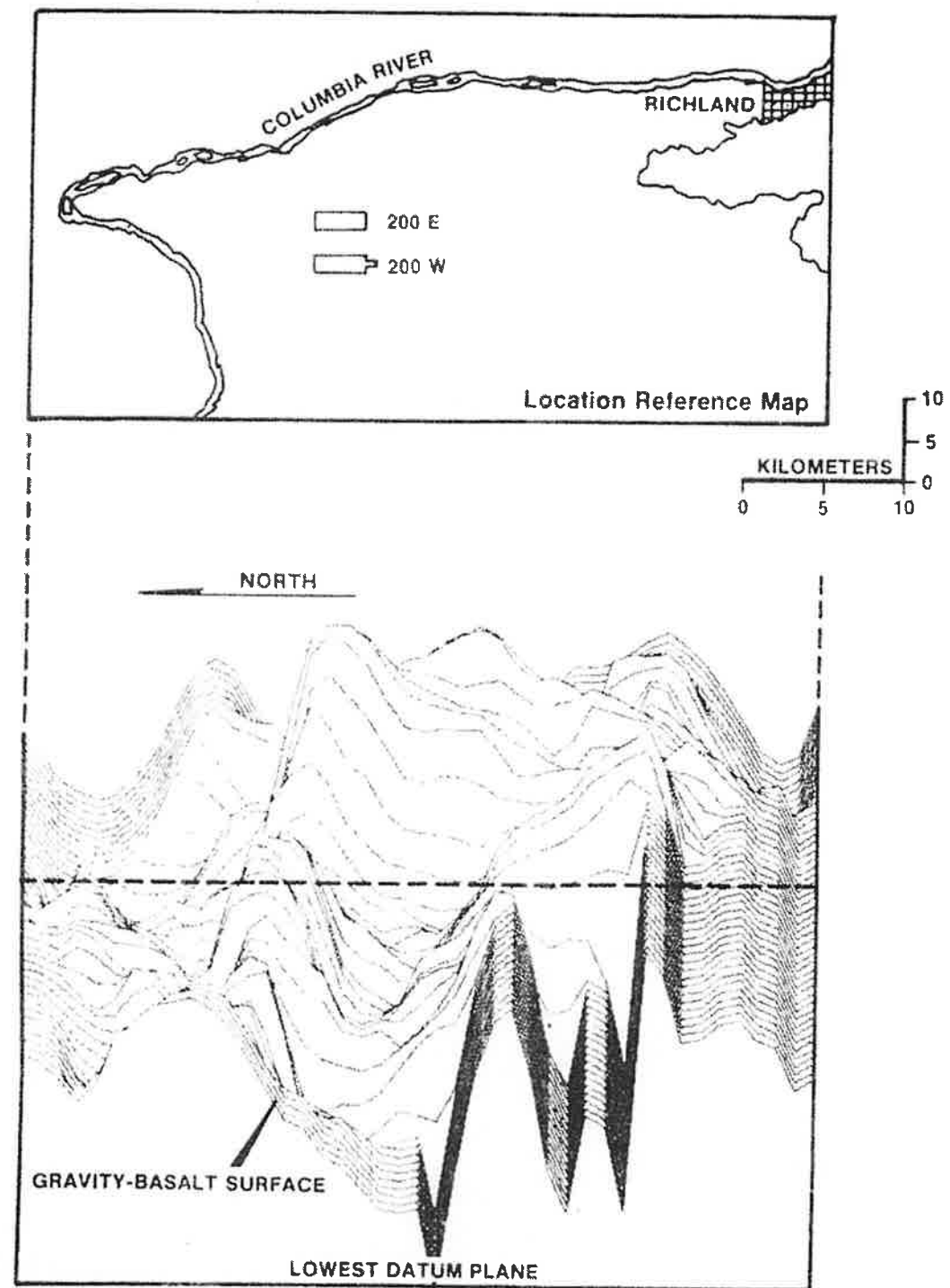


FIGURE B-6

HANFORD RESERVATION DEJU AND RICHARD RESIDUAL GRAVITY MAP, WEST VIEW

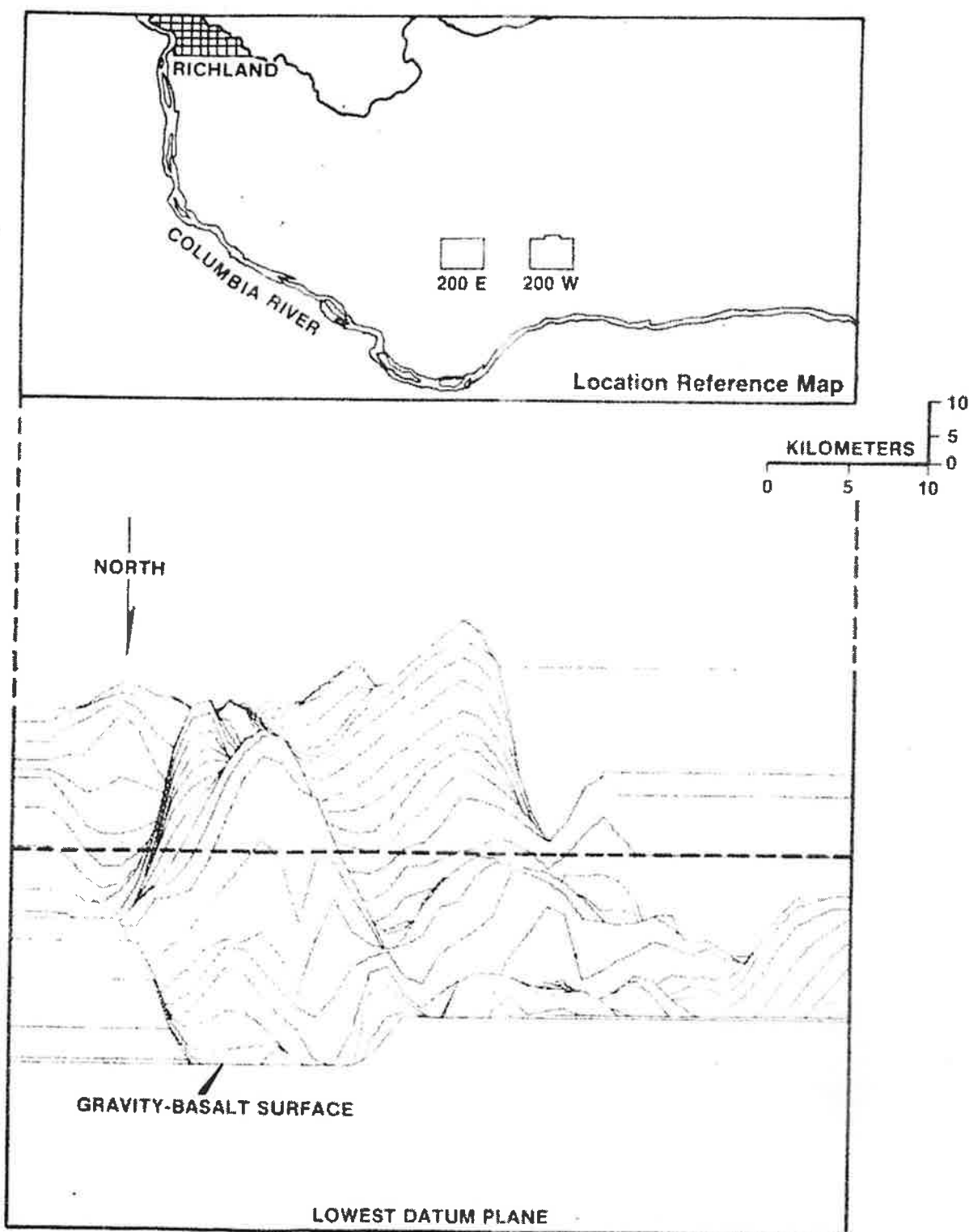


FIGURE B-7

HANFORD RESERVATION DEJU AND RICHARD RESIDUAL GRAVITY MAP, NORTH VIEW

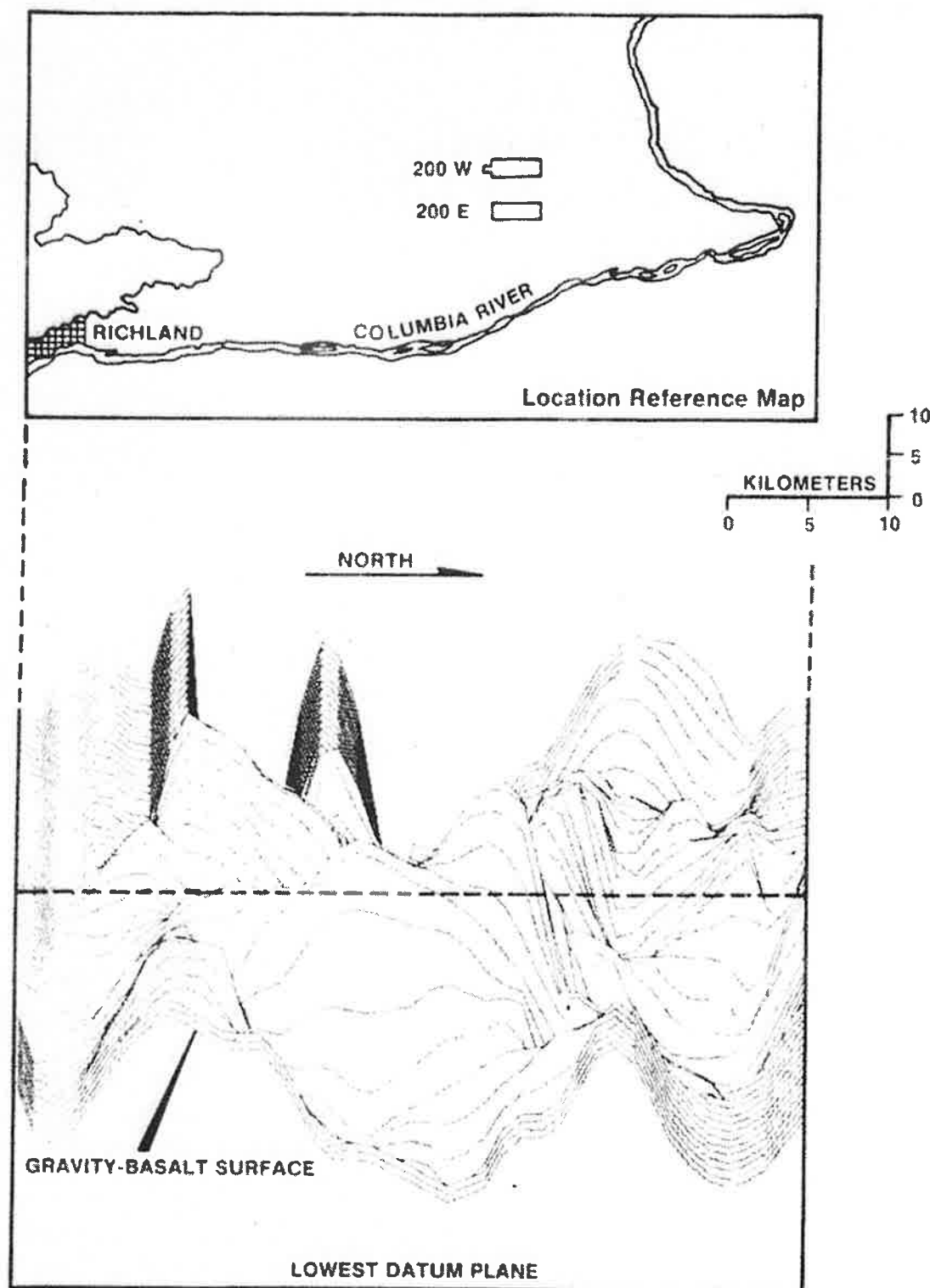


FIGURE B-8

HANFORD RESERVATION DEJU AND RICHARD RESIDUAL GRAVITY MAP, EAST VIEW

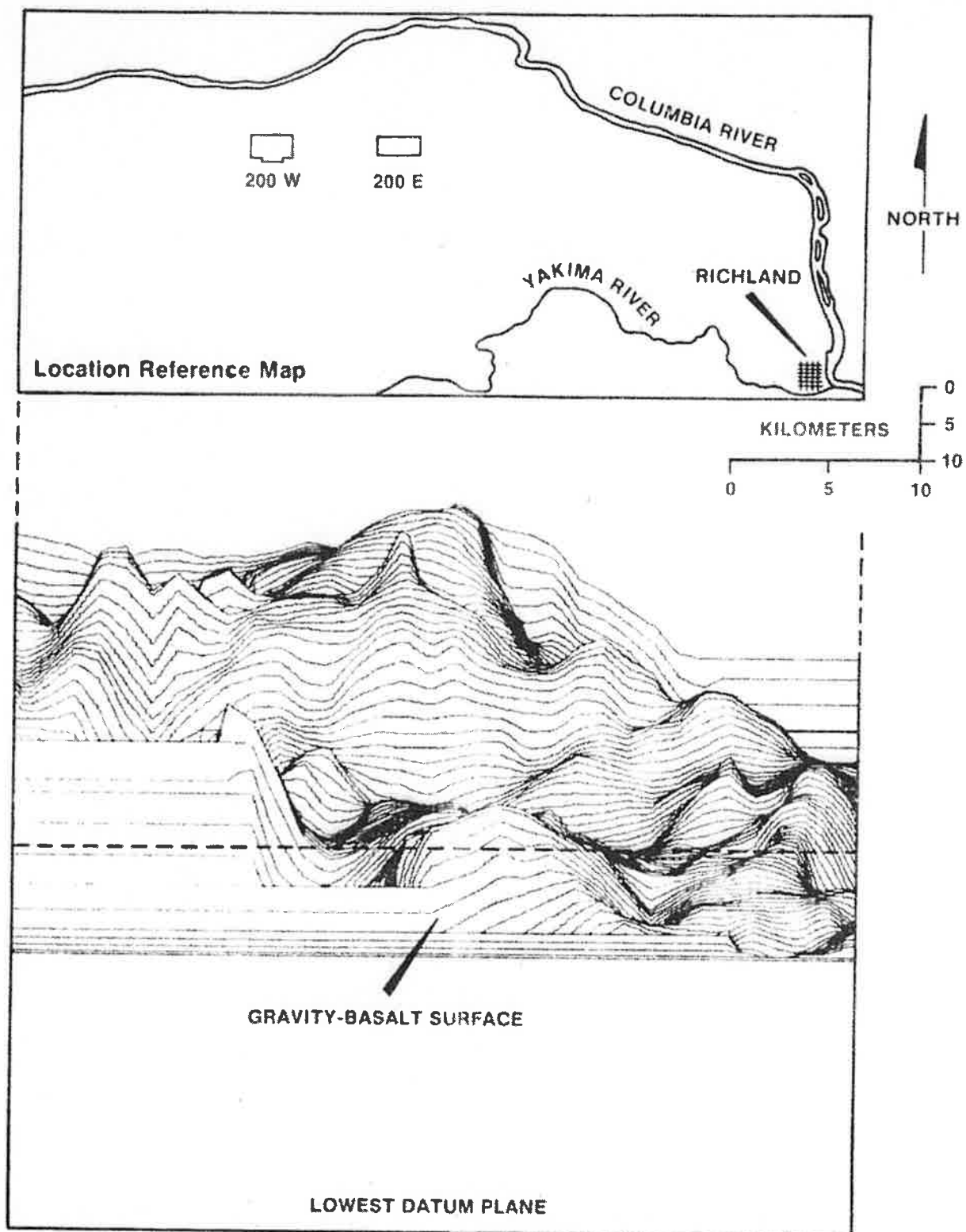


FIGURE B-9

HANFORD RESERVATION 499-POINT GRAVITY BEDROCK MAP, SOUTH VIEW

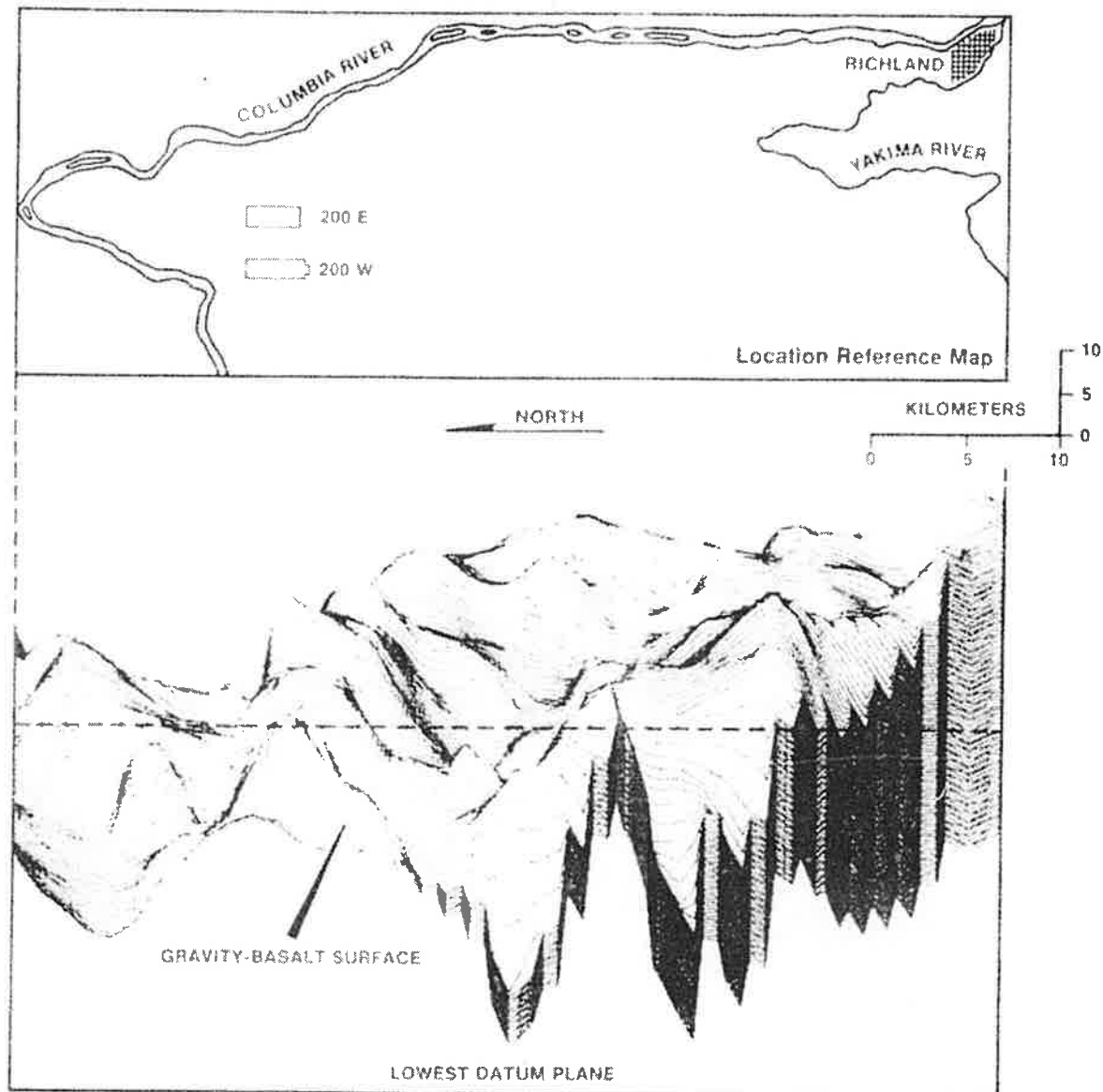


FIGURE B-10

HANFORD RESERVATION 499-POINT GRAVITY BEDROCK MAP, WEST VIEW

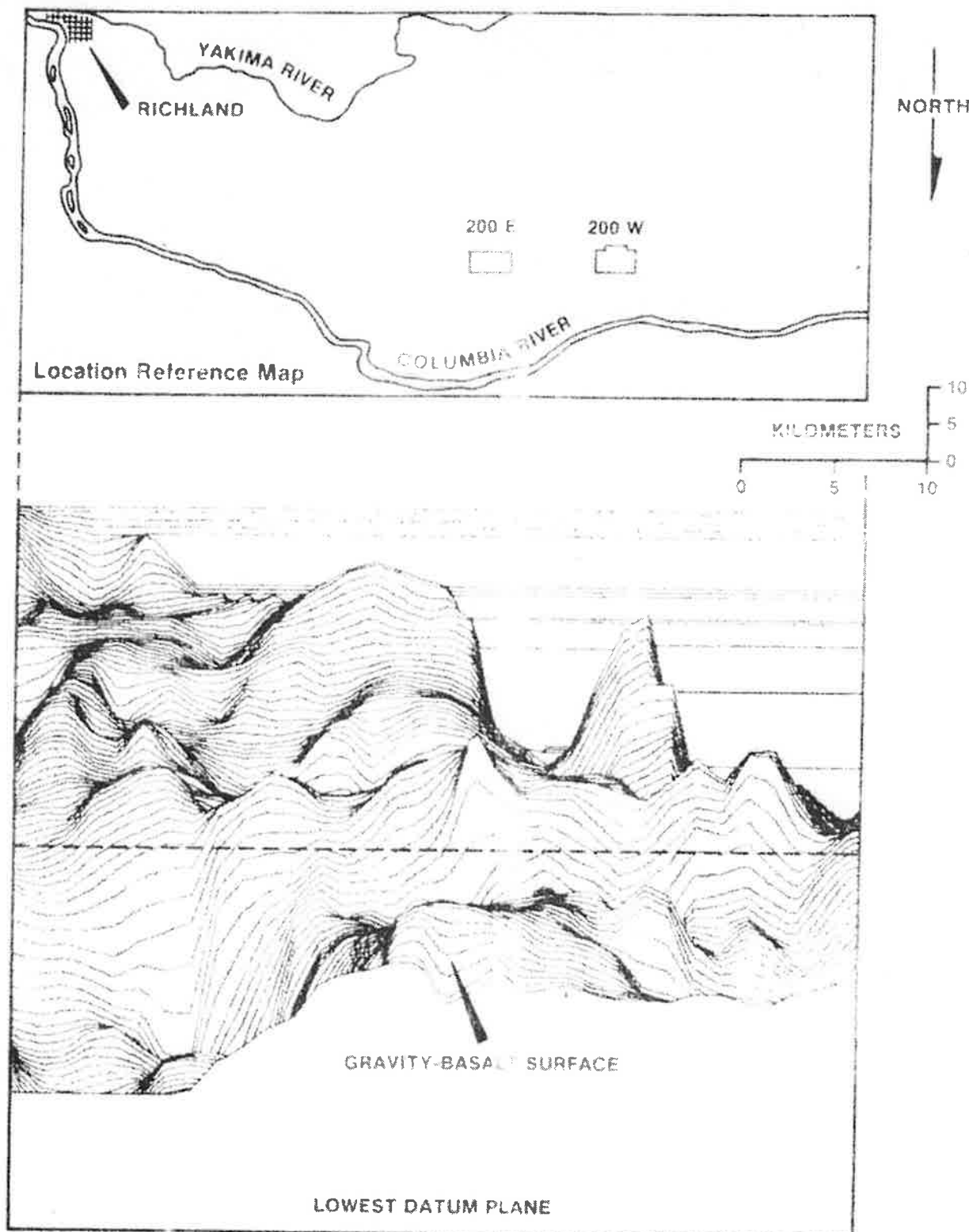


FIGURE 4-11

HANFORD RESERVATION 499-POINT CREDITY BEDROCK MAP, NORTH VIEW

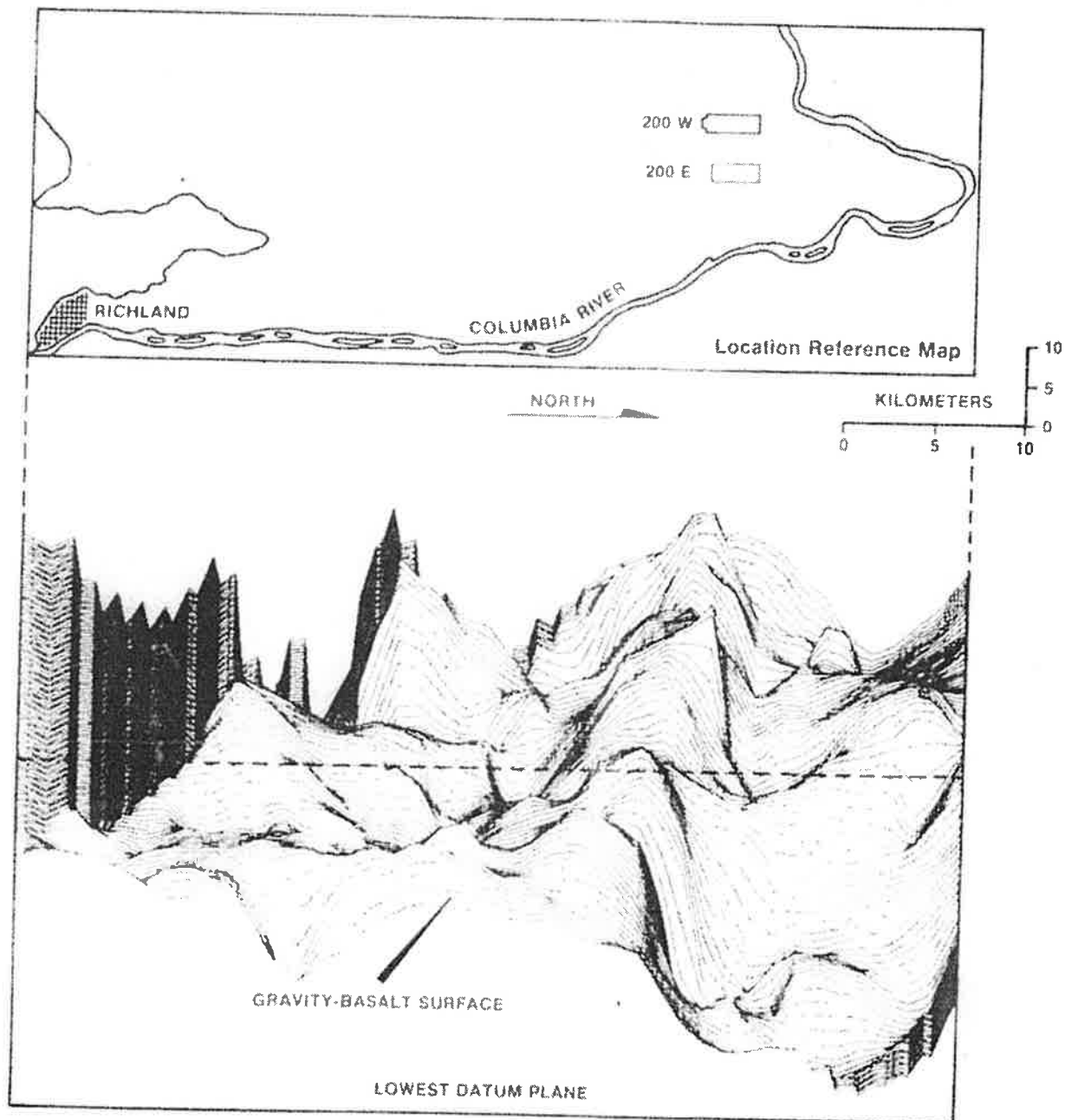


FIGURE B-12

HANFORD RESERVATION 499-POINT GRAVITY BEDROCK MAP, EAST VIEW

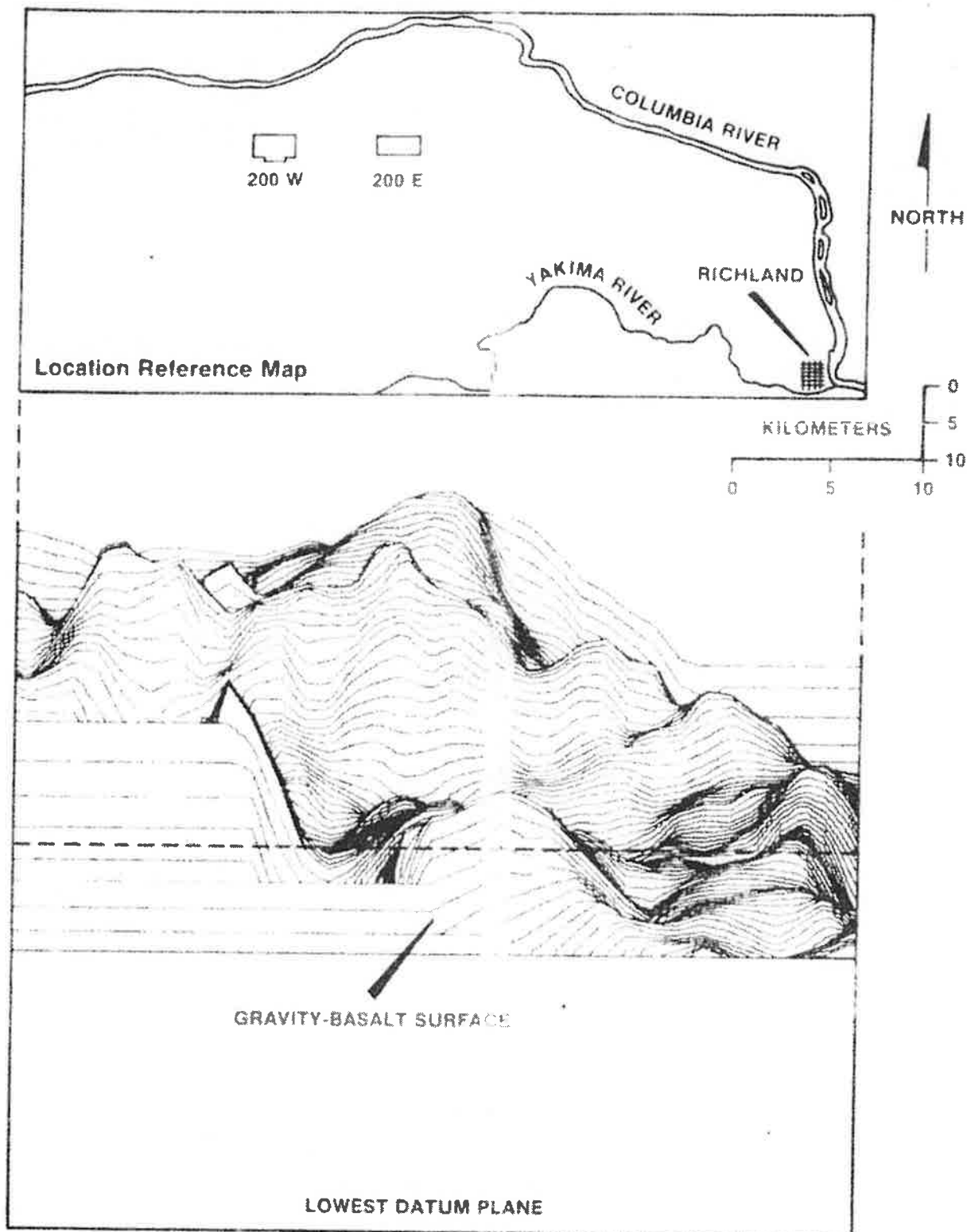


FIGURE I-13

HANFORD RESERVATION 344-POINT GRAVITY BEDROCK MAP, SOUTH VIEW

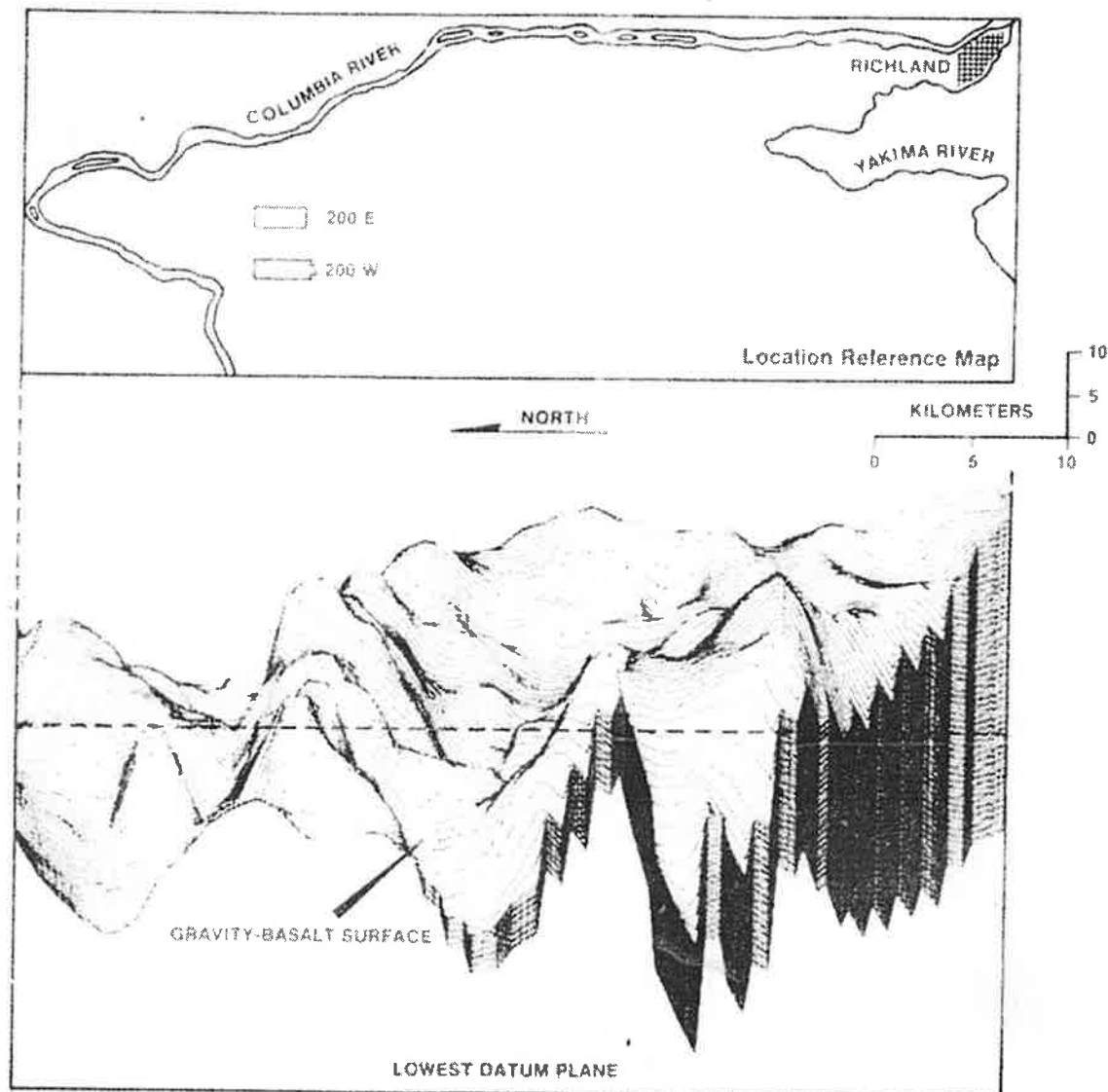


FIGURE B-14

HANFORD RESERVATION 344-POINT GRAVITY BEDROCK MAP, WEST VIEW

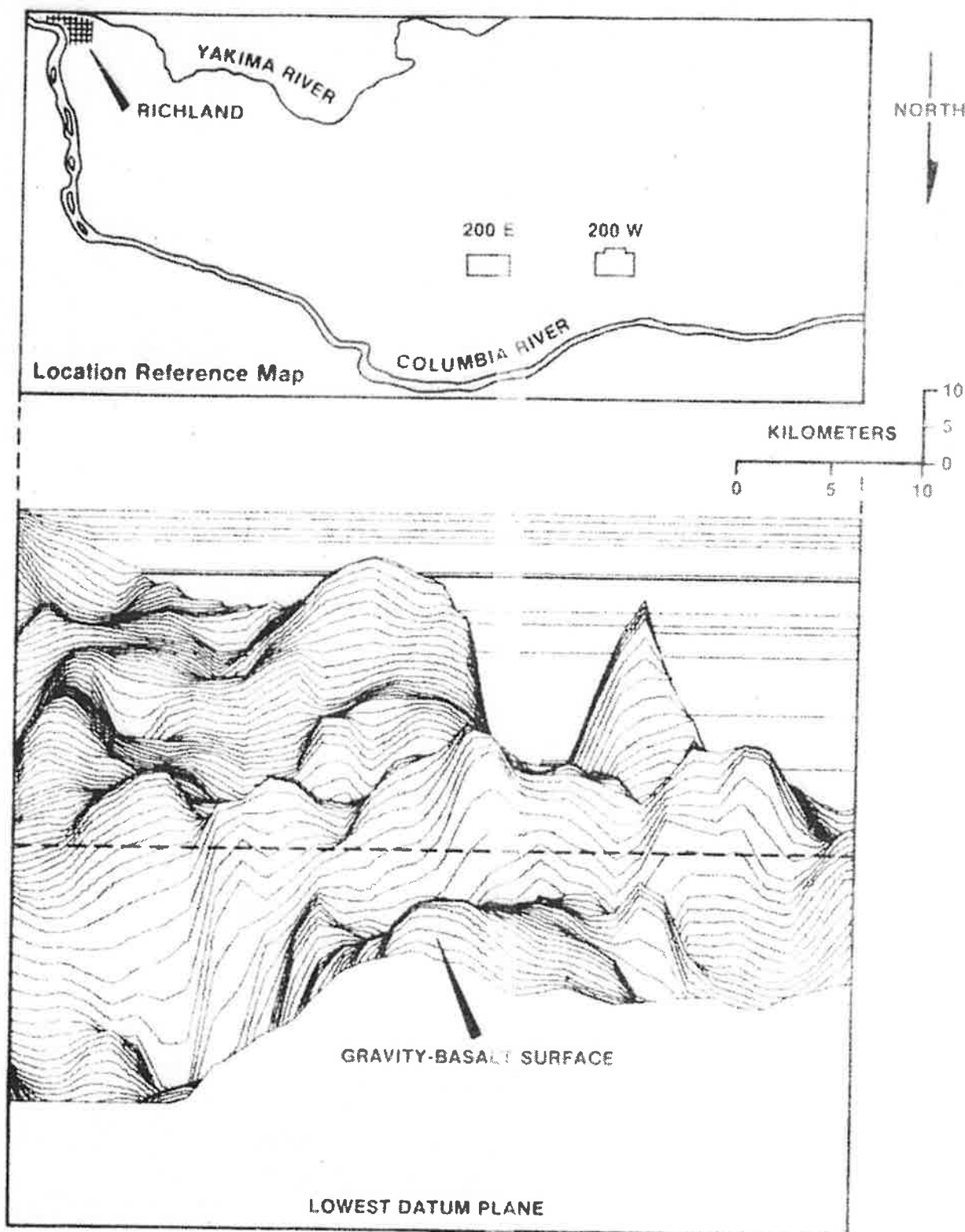


FIGURE B-15

HANFORD RESERVATION 344-POINT GRAVITY BEDROCK MAP, NORTH VIEW

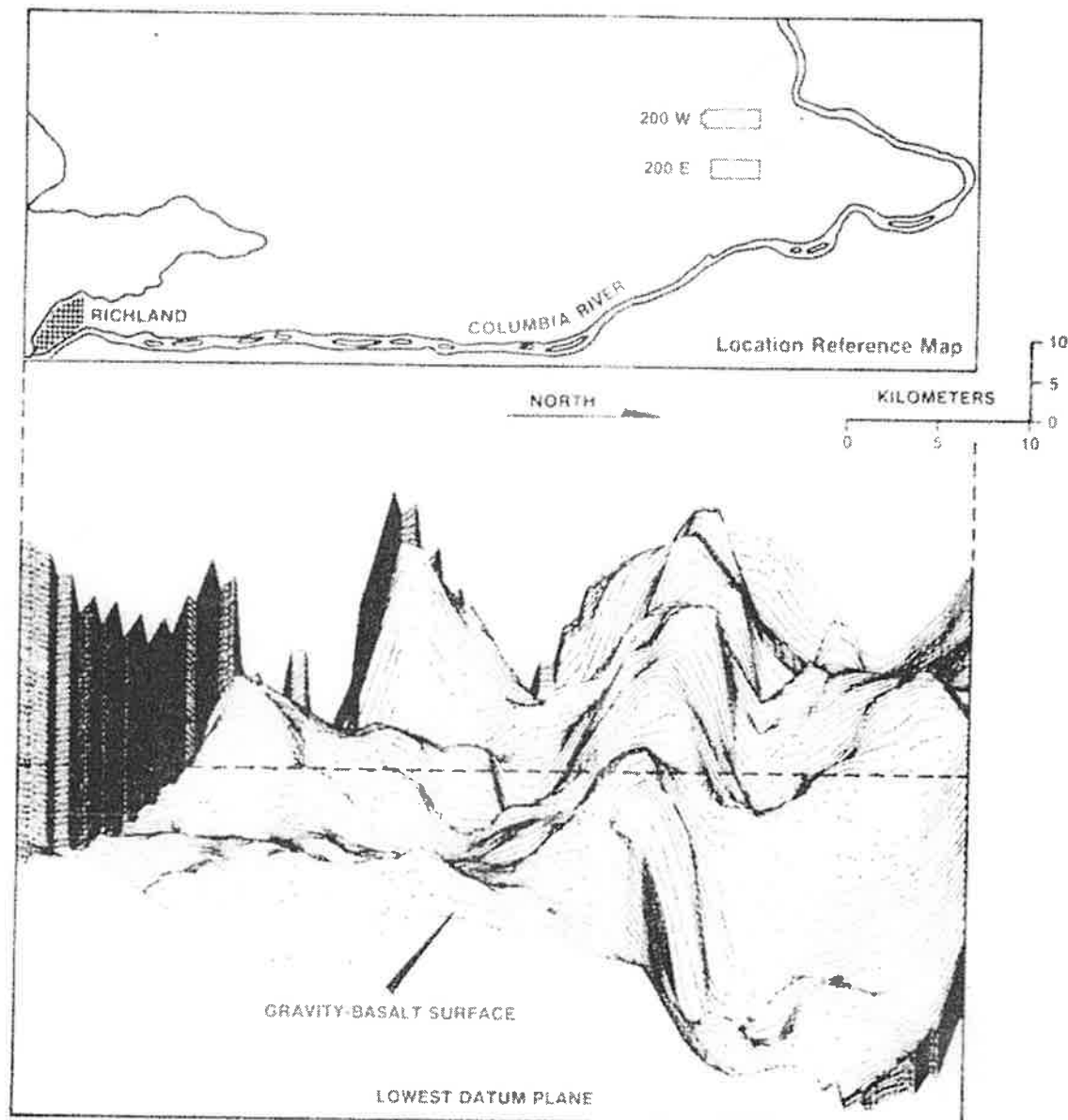


FIGURE B-16

HANFORD RESERVATION 344-POINT GRAVITY BEDROCK MAP, EAST VIEW

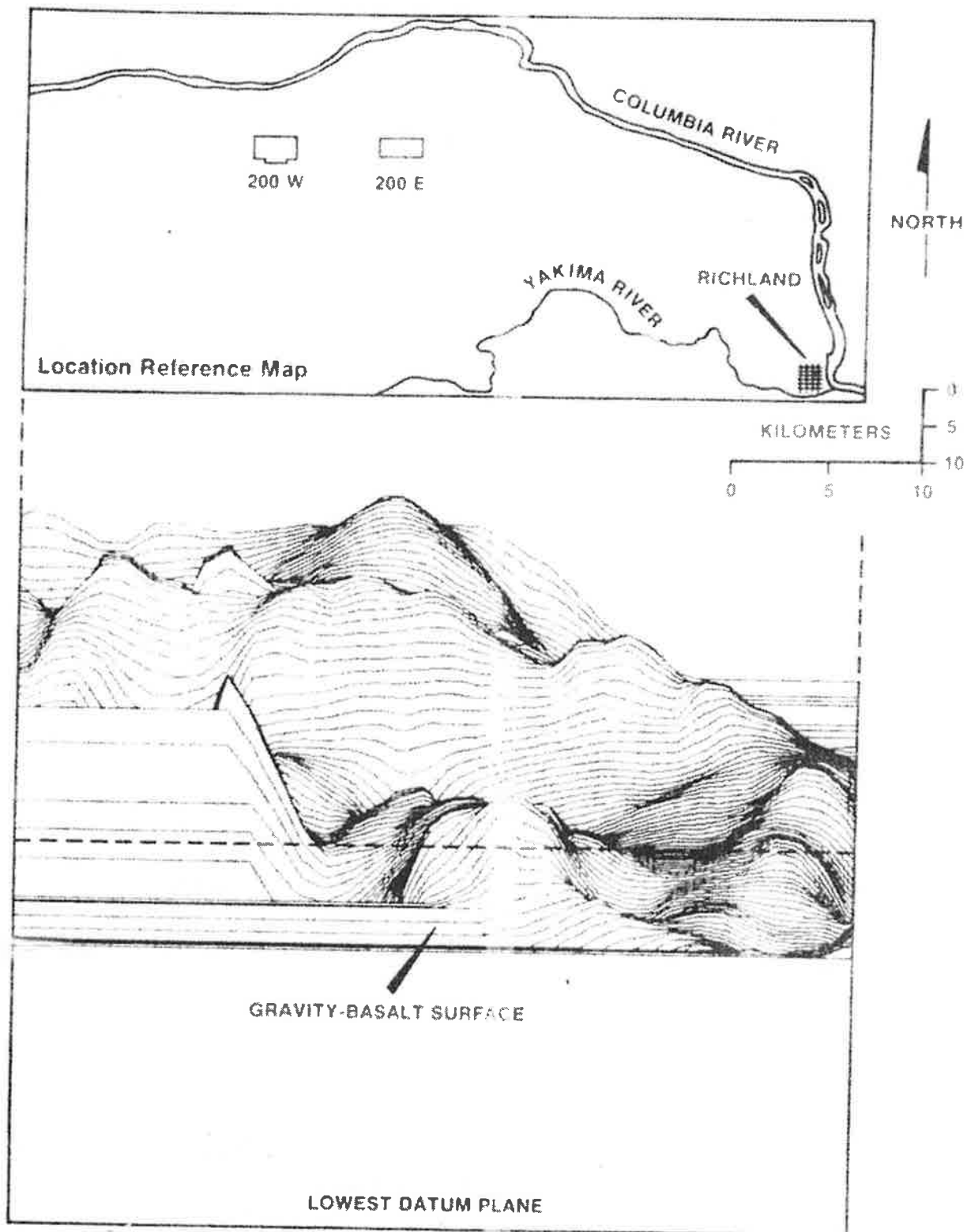


FIGURE A-17

HANFORD RESERVATION 166-POINT GRAVITY BEDROCK MAP, SOUTH VIEW

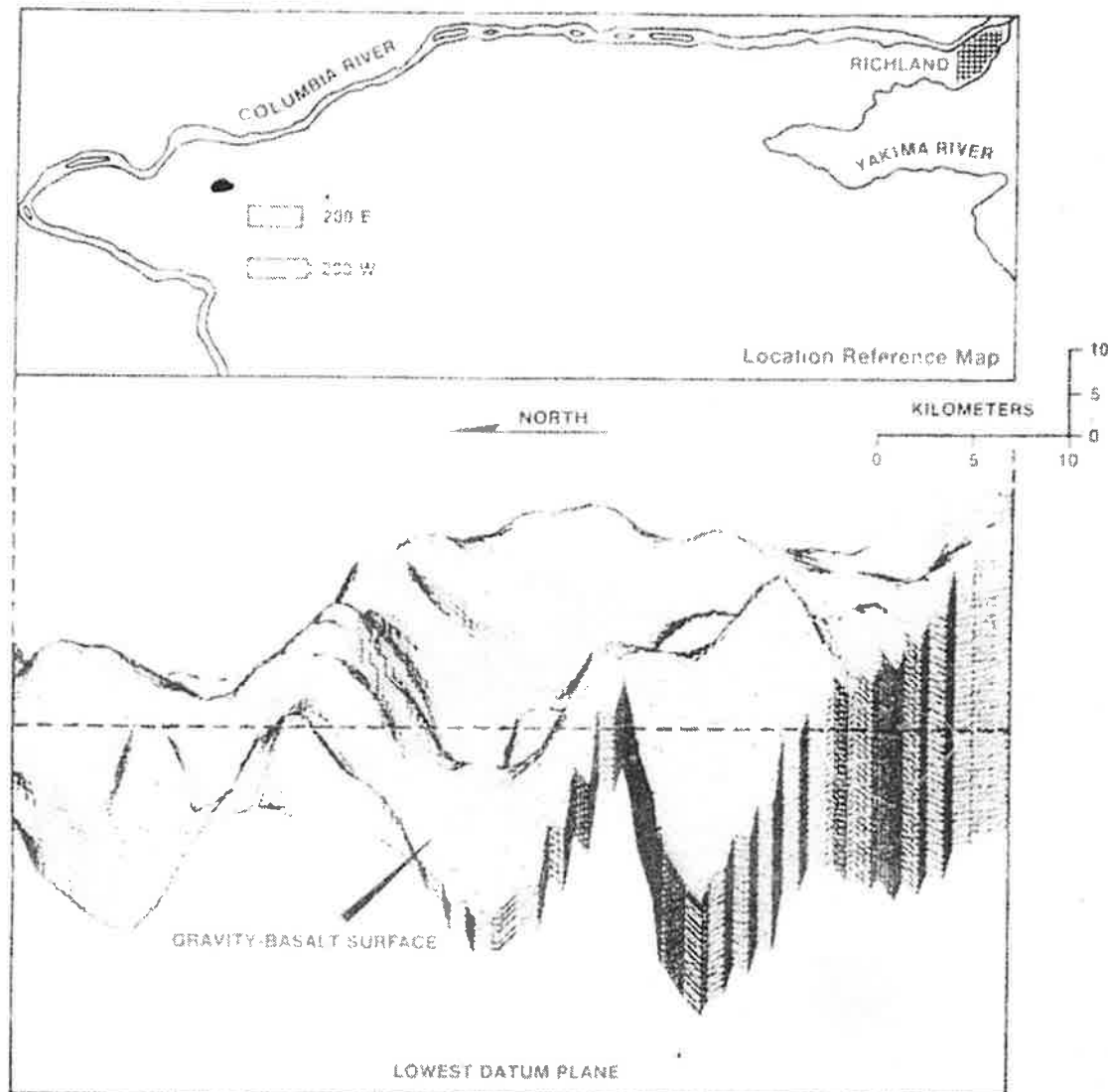


FIGURE B-16

HANFORD RESERVATION 166-POINT GRAVITY BEDROCK MAP, WEST VIEW

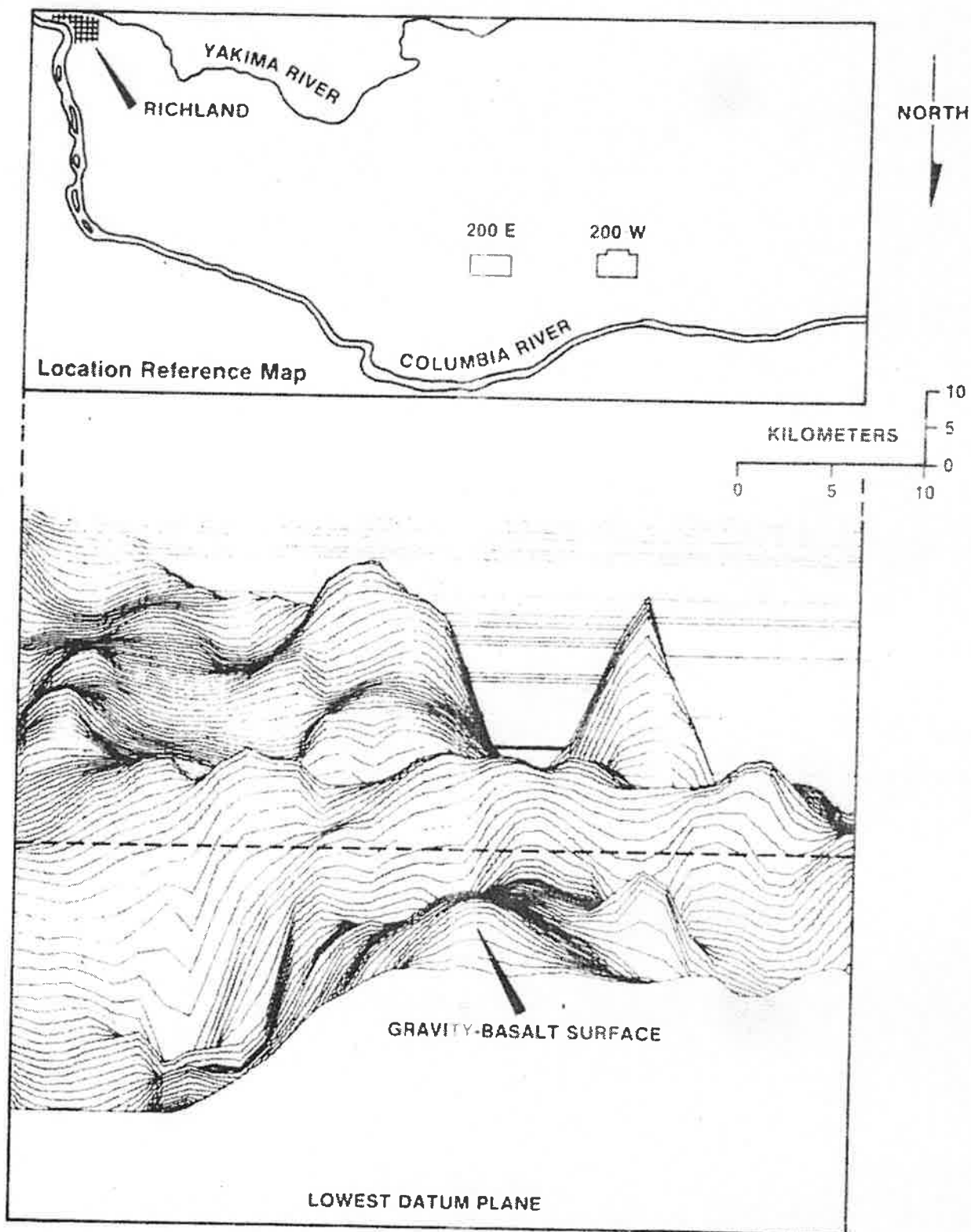


FIGURE 8-19

HANFORD RESERVATION 166-POINT GRAVITY BEDROCK MAP, NORTH VIEW

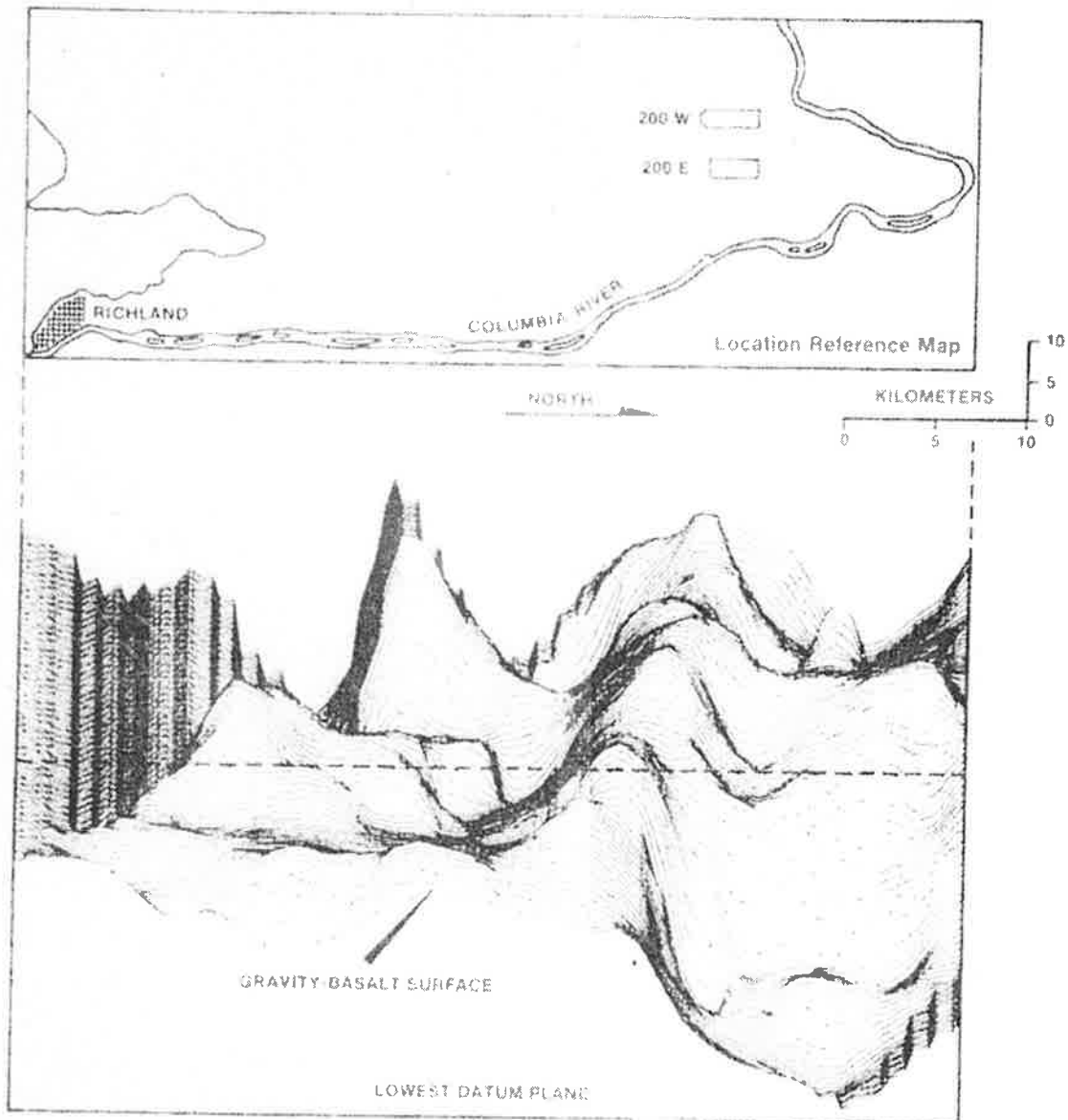


FIGURE B-20

HANFORD RESERVATION 166-POINT GRAVITY BEDROCK MAP, EAST VIEW

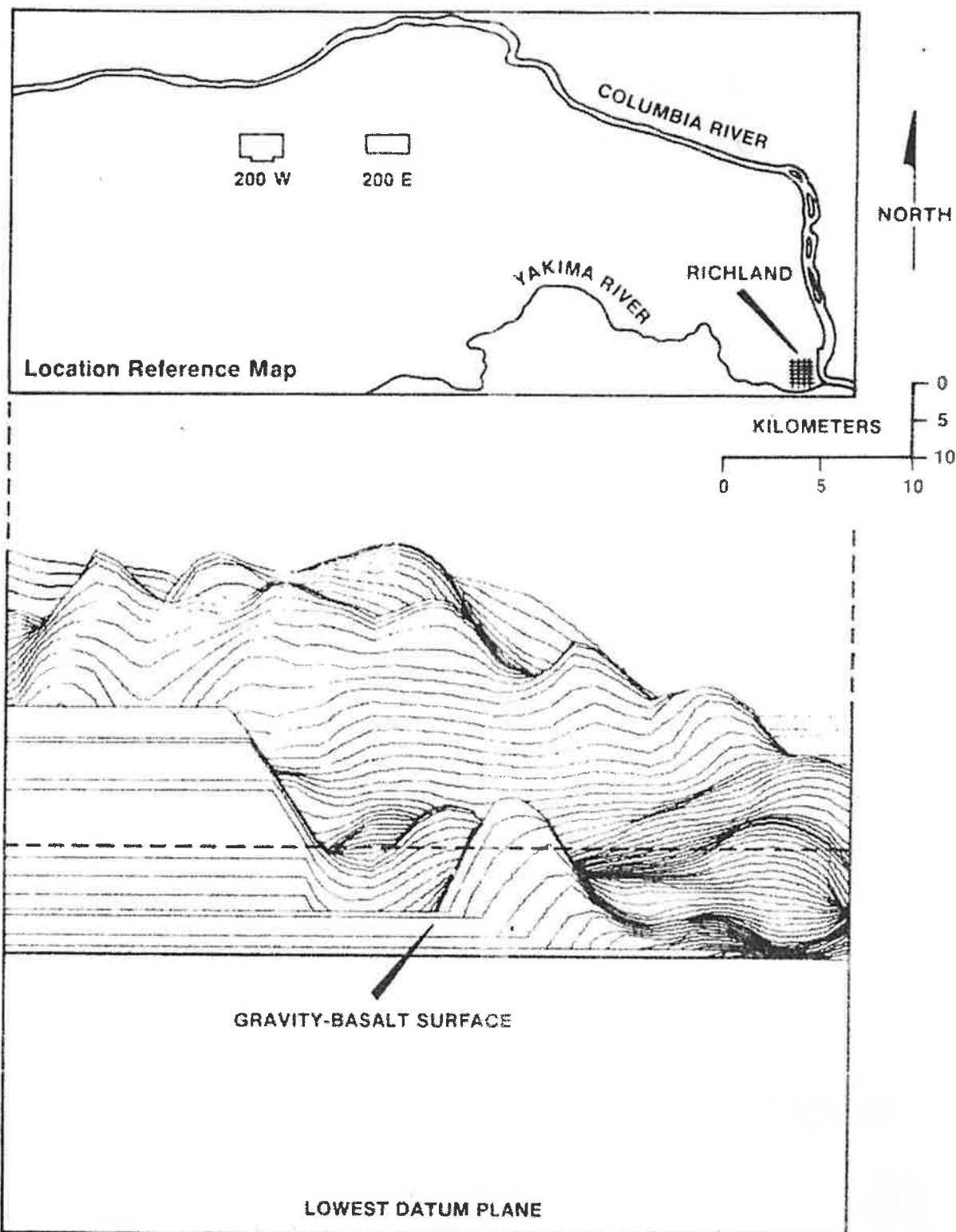


FIGURE B-21

HANFORD RESERVATION 88-POINT GRAVITY BEDROCK MAP, SOUTH VIEW

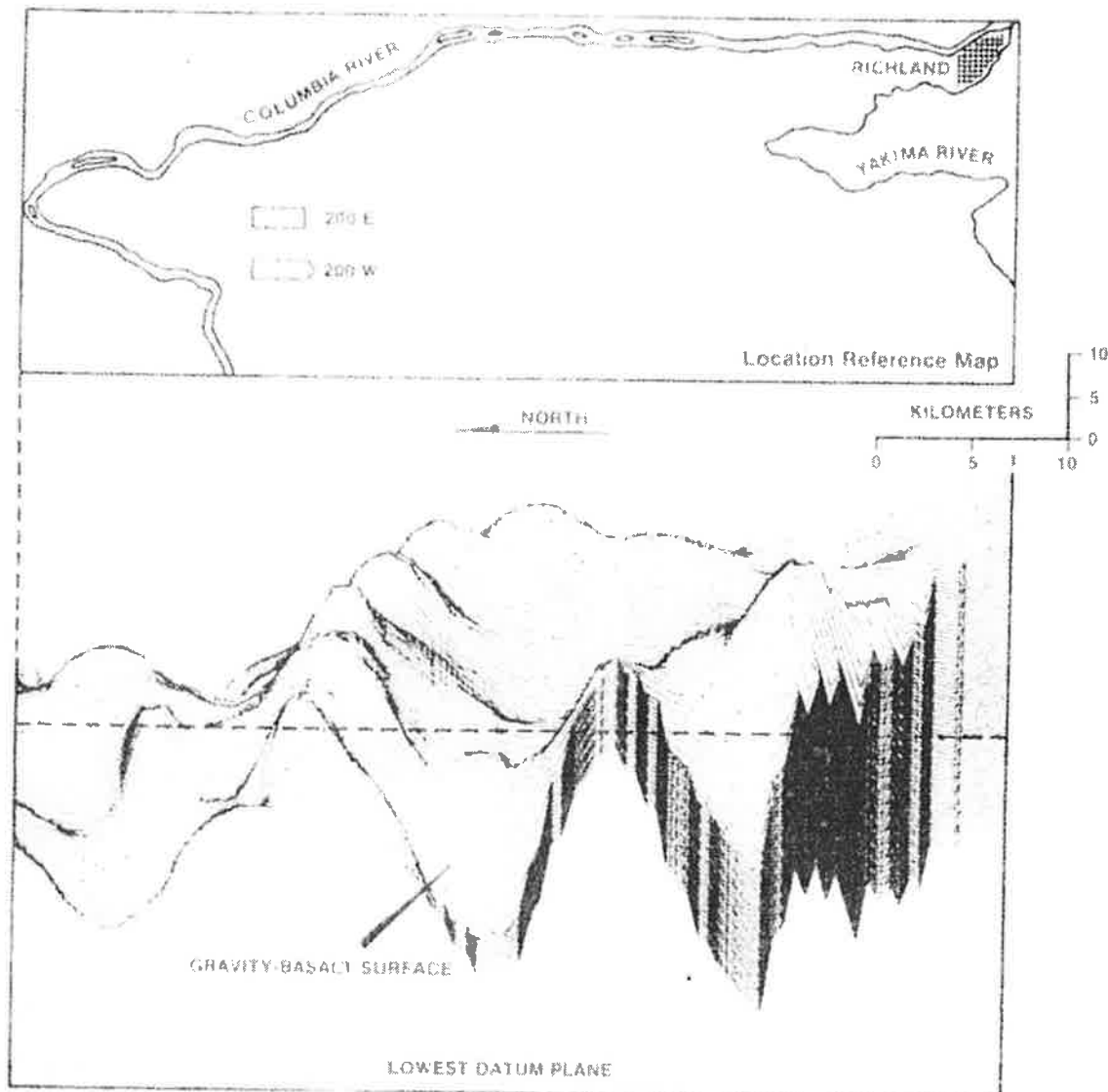


FIGURE B-22

HANFORD RESERVATION 88-POINT GRAVITY BEDROCK MAP, WEST VIEW

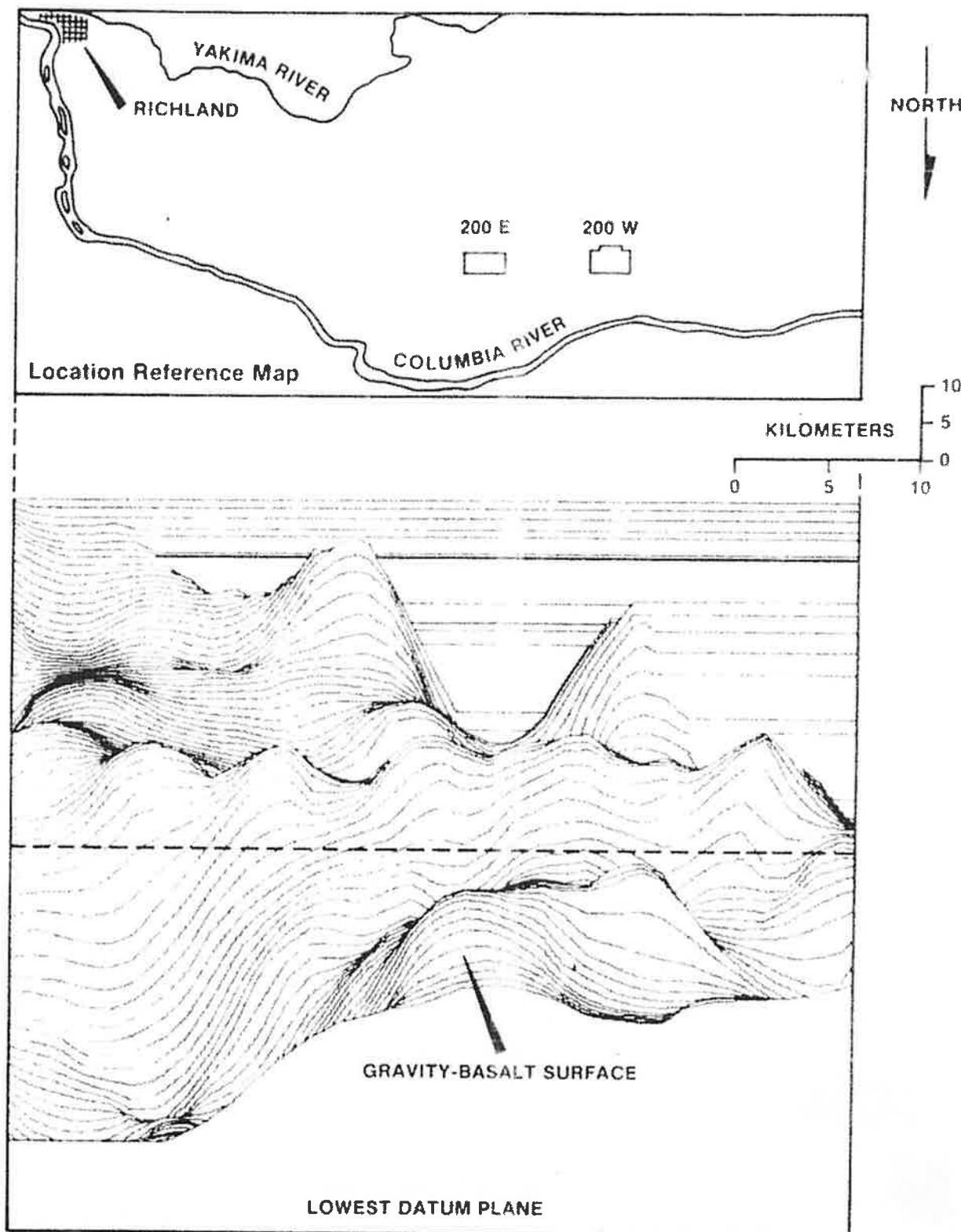


FIGURE B-23

HANFORD RESERVATION 38-POINT GRAVITY BEDROCK MAP, NORTH VIEW

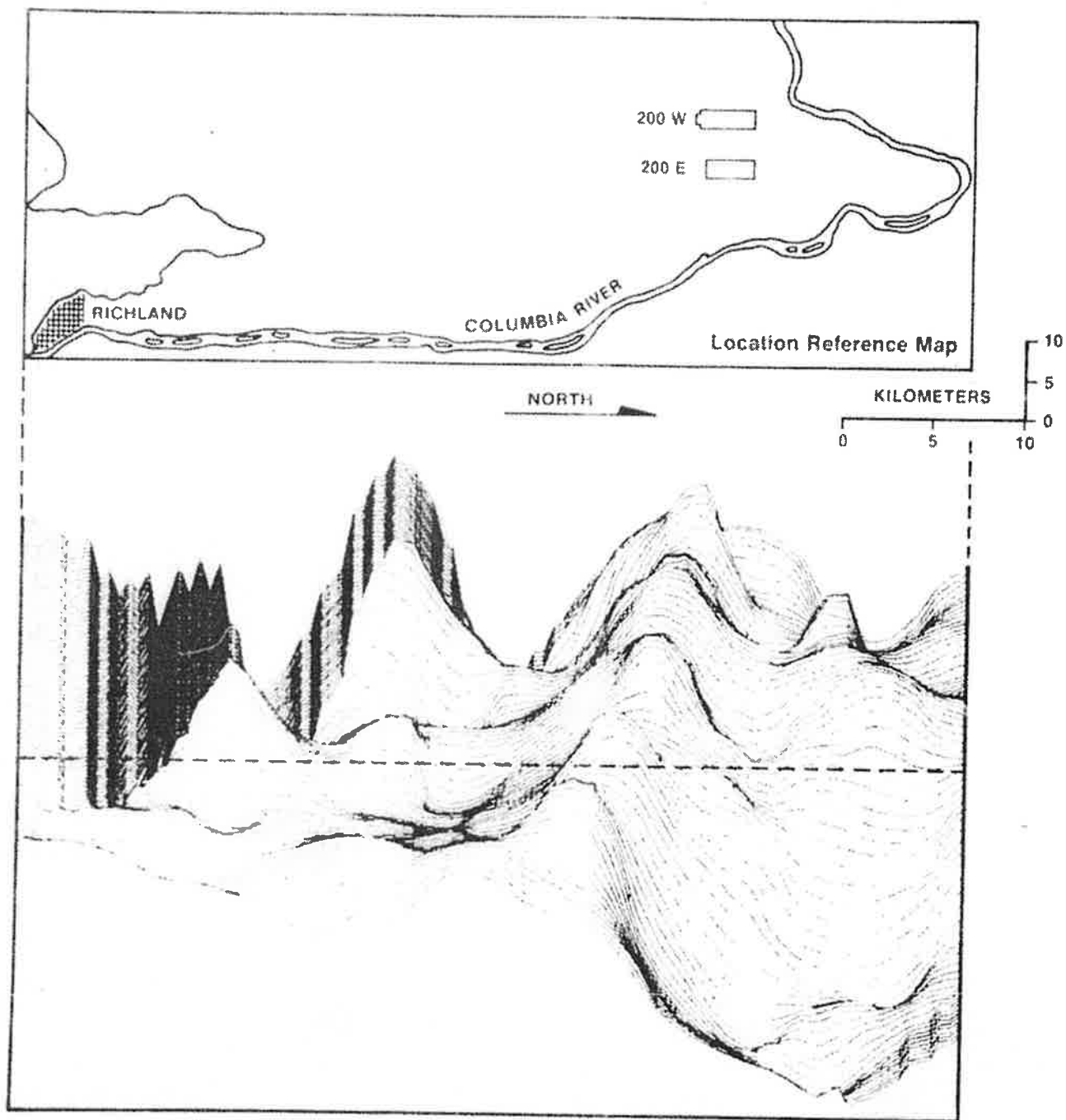


FIGURE B-24

HANFORD RESERVATION 88-POINT GRAVITY BEDROCK MAP, EAST VIEW

REFERENCES

1. D. E. Peterson, Variations in the Earth's Gravity Field at Hanford, BNWL-235 3, Battelle, Pacific Northwest Laboratories, Richland, Washington (1965).
2. D. E. Peterson, Bouguer Gravity Anomalies on the Hanford Reservation, BNWL-481 3, Battelle, Pacific Northwest Laboratories, Richland, Washington (1966).
3. R. A. Deju and B. H. Richard, A Regional Gravity Investigation of the Hanford Reservation, RAD-6, Deju Associates, Kennewick, Washington (1975).
4. M. B. Dobrin, Introduction to Geophysical Prospecting, McGraw-Hill, New York, New York (1960).
5. J. M. Adams, W. J. Hinze and L. A. Brown, Improved Application of Geophysics to Groundwater Resource Inventories in Glaciated Terrains, Technical Report Number 59, Purdue University Water Resources Research Center, West Lafayette, Indiana (1975).

DISTRIBUTION

Number of
Copies

4

BATTELLE-NORTHWEST

P. A. Eddy
J. R. Eliason
J. R. Raymond
R. W. Wallace

1

BOEING COMPUTER SERVICES RICHLAND, INC.

R. W. Nelson

1

GEOSCIENCE RESEARCH CONSULTANTS

J. G. Bond

1

W. K. SUMMERS AND ASSOCIATES

W. K. Summers

5

U. S. DEPARTMENT OF ENERGY-RICHLAND OPERATIONS
OFFICE

O. J. Elgert
R. B. Goranson
A. G. Lassila

D. J. Squires
M. W. Tiernan

Number of
Copies

1 UNIVERSITY OF IDAHO
 M. Miller
2 WASHINGTON PUBLIC POWER SUPPLY SYSTEM, INC.
 W. H. Riggsbee
 D. D. Tillson
1 WASHINGTON STATE UNIVERSITY
 J. W. Crosby, III
63 ROCKWELL HANFORD OPERATIONS
 H. Babad J. T. Lillie
 D. J. Brown W. H. Price (12)
 T. A. Curran (11) B. H. Richard
 R. A. Deju Waste Isolation
 R. E. Isaacson Program Library (25)
 A. G. Law (5) Document Services (4)